

Electrospinning of Cellulose Based Wound Dressing

A thesis submitted in partial fulfilment of the requirements
for the degree of

Doctor of Philosophy

By

Maryam Rachel Crabbe-Mann

Department of Mechanical Engineering
University College London
Torrington Place, London WC1E 7JE

UK

March, 2019

Declaration

I, Maryam Crabbe-Mann, confirm that the work presented in this thesis is my own. Where information has been derived from other sources, I confirm that this has been indicated in the thesis.

Maryam Crabbe-Mann

Dedication

To

My Mother;

Saada Ibrahim

And Grandmothers;

Elnora Naa Adawa Mann and Maryan Abdullahi Yusuf

The women whose shoulders I stand on

And in loving memory of my Grandpa;

John Peter Mann

He always remembered

Abstract

Cellulose is the most abundant polymer found on the face of the earth with plants and bacteria producing over 10¹¹ 10³ kg every year. Not only is this material widely available, it is renewable, sustainable and cheap, making it an attractive selection across many industries. The return to naturally derived materials in the medical field is driven by two motivations; the increased cases of resistance in bacteria to conventional drugs, and more relatedly, the need to reduce dependence on non-renewable resources when producing medical materials. Cellulose and its derivatives, are already used widely in the biomedical field in varying applications; drug delivery to eye drops. When manufacturing biomaterials from cellulose, the techniques used usually contain many steps and can be quite costly, this is where electrohydrodynamic (EHD) processing comes in. EHD is a one step process where under the influence of an electric field, a polymer solution or melt can be processed into micro- and nano-scale structures as a function of the polymer solution/melt properties such as concentration, molecular weight, solvent and processing properties such as voltage, flow rate and collection distance.

In the first instance, this work investigated the electrospinning of three cellulose derivatives, ethyl cellulose, cellulose acetate and carboxymethyl cellulose; changing parameters aforementioned and observing the effect on the microstructures produced.

Bacterial cellulose produced by the *Gluconacetobacter xylinus* bacteria, is chemically identical to plant cellulose, but is purer, not needing any separation or purifying post production. The most attractive feature of this bacterial cellulose (BC) is its liquid absorption capacity, it can hold many times its weight in liquid and proves to be useful in managing the exudate of diabetic ulcers. This BC was blended with different polymers and anti-diabetic drugs, after which *in vitro* behaviour was assessed.

List of Publications

- Crabbe-Mann, M., D. Tsaoulidis, M. Parhizkar, and M. Edirisinghe, Ethyl cellulose, cellulose acetate and carboxymethyl cellulose microstructures prepared using electrohydrodynamics and green solvents. *Cellulose*, 2018. 25(3): p. 1687-1703.
- Altun, E., M.O. Aydogdu, F. Koc, M. Crabbe-Mann, F. Brako, R. Kaur-Matharu, G. Ozen, S.E. Kuruca, U. Edirisinghe, O. Gunduz, and M. Edirisinghe, Novel Making of Bacterial Cellulose Blended Polymeric Fiber Bandages. *Macromolecular Materials and Engineering*, 2018. 303(3): p. 1700607.
- Aydogdu, M.O., E. Altun, M. Crabbe-Mann, F. Brako, F. Koc, G. Ozen, S.E. Kuruca, U. Edirisinghe, C.J. Luo, O. Gunduz, and M. Edirisinghe, Cellular interactions with bacterial cellulose: Polycaprolactone nanofibrous scaffolds produced by a portable electrohydrodynamic gun for point-of-need wound dressing. *International Wound Journal*, 2018. 5(15): p. 1-9
- Altun, E., M.O. Aydogdu, M. Crabbe-Mann, J. Ahmed, F. Brako, B. Karademir, B. Aksu, M. Sennaroglu, M.E. Eroglu, G. Ren, O. Gunduz, and M. Edirisinghe. Co-culture of Keratinocyte-Staphylococcus aureus on Cu-Ag-Zn/CuO and Cu-AgW nanoparticle loaded Bacterial Cellulose:PMMA bandages. *Macromolecular Materials and Engineering*, 2018.
- Altun, E., M. O. Aydogdu, S.O. Togay, A. Z. Sengil, N. Ekren, M.E. Haskoylo, E. T. Oner, N. A. Altuncu, G. Ozturk, M. Crabbe-Mann, J. Amhed, O. Gunduz and M. Edirisinghe, Bioinspired Scaffold Induced Regeneration of Neural Tissue. *European Polymer Journal*, 2019. (114): p.98-109.

List of Conference Presentations

Oral Presentations

- Crabbe-Mann M., Parhizkar M., and Edirisinghe M. Ethyl Cellulose, Cellulose Acetate and Carboxymethyl Cellulose Microstructures Prepared using Electrohydrodynamics and Green Solvents, 2018 MRS Spring Meeting, Phoenix, Arizona, USA, (2018).
- Crabbe-Mann M., Parhizkar M., and Edirisinghe M. Electrospinning of Bacterial Cellulose, 8th APS International PharmSci Conference, University of Hertfordshire, UK, (2017).
- Crabbe-Mann M., Parhizkar M., and Edirisinghe M. Electrospinning of Cellulose Derivatives, PhD Forum, Department of Mechanical Engineering, UCL, London, UK, (2016).
- Crabbe-Mann M., Parhizkar M., and Edirisinghe M. Electrospinning of Ethyl Cellulose, PhD Forum, Department of Mechanical Engineering, UCL, London, UK, (2015).

Poster Presentations

- Electrospinning of Bacterial Cellulose, 8th APS International PharmSci Conference, University of Hertfordshire, UK, September 2017

- Electrospinning of Bacterial Cellulose, EPSRC EHDA UCL Conference, UCL, UK, July 2017
- Electrospinning of Cellulose Derivatives, EPSRC EHDA Network: International PharmTech Conference 2016, De Montfort University, UK, November 2016
- Electrospinning of Cellulose Derivatives, UCL Mechanical Engineering Conference, UK, May 2016
- Electrospinning of Ethyl Cellulose, UCL Mechanical Engineering Conference, UK, June 2015

Acknowledgement

I would first and foremost like praise God Almighty for making this endeavour possible, and placing me in the best possible arena to conduct it in.

My supervisors; Prof. Mohan Edirisinghe and Dr. Maryam Parhizkar. Quite simply, they have tolerated me and got me to this stage, without them I would not have completed this work. Prof. Edirisinghe has offered me many, many opportunities, which extend far beyond just completing this PhD. Dr. Parhizkar teaches me something new every time I encounter her. Again, without these two people, I would not be in this position.

To the Biomaterials Processing Laboratory group, Miss Xinyue Jiang, it has been a pleasure sharing every step with you. Mrs Amalina Amir and Dr. Anouska Nithyanandan, both helped me keep the faith in God and myself. Dr. Keith Lau, Dr. Francis Brako, Dr. Chaojie Luo, Dr. Sunthar Mahalingam, Dr. Siqi Zhang, Dr. Zewen Xu, Yue Zhang, Jubair Ahmed, Rupy Matharu, Dr. Talayeh Shams, Mahroo Karimpoor have all supported me in some way or another.

And a special thank you to all my collaborators, Esra Altun, Onur Aydogdu and Dr. Muhammet Cam. They all helped take my work to another level.

Finally, my family; my father; Peter Crabbe-Mann, my siblings; NiiKofi, Niidaki, Kobina, Talabi, Aliyah, Abdul Karim and my friends; Attallah, Aisha and Alex, all of whom are my backbone and my unfailing support.

Contents

Declaration	ii
Dedication	iii
Abstract	iv
List of Publications	v
List of Conference Presentations	vi
Acknowledgement	viii
List of Figures	xiv
List of Tables	xx
1 Chapter 1	1
Introduction and Background.....	1
1.1 Background.....	1
1.2 Objectives	4
1.3 Thesis structure.....	5
2 Chapter 2	7
Literature Review.....	7
2.1. Introduction	7
2.2. Cellulose.....	9
2.1.1 Cellulose in Medicine.....	13
2.1.2 Cellulose Derivatives	14
2.1.3 Bacterial Cellulose.....	18
2.1.4 Other biomedical polymers	21
2.2 Solvent Selection	23
2.3 Other Spinning methods.....	26
2.4 EHD Processing.....	33
2.4.1 Brief history and Introduction.....	34
2.4.2 Electrospinning	36
2.4.3 Solution parameters affecting electrospinning.....	37
2.4.4 Processing parameters affecting electrospinning	40

2.5	Wound Healing Patches	41
2.5.1	Electrospun Wound Healing Patches.....	42
2.6	Drug release from electrospun fibres	44
2.7	Diabetic medication expand.....	46
3	Chapter 3.....	47
	Experimental Details	47
3.1	Introduction	47
3.2	Materials.....	47
3.2.1	Ethyl Cellulose	48
3.2.2	Cellulose Acetate.....	48
3.2.3	Carboxymethyl Cellulose	48
3.2.4	Polyethylene oxide	49
3.2.5	Bacterial Cellulose.....	49
3.2.6	Polycaprolactone	49
3.2.7	Gelatin	49
3.2.8	Glybenclamide	50
3.2.9	Metformin.....	51
3.2.10	Solvents	52
3.2.11	Glutaraldehyde.....	53
3.2.12	Phosphate buffered saline	53
3.3	Solution Characterisation	54
3.3.1	Viscosity	54
3.3.2	Surface Tension.....	54
3.3.3	Electrical Conductivity.....	54
3.4	Preparation of solutions	55
3.4.1	Cellulose derivatives solutions	55
3.4.2	BC-PCL-Glybenclamide solutions	55
3.4.3	PB-Gel-Metformin suspension	55

3.5	Experimental setup.....	56
3.5.1	Table top set up.....	56
3.5.2	Portable EHD gun	57
3.6	Characterisation of electrospun microstructures	58
3.6.1	Optical Microscopy.....	58
3.6.1	Scanning electron microscopy	58
3.6.2	Measurement of microstructures	59
3.7	<i>In vitro</i> Testing.....	59
3.7.1	Release	59
3.7.2	UV Spectroscopy.....	59
3.7.3	Swelling.....	61
4	Chapter 4.....	62
	Results and Discussion	62
	Ethyl cellulose, cellulose acetate and carboxymethyl cellulose microstructures prepared using electrohydrodynamics and green solvents..	62
	Overview	62
4.1	Ethyl Cellulose.....	63
4.1.1	Solution characterisation	63
4.1.2	Solvent selection	64
4.1.3	Concentration.....	66
4.1.4	Voltage	71
4.1.5	Flow rate	73
4.1.6	Collector to tip distance	75
4.2	Cellulose Acetate	76
4.2.1	Solution characterisation.....	77
4.2.2	Solvent Selection.....	78
4.2.3	Solvent	79
4.2.4	Concentration.....	82

4.2.5	Voltage	84
4.2.6	Guard Plate	85
4.3	Carboxymethyl Cellulose.....	87
4.1.1	Solution characterisation.....	87
4.1.2	Molecular weight.....	88
4.8.2	CMC/PEO Content.....	90
4.4	Summary.....	91
5	Chapter 5.....	92
	Results and Discussion	92
	Electrohydrodynamic production of polycaprolactone and bacterial cellulose wound healing patches doped with Glybenclamide.....	92
	Overview	92
5.1	Solution characterisation and fibre production.....	93
5.1.1	Characterisation of PCI-BC-Glybenclamide solutions.....	94
5.1.2	Production of PCI-BC-Glybenclamide fibres.....	97
5.2	Characterisation of PCI-BC-Glybenclamide electrospun patches	98
5.2.1	Effect of concentration of PCI on morphology and diameter of fibres	99
5.2.2	Energy-dispersive X-ray spectroscopy	102
5.3	<i>In vitro</i> testing	105
5.3.1	Effect of BC on swelling characteristics.....	105
5.3.2	Effect release of glybenclamide from PCI-BC.....	108
6	Chapter 6.....	111
	Results and Discussion	111
	Production of gelatin and bacterial cellulose wound healing patches doped with Glybenclamide and Metformin using electrohydrodynamics.....	111
	Overview	111
6.1	Gelatin with Bacterial Cellulose and Metformin	112
6.1.1	Fibres.....	113
6.1.1	Elemental analysis	114

6.1.2	Drug release	115
6.2	Gelatin with Bacterial Cellulose and Metformin	117
6.2.1	Fibres.....	117
6.2.2	Elemental analysis	118
6.2.3	Drug release.....	119
7	Chapter 7.....	121
	Conclusions and future work	121
7.1	Conclusion	121
7.1.1	Electrospinning ethyl cellulose derivatives with ethanol and water 121	
7.1.2	Electrospinning of cellulose acetate.....	122
7.1.3	Electrospinning of carboxymethyl cellulose	122
7.1.4	Production of PCI-BC-Gb wound healing patches.....	123
7.2	Future work.....	123
7.2.1	Wound healing assays	123
7.2.2	Cytotoxicity testing	123
7.2.3	MTT Assay	124
8	References	125

List of Figures

Figure 1: An anhydroglucose monomer that makes up the cellulose polymer	9
Figure 2: Some hydrogen bonding found in cellulose; intermolecularly (black) and intramolecularly (red) [23].....	10
Figure 3: The constituents of the plant cell wall. The purple cellulose rods are produced by complexes found in the plasma membrane and the hemicelluloses and pectins are produced by the Golgi apparatus and secreted via vesicles [27]	11
Figure 4: A cellulose microfibril with the crystalline regions highlighted in green and amorphous regions highlighted in red	12
Figure 5: Cellulose is reacted with ethyl chloride in the presence of sodium hydroxide to produce EC	15
Figure 6: Cellulose is reacted with acetic anhydride in the presence of sulphuric acid to produce CA	17
Figure 7: Cellulose is reacted with monochloroacetic acid in the presence of sodium hydroxide to produce CMC.....	17
Figure 8: L –R Transmission electron micrograph of single BC ribbon (white ribbon) being produced by a <i>Gluconacetobacter xylinus</i> cell (black arrow) [71] and scanning electron micrograph of <i>Gluconacetobacter xylinus</i> entrapped in BC pellicle [68]	19
Figure 9: Image demonstrating wet spinning.....	26
Figure 10: Image showing dry-jet wet spinning	27
Figure 11: Schematic of dry spinning process.....	28
Figure 12: Diagram of melt spinning method	29
Figure 13: Diagram showing gel spinning of UHMWPE	30

Figure 14: Image of centrifugal spinning (left) and pressurised gyration (right)	31
Figure 15: Schematic image of electrospinning set up with a magnified Taylor cone [151].	36
Figure 16: Image highlighting the benzamido and sulfonyl groups on the Gb molecule	50
Figure 17: Image of metformin molecule	51
Figure 18: Schematic illustration showing electrospinning set-up	57
Figure 19: Image of A) portable EHD gun, B) gun in use, C) resulting patch produced in situ and, D) a detailed image of the applicator [190]	58
Figure 20: UV calibration curve of glybenclamide	60
Figure 21: UV calibration curve of metformin	60
Figure 22: Optical micrographs of (a) 5wt% particles, (b) 10wt% particles, (c) 15wt% particles, (d) 20wt% beaded fibres, (e) 25wt% fibres and ribbons, (f) 30wt% ribbons, the flow rate, applied voltage and working distance were 100 μ L/min, 15kV and 100mm, respectively.	67
Figure 23: Effect of concentration on microstructure morphology the flow rate, applied voltage and working distance were 50 μ L/min, 15kV and 100mm, respectively, a) 17wt%, b) 25wt%, respective microstructure distributions below.	68
Figure 24: Effect of concentration on microstructure diameter at constant flow rate, applied voltage and working distance of 100 μ L/min, 19kV and 150mm, respectively a) 17wt%, b) 18wt%, c) 19wt%, d) 20wt%, e) 21wt%, f) 22wt%, g) 23wt%, h) 24wt% and i) 25wt%, each with their corresponding microstructure size distribution.....	70
Figure 25: Effect of voltage on fibre diameter collected at flow rate, concentration and working distance used were 50 μ L/min, 25wt% and 100mm	

a) 13kV, b)14kV, c)15kV, d)16kV, e)17kV, f)18kV, g)19kV and h)20kV, and graph showing the fibre diameter trend across the voltages. 72

Figure 26: Graph showing fibre diameter with increase in applied voltage for 22wt% CA dissolved in 80:20 acetone/water and 100:0 acetone/water. 80

Figure 27: CA fibres electrospun from 10wt% solution at flow rate, voltage and working distance used were 4ml/h, 13kV and 100mm, respectively, with the following solvents; a) 95:5, b) 90:10, c) 85:15 and d) 80:20. 81

Figure 28: Correlation between fibre diameter and polymer concentration, the flow rate, applied voltage and working distance were 4ml/h, 12kV and 100mm, respectively. 82

Figure 29: Optical micrographs of cellulose acetate fibres electrospun at 12kV, 6ml/h with the following solution concentrations L-R 10, 12.5, 15 and 17.5wt% (in acetone only). 83

Figure 30: Graph representing the change in fibre diameter by increasing the applied voltage, fibres were collected at a constant flow rate; 6ml/h with a guard plate attached. 85

Figure 31: Graph showing the diameter of fibres at variable applied voltage with and without guard plate 80:20 (acetone/water) solvent at concentration, flow rate and working distance used were 10wt%, 6ml/h, and 100mm, respectively. 85

Figure 32: Optical microscope images and corresponding size distribution graphs for fibres produced from 80:20 (acetone: water) solvent, at concentration, flow rate, voltage and working distance used were 10wt%, 6ml/h, 15kV and 100mm, respectively. Top image: Without guard plate, bottom image: With guard plate. 86

Figure 33: L-R Optical micrographs of carboxymethyl cellulose/poly(ethylene oxide) fibres electrospun at 16kV with 5 μ L/min flow rate with 100mm needle tip to collector distance, showing L-R 250,000g mol⁻¹ and 700,000 g mol⁻¹. 88

Figure 34: L-R Optical micrographs of carboxymethyl cellulose/poly(ethylene oxide) fibres electrospun at 15kV with 5µL/min flow rate with 100mm needle tip to collector distance, showing L-R 250,000 g mol ⁻¹ and 700,000 g mol ⁻¹	89
Figure 35: Optical micrographs of CMC (Mw 250,000)/PEO fibres electrospun at 16kV, 5µL/min at the following blends PEO:CMC a) 90:10, b) 86:14 and c) 75:25.	90
Figure 36: Graph showing effect of CMC proportion in solution on fibre diameter. Samples were collected at 15kV, with 5µL/min flow rate with 100mm needle tip to collector distance.	90
Figure 37: A(1) SEM image of 10wt% PCI fibres with A(2) accompanying histogram of fibre size. B(1) SEM image of 15wt% PCI fibres with B(2) accompanying histogram	100
Figure 38: A(1) SEM image of 10wt% PCI fibres with A(2) accompanying histogram of fibre size. B(1) SEM image of PCIBCGb-10 fibres with B(2) accompanying histogram	101
Figure 39: A(1) SEM image of 15wt% PCI fibres with A(2) accompanying histogram of fibre size. B(1) SEM image of PCIBCGb-15 fibres with B(2) accompanying histogram	101
Figure 40: A(1) SEM image of PCIBCGb-15 fibres with A(2) accompanying histogram of fibre size. B(1) SEM image of PCIBCGb-10 fibres with B(2) accompanying histogram	102
Figure 41: SEM image and elemental dispersive spectrum of glybenclamide drug.....	103
Figure 42: SEM image and elemental dispersive spectrum of PCIBCGb-10	104
Figure 43: SEM image and elemental dispersive spectrum of PCIBCGb-15	104

Figure 44: Graph showing swelling behaviours of PCI and PCL-BS patches over time	105
Figure 45: Drug release profile from PCIBCGb-10	108
Figure 46: Drug release profile from PCIBCGb-15	109
Figure 47: Comparison between PCIBCGb-10 and PCLBCGb-15.....	110
Figure 48: Release profiles of all four PCI based fibres	110
Figure 51: Gelatin and Met fibres with fibre diameter distribution.....	113
Figure 52: Gelatin, BC and Met fibres with fibre diameter distribution	113
Figure 53: SEM image and elemental dispersive spectrum of metformin drug	114
Figure 54: SEM image and elemental dispersive spectrum of Gel-Met	114
Figure 55: SEM image and elemental dispersive spectrum of Gel-BC-Met	114
Figure 56: Release of Met from cross linked Gel only.....	115
Figure 57: Release of Met from cross linked Gel compared to non cross linked Gel.....	115
Figure 58: Release of Met from cross linked Gel-BC only.....	116
Figure 59: Release of Met from cross linked Gel-BC compared to non cross linked Gel-BC.....	116
Figure 60: Gelatin and Gb fibres with fibre diameter distribution.....	117
Figure 61: Gelatin-BC and Gb fibres with fibre diameter distribution.....	117
Figure 62: SEM image and elemental dispersive spectrum of glybenclamide drug.....	118
Figure 63: SEM image and elemental dispersive spectrum of Gel-Gb.....	118
Figure 64: SEM image and elemental dispersive spectrum of Gel-BC-Gb	118

Figure 65: Release of Gb from cross linked Gel only	119
Figure 66: Release of Gb from cross linked Gel compared to non cross linked Gel	119
Figure 67: Release of Gb from cross linked Gel-BC only	120
Figure 68: Release of Gb from cross linked Gel-BC compared to non cross linked Gel-BC	120

List of Tables

Table 1: Solvents used with ethyl cellulose, cellulose acetate and CMC.....	25
Table 2: Various spinning methods [121].	33
Table 3: Properties of the CDs used.....	62
Table 4: Characteristics of ethyl cellulose solutions	64
Table 5: Literature values of desirability/safety of solvents used with ethyl cellulose of all the solvents checked, only water and ethanol were given the “green light” across the board by ref. 105, 106, 193 and 194. The values listed correspond to the health score from American Chemistry Society (ACS), health (acute and chronic effects on human health and exposure potential) from GlaxoSmithKline (GSK), overall ranking from Sanofi and guide for medicinal chemistry from Pfizer.	65
Table 6: Fibre diameter as a function of flow rate.....	73
Table 7: Effect of flow rate on morphology; tip to collector distance: 100mm.	74
Table 8: Effect of collector distance on morphology, voltage: 20kV, flow rate: 100 μ L/min.	76
Table 9: Characteristics of cellulose acetate solutions	77
Table 10: Literature values of desirability/safety of solvents used with cellulose acetate.	78
Table 11: Characteristics of carboxymethyl cellulose solutions	87

Table 12: Fibre diameter as a function of molecular weight	89
Table 13: Designations of polycaprolactone, bacterial cellulose and glybenclamide solutions.....	94
Table 14: Characteristics of polycaprolactone, bacterial cellulose and glybenclamide solutions.....	95
Table 15: Processing parameters used to electrospin polycaprolactone, bacterial cellulose and glybenclamide solutions.....	97
Table 16: Showing fibre diameters of BC and PCL-BC-Gb fibres.....	100
Table 17: Showing swelling value over time with peak swelling values highlighted	106
Table 18: Showing swelling value of PCL10 and PCI10BC10 and their ratio	Error! Bookmark not defined.
Table 19: Showing swelling value of PCL 15 and PCIBC-15 and their ratio	108

1 Chapter 1

Introduction and Background

1.1 Background

The importance of cellulose to humanity should not be underestimated [1]. Plants have been used in wound healing for millennia. Herbs and resins were used throughout the ancient world to clean and seal wounds [2]. Honey, minerals and animal derived products were also used by the ancients, in a bid to heal wounds [3]. As time progressed and we came to understand our own physiology, the width and breadth of wounds dressing available exploded, until the present day, where there are now over 5000 wound dressing products available. These range from basic occlusive dressings to more technical negative pressure therapies [4].

The use of cellulose is on the rise, but not more so in the medical industry where a return to naturally derived medicines and materials is favourably viewed. The versatility of cellulose, its low price, sustainability, biocompatibility, strength and availability make it an attractive material at a time when sustainability is essential [5].

An important development in that time is the understanding that maintaining a moist wound environment is conducive to healing [6], where the consensus was keeping the wound area dry was necessary. This is where cellulose has come into its own as a wound dressing, with its capacity to absorb large amounts of exudate but still maintain a moist environment [7]. Wounds such as diabetic ulcers found on lower limbs produce large amounts of exudate which must be managed to prevent necrosis and allow normal healing to proceed. With cellulose possessing an essential property needed in the treatment of diabetic ulcers, it forms a natural conclusion that cellulose should be used as or part of the biomaterial used to dress and treat diabetic ulcers.

The form this takes has been discussed abundantly in the literature. Oxidised regenerated cellulose and bacterial (microbial) cellulose are the most mentioned celluloses in the literature with regards to treating diabetic ulcers [8-12].

There are many different processes used to transform the cellulose from its raw form into a medically viable material, however, this typically involves lengthy multiple step procedures and the use of solvents. The solvents typically used for this are toxic, such that if they were to come into contact with a wound, more damage would occur rather than healing.

Cellulose in its native state is difficult to process and requires strong solvents but cellulose derivatives do not. The addition of a functional group along the cellulose polymer chain allows it to be solubilised in safer solvents which pose no threat to the wound or healing process. This is not explored widely, as these “safer” solvent do not possess the ideal properties for electrospinning. Although, the electrospinning of cellulose is already prevalent in the literature [13-17]; this project works to highlight the use of cheap, renewable, biocompatible and readily available solvents, which has not been as readily exploited in the literature. But as sustainability and environmental concerns taken into consideration, it is a difficulty we must overcome.

Electrohydrodynamic processing is a process that allows the production of a wide range of micro- and nano-structures from particles to beaded fibres to smooth fibres to ribbons [18]. From a single cellulose solution, changes to its characteristics or the parameters under which it is processed can drastically change the morphology of the structures produced [19, 20].

The motivation behind this work is to combine the medically relevant properties of cellulose with EHD, a simple one step process, to form micro- and nano-scaled structures to be used as wound healing patches to serve to two purposes; 1) accelerate wound healing thereby increasing quality of life for a patient, and 2) to follow the trend of returning to naturally derived medicines and materials, detracting from the use of non-renewable resources.

This is all with the aim of producing wound healing patches that eventually will be deposited directly onto patients' wounds using a portable point of need set up. Solvents play a large role in electrospinning and has a substantial effect on the morphology of the products made, as such, particular attention was paid to the solvents used, ensuring they were biocompatible, renewable and safe to use.

1.2 Objectives

There are two main aims to this work:-

1. Produce cellulose derivative microstructures using only safe solvents
2. To produce bacteria cellulose (BC) based biomaterials doped anti diabetic medications to make wound healing patches to treat chronic diabetic ulcers with the portable electrospinning gun capable of applying the dressing *in situ*

In order to achieve aim 1. ethyl cellulose, cellulose acetate and carboxymethyl cellulose were subjected to a range of solution and processing parameters with the structures produced observed and evaluated.

The objective for aim 2. was to manufacture bacterial cellulose based wound healing patches. As BC does not electrospin on its own it was blended with a synthetic polymer; polycaprolactone and a natural polymer; gelatin, separately. The morphology and some *in vitro* properties were observed. These were produced using the portable electrohydrodynamic gun, designed to allow the wound dressings to be applied *in situ*.

1.3 Thesis structure

The layout of this thesis is given here. This **chapter 1** details the background information gives details of the materials used, electrospinning process, the applications and motivations behind it all.

Chapter 2 gives an in depth literature review. Detailing various fibre forming techniques available alongside electrospinning, with the various parameters involved in the process. Background on the materials used are given, as well as properties of wound healing materials.

Chapter 3 describes the materials, experimental set ups, production methods, and characterisation procedures used to produce and analyse the various products made.

Chapter 4 shows the results of processing three different cellulose derivatives using only safe solvents are given. **Section 4.1** observes the changes to morphologies of ethyl cellulose structures when changes are applied to the processing parameters and solution concentration. **Section 4.2** investigates the effect on cellulose acetate when the applied voltage and flow rate are varied, along with polymer and solvent content. Finally, **section 4.3** investigates how changes to the degree of substitution and compositions of carboxymethyl cellulose change to fibres produced.

Chapter 5 describes the results of bacterial cellulose and polycaprolactone blended fibres. The anti-diabetic drug, glybenclamide, was incorporated into the fibres to make drug eluting wound dressings. The processing details, fibre analysis, drug release and swelling properties are also described.

Chapter 6, examines the results of bacterial cellulose and gelatin blended fibres. The fibres were incorporated with glybenclamide and metformin (another anti-diabetic medicine), separately. Comparisons between cross linked and non-cross linked *in vitro* behaviours were compared.

Chapter 7, draws up the conclusions found during this work and lists the future work that could follow these investigations.

2 Chapter 2

Literature Review

2.1. Introduction

The objective of this work was to explore the electrospinning process to produce cellulose based wound healing patches. The end target of this to be the treatment of chronic diabetic ulcers with cellulose based patches eluting anti diabetic medications to help overcome arrested healing.

The literature was surveyed as follows:

- **Cellulose and cellulose derivatives:** the structure and properties of cellulose which make it suitable for this application are discussed. Cellulose derivatives, are a form of cellulose which allows for a different approach in processing. The preparation of cellulose derivative is detailed, the addition of various functional groups, changes the chemistry such that common polar solvents can be used to dissolve the polymer. Bacterial cellulose, most commonly sourced from bacterium *Gluconacetobacter xylinus*, is also introduced. Its production, properties and uses, particularly, in wound healing are described. Polycaprolactone and gelatin were also used in this work and other relevant biomedical polymers are described.

- **Other fibre producing techniques:** many different methods are available to prepare fibres; wet spinning, dry spinning, flash spinning, melt spinning, dry-jet spinning, gel spinning and emulsion spinning are all described therein and compared to the chosen process; electrospinning.
- **Electrohydrodynamic processing:** the overall process is described and the effect of the various parameters involved, processing parameters; applied voltage, flow rate, collection distance and solution properties such as; concentration, surface tension, conductivity and viscosity. Along with the range of materials and structures this process can give rise to. Electrospinning falls under the umbrella of electrohydrodynamic processing, particular attention is paid to this, as it forms a fundamental part of this research.
- **Wound healing patches:** the wound healing process is complex, but materials can be used to aid in the progression or speed of healing. The requirements of a wound healing patch are listed. There is a focus on electrospun patches and how there have been able to successfully fulfil these requirements, as described in the literature. Examples of different materials for treating a range of different wounds is detailed.
- **Drug delivery in wound healing:** numerous agents can be added wound healing materials, again to aid the healing process. The mechanisms in which they are released, advantages of incorporating them into the materials and examples of specific applications are discussed.

- **Diabetic medication:** in order to treat diabetic ulcers specifically, research has shown applying some anti diabetic medications to the wound directly helps; this is elucidated here.

2.2. Cellulose

Cellulose (referring to plant cellulose) is the single most available biopolymer on earth, with an estimated production rate of 10^{13} kg per year via photosynthesis [21]. Cellulose is a polysaccharide most commonly found in the cell wall of plant cells. Plants are the primary source of cellulose; however, they do not exclusively produce it. It is also found in bacteria, algae, fungi and tunicate (marine invertebrate) [5]. In plants, it chiefly serves a mechanical purpose, maintaining the cellular and in turn the plant structure in times of turgidity and flaccidity.

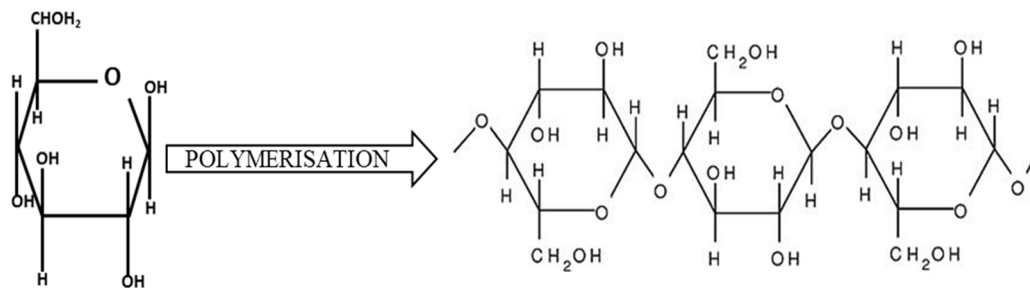


Figure 1: An anhydroglucose monomer that makes up the cellulose polymer

Cellulose has a very hierarchical structure, each level leading to the overall structure and properties of the polymer. Cellulose is made up of anhydroglucose monomer units ($C_6H_{12}O_6$) with 1,4-β-glycosidic linkages joining carbon-1 and carbon-4 of adjacent residues; these covalent bonds and intramolecular bonds are the source of the polymers rigidity and strength. The

chain length, defined as the number of monomers present, can range from few hundreds to 10,000 depending on the source [5]. The difficulty in processing cellulose i.e. its inability to dissolve in the majority of solvents, stems from the presence of hydrogen bonding [22].

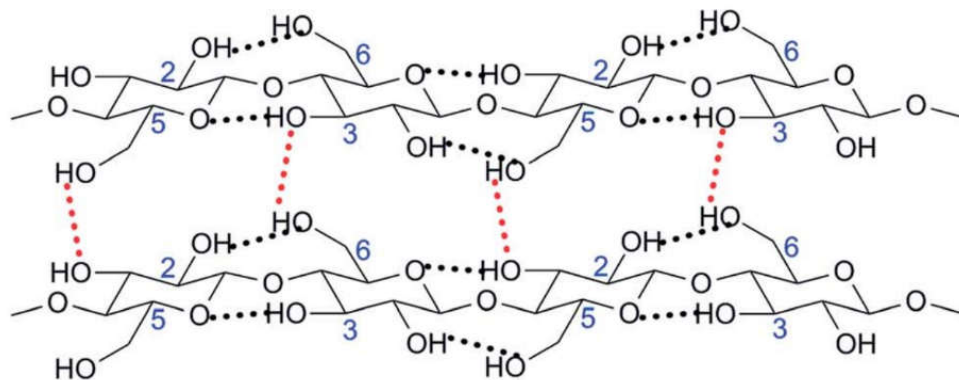


Figure 2: Some hydrogen bonding found in cellulose; intermolecularly (black) and intramolecularly (red) [23]

The oxygen atoms present in the hydroxyl groups, within the ring itself and in the glycosidic bond all partake in hydrogen bonding, both within and between the polymer chains giving rise to the 3D structure [24]. As a result of the large number of –OH groups present cellulose is hydrophilic; however, it is not solubilised in water along with many other solvents because of its massive molecular weight. The hydrogen bonds and van der Waals force draw polymer chains together to form microfibrils, with crystalline and amorphous regions [25], as shown in Fig. 4. These microfibrils aggregate in an aligned manner to form macrofibrils dispersed within hemicellulose and pectin matrix approximately [26], as shown in Fig. 3.

It was not until the 1800's that the molecular structure and morphology was identified by two researchers Henri Braconnot (1833) and Anselme Payen (1842). The extraction of cellulose from plant material was first discovered by the latter, where he introduced various plant parts to an acid-ammonia solution and then water, unknowingly extracting a substance which was named by the French Academy "cellulose" [1]. Before this Henri Braconnot (1833), by the dissolution of "plant substances" in nitric acid came to produce *xyloidine*, the first precursor nitrocellulose, commonly used as an explosive material and in the plastics industry [60].

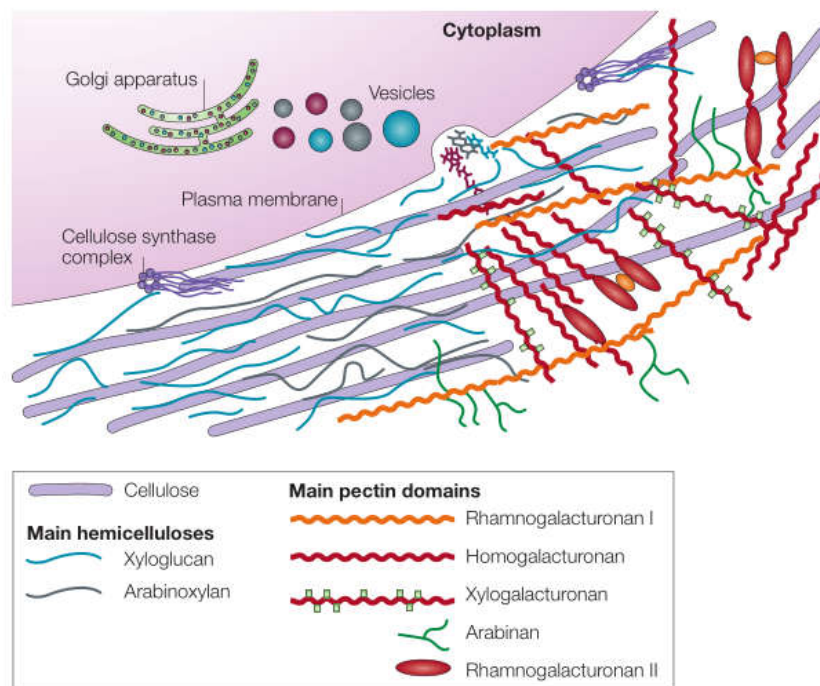


Figure 3: The constituents of the plant cell wall. The purple cellulose rods are produced by complexes found in the plasma membrane and the hemicelluloses and pectins are produced by the Golgi apparatus and secreted via vesicles [27]

Cellulose also forms the fibre consumed in our diet. Although cellulose is made up of the same monomer as carbohydrates, it is not digested in the human body as we lack the enzyme to break the 1,4- β -glycosidic bond found in cellulose but we do produce the amylase enzyme which is able to break down the bonds 1,4- α -glycosidic bond found in starch [28]. Cellulose is rarely found in its pure form *in vivo*. In the cell wall it has strong associations with other polysaccharides such as hemicellulose and pectin as shown in Fig. 3. Extraction of cellulose is typically a two-step process; the first step is an alkali treatment followed by a bleaching regime [24].

The difficulty with working with cellulose, especially within the remit of this work, is its inability to be solubilised by conventional solvents. This is attributed to the chemical bonding of the polysaccharide, despite the presence of –OH groups, the sheer size of the molecule and the large presence of hydrogen bonding means not all of the polymer chains are not exposed to the solvent, making it very difficult to dissolve and impossible to melt, it disintegrates upon heating [23, 29].

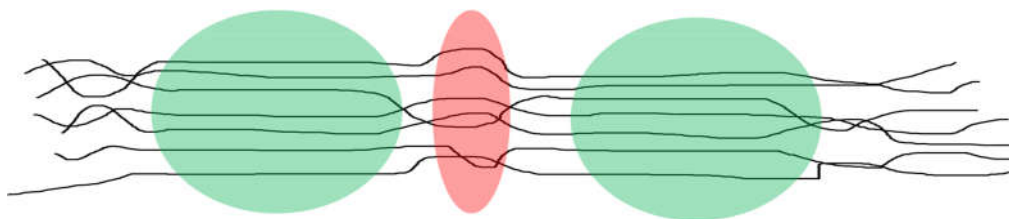


Figure 4: A cellulose microfibril with the crystalline regions highlighted in green and amorphous regions highlighted in red

Cellulose is a semi crystalline polymer, with crystalline and amorphous regions as shown in Fig. 4. The crystalline regions have a higher quantity of hydrogen bonds. The amorphous regions with less tightly packed chains allow water and other solvents to penetrate and form bonds, allowing the polymer to swell but not dissolve [30].

Exhausting non-renewable energy reserves is something we approach closer to everyday, along with increasing the levels of pollution associated with its use [31]; this is where cellulose may be able to fill this gap. Cellulose is biodegradable, it will not add to the growing issue of landfill waste, some of which will takes many years to degrade with toxic results.

2.1.1 Cellulose in Medicine

Cellulose is biodegradable, biocompatible, renewable, sustainable and inexpensive; with these properties it is steadily replacing non-renewable materials [32]. The use of native cellulose in pharmacy is also well documented, it is used as a laxative and artificial tears [33]. Cellulose is a cationic polysaccharide which has been shown to promote healing and prevent infection while also reducing blood loss [34, 35]. Native cellulose is not readily degradable in living tissue and not digestible; which is attributed to its highly ordered structure [36].

2.1.2 Cellulose Derivatives

2.1.2.1 *Introduction*

Cellulose derivatives (CD) are derived from native cellulose but purified with functional groups added [13]. The use of cellulose derivatives allows for much safer solvents to be used, and makes for much easier processing especially in the case of electrohydrodynamic (EHD) processing. As cellulose cannot be melted, it must be processed as a solution, which involves solvents. The addition of functional groups distorts the cellulose polymer chain and allows solvents such as ethanol, acetone and water to completely solvate the polymer and form solutions [30, 37]. This reduced the need to use solvents such as N-methylmorpholine-N-oxide (NMMO) hydrate, which is used prolifically with cellulose [29, 38]. NMMO is able to dissolve cellulose without altering the chemical formula [38]. However, electrospinning with NMMO must be done at elevated temperatures and measures taken to wash any residue [39]. After this are the binary solvent systems N, N-dimethylacetamide & lithium chloride (DMAc & LiCl) [40] and dimethylsulfoxide & tetrabutylammonium fluoride (DMSO & TBAF) [29] are most popular.

There are examples where electrospun CD fibres have performed better than those made by other processing techniques. Hydroxypropoxy methylcellulose (HPMC) was electrospun with a poorly water soluble drug (itraconazole), the high surface to area ratio showed a more controlled release of the drug overtime compared to a solvent cast film and melt extruded samples of the same polymer-drug combination [41].

2.1.2.2 *Ethyl Cellulose*

Ethyl cellulose (EC) is a non toxic, stable, inert and hydrophobic polymer [42]. EC is non-ionic and although hydrophobic, it is soluble in other polar solvents [43]. EC is thermo-stable and has shown some electrical properties [44, 45]. Every year an estimated 40000 kg of EC is produced and used primarily in the biomedical field [23]. EC is tasteless and is used in masking undesirable flavours, as well as filtration and protective clothing [17, 46]. Most commonly used in pharmaceuticals, it is used as an insoluble component, to coat active ingredients, allow compression of tablets, or used in conjunction with other polymers to mediate drug release profiles and as a dissolution rate controlling polymer sustained release forms [47, 48]. It is a favoured polymer in drug delivery systems, be it in tablets, microspheres and film encapsulating both soluble and non-soluble drugs [49, 50]. Liakos et al., has used EC with essential oils to produce wound healing patches. EC fibres has the capability to be loaded with therapeutic agents to increase its healing ability further [51]. Miyamoto et al. showed: ethyl cellulose (EC) was not absorbed by living tissue in dogs, and only initiated a mild foreign body reaction after 4 weeks of implantation. It was also shown the degree of tissue absorbance is relative to hydrophilicity and, due to the hydrophobic nature of EC, it is not absorbed by the body [36].

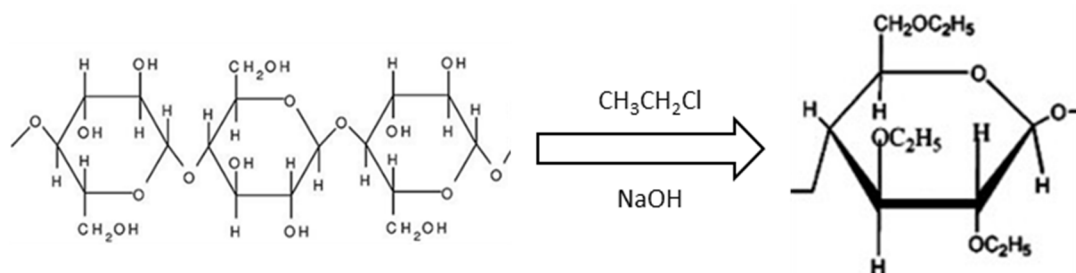


Figure 5: Cellulose is reacted with ethyl chloride in the presence of sodium hydroxide to produce EC

2.1.2.3 Cellulose Acetate

Cellulose acetate (CA) is produced via acetylation of cellulose; cellulose is reacted with acetic anhydride in the presence of sulphuric acid [52]. It is amorphous, non toxic and soluble in acetone [53]. CA is most commonly used as a semi permeable membrane for molecular filtration in chemistry [54]. It is used to produce regenerated cellulose, where cellulose acetate is processed via deacetylation in a strongly ionising agent such as sodium hydroxide or potassium hydroxide [54], this is commonly used in textiles.

Electrospun CA is used widely including medical applications such as cell culture and regenerative medicine [55], anti microbial mat (with anti-bacterial agents added) [56] and drug delivery [57].

CA has excellent water retention properties which are a desirable trait in a wound dressing where absorbing wound exudate is an important function [58]. Son et al. electrospun CA with AgNO_3 where Ag^+ ions, well known antibacterial agent, were released via UV light exposure [14]. Suwantong et al. electrospun

CA with curcumin (an component of turmeric), a historical remedy used in the eastern world, and has been shown to increase cutaneous wound healing in test animals [59].

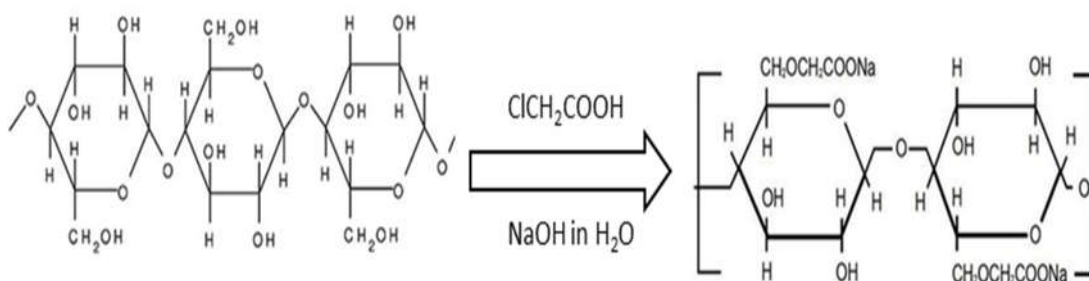


Figure 6: Cellulose is reacted with acetic anhydride in the presence of sulphuric acid to produce CA

2.1.2.4 Carboxymethyl Cellulose

Carboxymethyl cellulose (CMC) is a water soluble derivative of cellulose, made so by the addition of carboxymethyl functional groups to the cellulose backbone [60]. CMC is a non-toxic and water soluble polymer [61]. It has mucoadhesive properties [62]. CMC is used as a flocculant, drag reduction, detergent, in textiles and paper making, as well as food and drugs [63]. PEO is used a spinning agent [62]. CMC produced through an esterification process, bleached cellulose is activated with sodium hydroxide. Then monochloroacetic acid is added in the presence of the alkali [64].

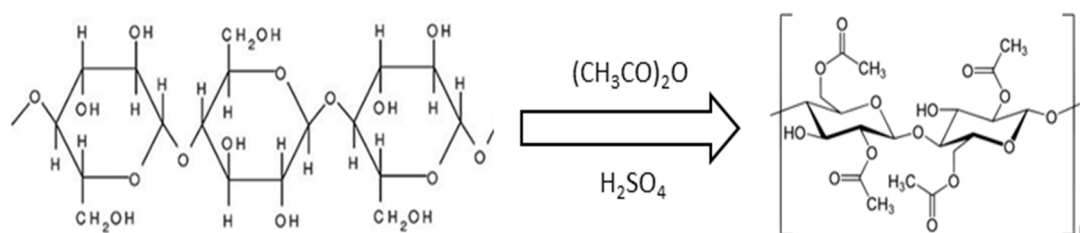


Figure 7: Cellulose is reacted with monochloroacetic acid in the presence of sodium hydroxide to produce CMC

2.1.3 Bacterial Cellulose

2.1.3.1 Introduction

Many bacteria produce cellulose but only *Gluconacetobacter xylinus* is used to produce bacterial cellulose (BC) on a commercial scale [65]. It is superior to plant cellulose produced with its high purity, containing no lignin, hemicelluloses, pectin and waxes unlike plant cellulose. *Gluconacetobacter xylinus* is a Gram-negative, acetic acid bacteria which was first found to produce BC on the surface of a vinegar fermentation by Brown in 1886 [66]. Following this in 1954, Hestrin and Schramm reported the bacteria producing BC in medium high in glucose [67]. Following the commercialisation of BC production, reactors and culture conditions were fashioned to maximise production [67]. In 1886, it was Brown who definitively showed the pellicle was made up of cellulose, using a number of reactions and chemical analysis [66, 68].

2.1.3.2 Production

BC is produced in the form of a wet membrane comprised of approximately 99% water at the air-liquid interface [69]. The pellicle is produced as a succession of layers, entrapping the bacteria within them [66], as shown in Fig. 8, it is formed at the liquid-air interface in static cultures [70]. The *G. xylinus* is capable of producing BC from a wide range of carbon sources, such as; glucose, sucrose proteose and peptone [70].

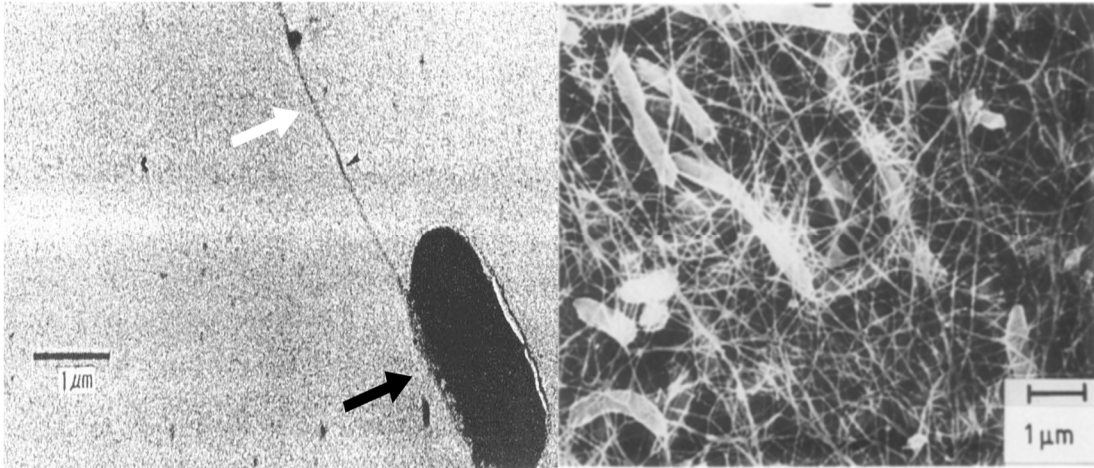


Figure 8: L –R Transmission electron micrograph of single BC ribbon (white ribbon) being produced by a *Gluconacetobacter xylinus* cell (black arrow) [71] and scanning electron micrograph of *Gluconacetobacter xylinus* entrapped in BC pellicle [68].

2.1.3.3 Properties

BC is chemically equivalent to plant cellulose and has a distinct ultrafine fibrils that are in a nanosized 3D network [72]. This 3D network is made up of nano fibrils of 2-4 nm which come together to form fibrils of 130 nm [73, 74]. BC is highly crystalline, and has an ultrafine network structure and capable of absorbing 200 times its dry mass of water [67, 71]. Another desirable property of BC is the ability to chemically alter the polymer during synthesis by adjusting the feedstock of the bacteria [70]. The degree of polymerisation between plant cellulose and BC does differ, the former is typically made up of 13,000 to 14,000 residues but BC only contains 2000 to 6000 [67].

2.1.3.4 *Uses*

BC is typically cultivated in static cultures, which result in pellicles. The fibres are 100 times thinner than plant cellulose. Its biocompatibility has led to its introduction to the medical sector where it has been successfully used as artificial skin in treating burns, and artificial blood vessels in microsurgery [75-77]. BC is easily sterilised and has been found to be non-allergenic, these characteristics as well as the many others has made it a great candidate for use as wound dressing [78]. There are currently two major manufacturers of BC based biomaterials; BioFill Produtos Biotecnologicos from Brazil, they manufacture wound healing systems for treating burns and ulcers. They also have a product focussed on treating periodontal disease. The second is Xylos, based in USA. Their range includes an anti-microbial dressing and a product designed to specifically treat ulcers also [5, 67, 79, 80]. Attempts have been made to make paper from BC as done with plant cellulose, where it was showed "BC paper" had a greater Young's modulus and tensile strength compared to paper made from cotton lint [68]. This has also made it a potential candidate for electroacoustic transducer in speaker systems [81]. The porous nature of the material can allow the transfer of medicines whilst maintaining a barrier [79]. In food, BC is used as a stabiliser, thickener, used in pastry condiments and ice cream [82].

2.1.4 Other biomedical polymers

2.1.4.1 Polycaprolactone

PCI, specifically poly(ϵ -caprolactone) used in this work, is produced through the polymerisation of ϵ -caprolactone, the hexagonal ring molecule, through a ring opening polymerisation (ROP) process. There are four different ring opening mechanisms; anionic, cationic, monomer-activated and coordination-insertion, which all give rise to the aliphatic polycaprolactone [83]. PCI is a synthetic, biodegradable polymer, typically used in long term implants, it is semi crystalline and soluble in a number of solvents [84]. It is already used in implantable devices due to its biodegradable, biocompatible, presents good mechanical properties and has tissue compatibility [85].

Its slow degradation can be unfavourable in terms of drug release, however, compared to the fast degrading poly(lactic acid) and poly(glycolic acid), which are commonly used for their ability to degrade *in situ*

In terms of its use in electrospun biomaterials, PCI is widespread. Due to its ease in processing it is commonly used alone and in combination with other polymers and active pharmaceutical ingredients. It is a versatile material with references using it to produce cellular scaffolds [86, 87], drug delivery [88-90], scaffolds [91-93] and wound healing [94]. The variety of applications are also broad. Bölgen *et al.* used electrospun PCI soaked in an antibiotic to prevent abdominal adhesion following surgery [95], the use of the drug embedded patch hastened and improved the healing process, all while reducing adhesion. Huang *et al.* demonstrated the flexibility of PCI by successfully electrospinning it with a hydrophilic and hydrophobic drug, separately. Core-

shell fibres were made with the hydrophilic antibiotic, gentamycin sulphate and resveratrol, a hydrophobic antioxidant, both to be used in wound healing [88]. PCI has also been prepared to treat periodontal disease. PCI was blended with metronidazole benzoate, an antibiotic used to reduce the anaerobic bacteria associated with periodontal disease [96].

2.1.4.2 Gelatin

Gelatin is another important biopolymer like PCI, but unlike PCI it has natural origins. As such, it is almost entirely sourced from animal sources, with porcine and bovine being the most common [97]. Skin, bone and other fibrous tissues contain the greatest portions of collagen and therefore gelatin. Gelatin is made from the partial hydrolysis of collagen making it biodegradable and non-immunogenic. It is formed by exposing collagen to a degradative substance, either acidic or alkali, in the presence of heat. This brings about the irreversible breakdown of the fibrous structure [98]. Ironically, gelatin comes from gelatine. Gelatine is the entire material produced from the hydrolysis of collagen, this is made up of gelatin and other inorganic and organic impurities [98]. As it is partially hydrolysed, it is soluble in water and must be cross linked if it will be used *in vivo* to counteract the high water content of the physiological environment and improve thermo-mechanical properties [99]. Also like PCI, gelatin has been electrospun extensively, combined with other polymers and encapsulating various additives. Gelatin is a popular choice in biomaterials, especially as cellular scaffolds, because the extracellular matrix is mostly made up of proteins [100]. Gelatin was electrospun with cellulose acetate to exploit the non-adherent property of cellulose acetate and for the similarity between extracellular matrix and electrospun gelatin to treat wounds [101].

Gelatin was also blended with silk from the cocoons of *Bombyx mori* silkworms, to produce all-natural beaded fibres for controlled release applications [102]. Enayati *et al.* used gelatin to coat estradiol loaded PLGA particles in order to regulate the drug release and reduce the initial burst [103].

2.2 Solvent Selection

2.2.1 Introduction

The solvent used is another factor that needs to be taken into consideration. Table 1. lists solvents used in the literature with CA and EC. Many of those listed are considered unsafe (details in chap. 4; pages 38 and 48).

Solvents serve a very important purpose in electrospinning, especially in the case of polymers, which cannot be melted, like cellulose. Dissolving the polymer in a solvent produces solutions that allow the polymers to be electrospun. Solvents can alter characteristics of the solution making it easier or potentially more difficult to electrospin. Lu *et al.* [104] described how changing the solvent changed the interactions present in the solution. Ethylene/vinyl alcohol (EVOH) (polymer) mixed with isopropyl alcohol and water formed hydrogen bonds increasing the polymers relaxation time and in turn increasing the diameter of the fibres produced. Whereas EVOH mixed with DMAc did not result in hydrogen bond formation, thereby reducing the relaxation time leading to smaller fibre diameters [104]. When selecting solvents for this work only two points were considered; solubility of the polymer and toxicity.

2.2.2 Biocompatible and Green Solvents

A safe and green solvent does not induce an inflammatory response from a person and also has a minimal effect on the environment (i.e. aquatic life) when disposed of. Preferably its source is renewable with a near zero carbon footprint. Companies such as GSK [105], Sanofi [106] and others have published papers listing the safety of many solvents. They not only list toxicity to humans but also any environmental implications when disposing of the materials, safety in handling along with any regulatory considerations. As much as possible to only the two points previously mentioned were considered.

Despite some sources stating that up to 99% of solvent evaporates during the EHD process and does not remain in the fibre, this cannot be guaranteed and it is not currently included in the scope of this work to measure it. Therefore, it is imperative to use safe solvents, so in the case that there is solvent residue it will not cause harm to the patient. This aspect has not been paid much attention in the literature, especially in older papers, where safety practices have been informed and heightened over time. Haas et al. used benzene when casting ethyl cellulose in the 1950's [107]. But since the 1980's, benzene has been ruled a carcinogen [108], ruling out its use in the production of biomaterials.

Table 1: Solvents used with ethyl cellulose, cellulose acetate and CMC.

	Cellulose acetate	Ethyl cellulose	CMC
Single solvent	Acetone [54, 109] Chloroform [109] N,N-dimethylacetamide (DMAc) [109] N,N-dimethylformamide (DMF) [109] Dichloromethane (DCM) [109] Methanol (MeOH) [109] Formic acid [109] Pyridine [109] Acetic acid [110]	2,2,2-Trifluoroethanol (THF) [111, 112] Dichloromethane [113] Benzene [107] Chlorobenzene [107] 2-nitropropane [107]	Water [62]
Binary solvent system	Acetone/DMAc at 2:1 [114] Acetone [51] Acetone/DMAc at 1:1, 2:1, 3:1 [109, 115] Chloroform/MeOH(v/v) at 1:1, 3:2, 7:3, 4:1 and 9:1 [109] DCM/MeOH (v/v) at 1:1, 3:2, 7:3, 4:1, and 9:1 [109] Acetone/DMAc (v/v) at 2:1 [109] Acetic acid/DMAc at 1:2 and 1:3 [110] Acetone/water at 100:0-80:20 [14, 54]	THF/DMAc at 0:100-100:0 [44, 45] DMF/acetone at 5/0-0/5 [116] Ethanol/water at 80:20 [16] Benzene/carbon tetrachloride [107]	Water/methanol [117]
Ternary solvent system	Acetone/dimethylformamide/trifluoroethylene v/v/v at 3:1:1 [118]		

2.3 Other Spinning methods

2.3.1 Wet spinning

This is commonly used with polymers that must be processed in solution but the solvent must be removed via chemical means. The spinneret is immersed in a coagulation bath containing a coagulant, a non solvent of the polymer but is miscible with the polymer solvent [119]. Through mass transfer the non solvent replaces the polymer solvent in the precipitated fibre which will then evaporate as the fibres are drawn [120]. This step makes wet spinning slower than both melt and dry spinning. This process was developed in the 1900's and first used to produce the textile Rayon (from generated cellulose). There are also environmental considerations if the solvents used are hazardous along with the uncertainty involved over complete removal of the solvents [121].

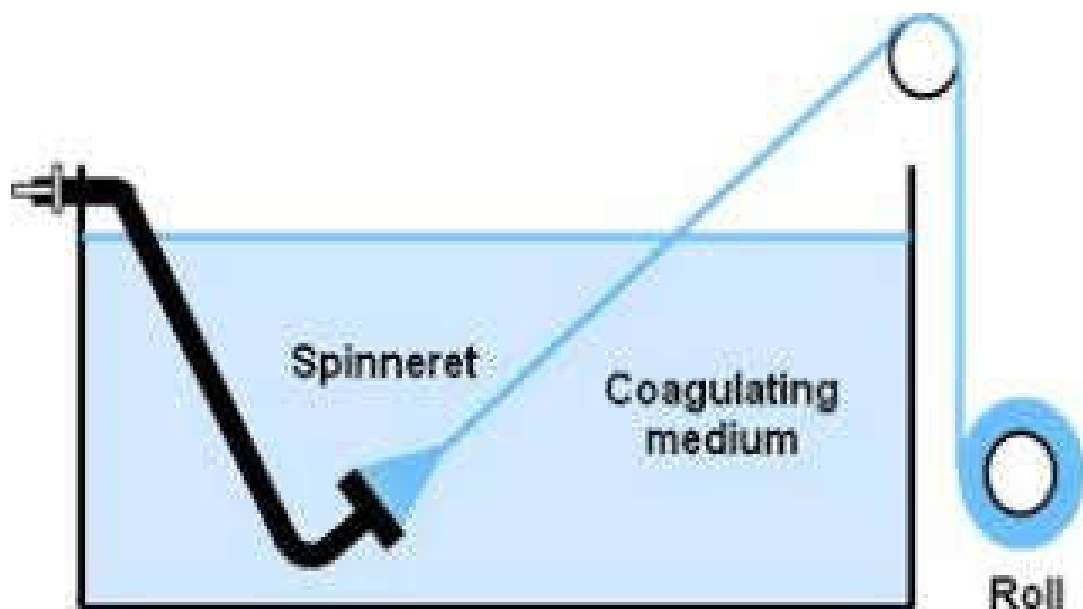


Figure 9: Image demonstrating wet spinning

2.3.2 Dry-jet wet spinning

The polymer solution is processed as in wet spinning except the spinneret is not submerged in liquid. Instead it is placed at a small distance (~1 cm) above the coagulation bath [122]. The polymer dries in air slightly before entering the bath [121]. The temperature of the coagulation bath can have an effect; where higher temperatures favour the diffusion of the solvent and rapid solidification weakening the filament. Lower temperatures prevent polymer relaxation and increases the strength of the filament [123].

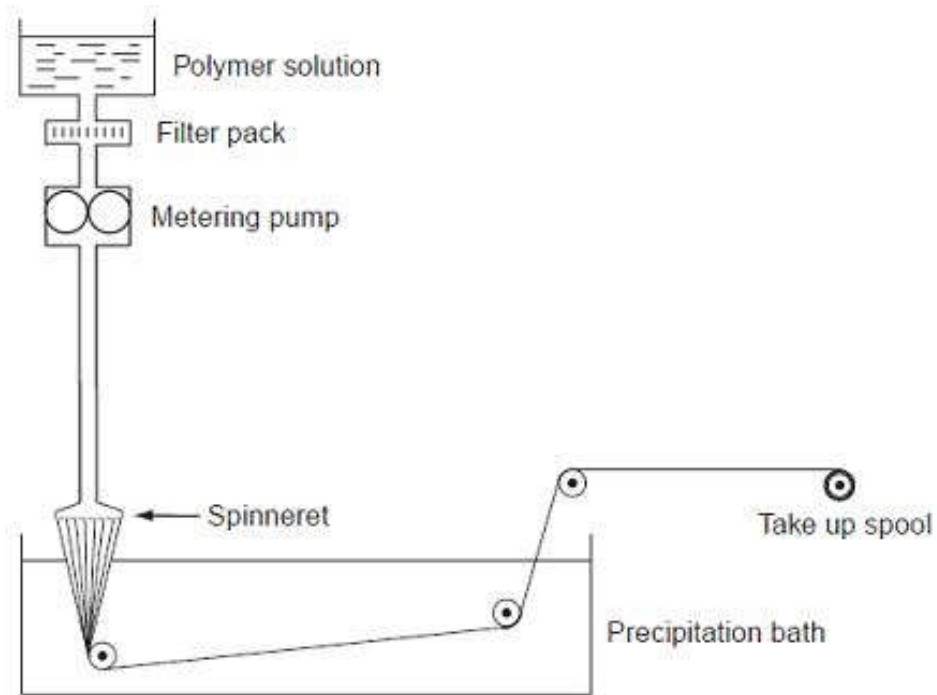


Figure 10: Image showing dry-jet wet spinning

2.3.3 Dry spinning

The polymer solution in this process is dried solely by the blowing of air or some inert gas to encourage the evaporation of the solvent from the fibre, making it one of the simplest methods. Following the drying stage the fibres are drawn to increase the axial orientation and consequently the strength [124] [121]. Dry spinning was used by Chaochai et al. to produce gelatin fibres from a solution with water. These fibres were intended for biomedical use, the use of a safe solvent was important, they were consequently cross linked to prevent them redissolving in water [125].

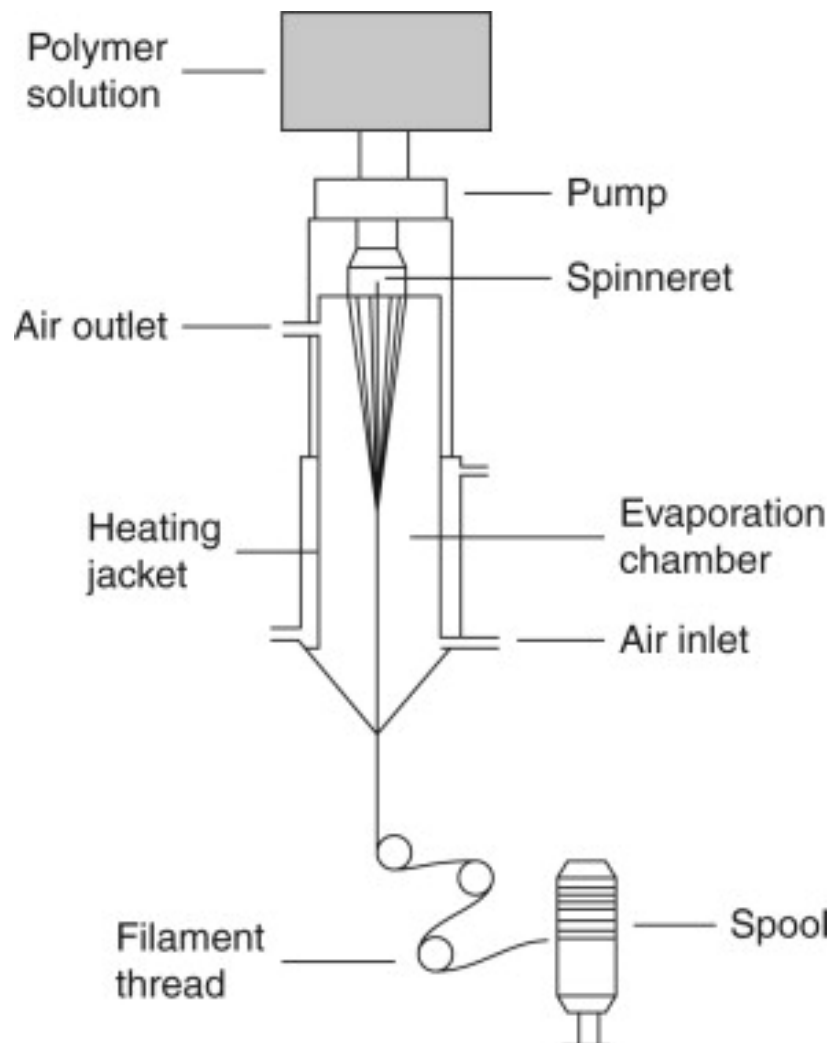


Figure 11: Schematic of dry spinning process

2.3.4 Melt spinning

Thermoplastic polymers which do not need to be solvated in order to be spun can be processed with this method. Here the polymer is heated, usually with a heated extruder. The melt is passed through the spinneret where it is then quenched. This relies on heat transfer, making it the fastest spinning process as it is much speedier than mass transfer used in wet spinning. [121] [126].

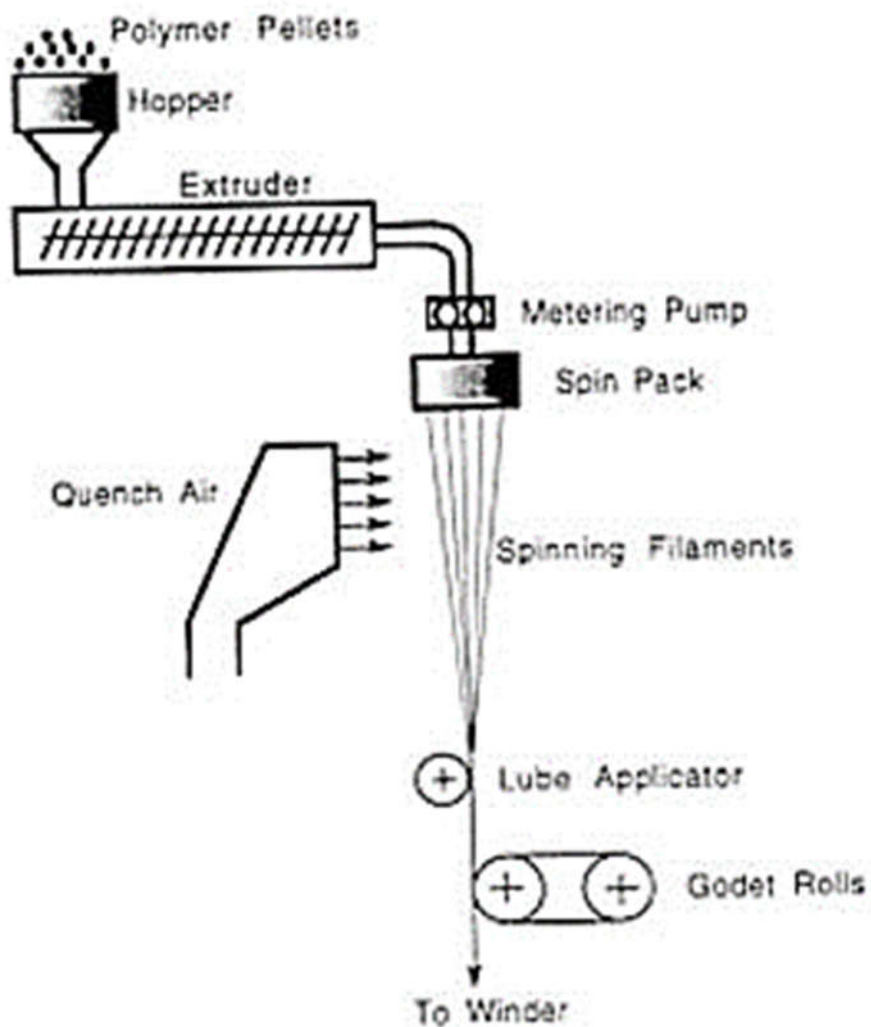


Figure 12: Diagram of melt spinning method

2.3.5 Flash spinning

A polymer solution is formed by dissolving a polymer in a solvent at high pressure. This solvent would ordinarily be a non solvent at atmospheric conditions [121]. The solution is then extruded into an area of lower pressure and temperature, causing the solvent to evaporate. This is usually used for crystalline polyhydrocarbons like polyethylene [127].

2.3.6 Gel spinning

Polymer gels are highly saturated solutions like ultra-high molecular weight poly(ethylene) (UHMWPE), where the high concentrations are needed as the chain lengths do not possess sufficient properties needed for engineering materials [128]. Using such a high molecular weight magnifies the effect of the van der Waals forces throughout the polymer. The high molecular weight also allows the molecules to be drawn thereby increasing tensile strength [121]. In this method the polymer solution is passed through an extruder. It is air dried as it passes through an air gap then quenched, UHMWPE is quenched in

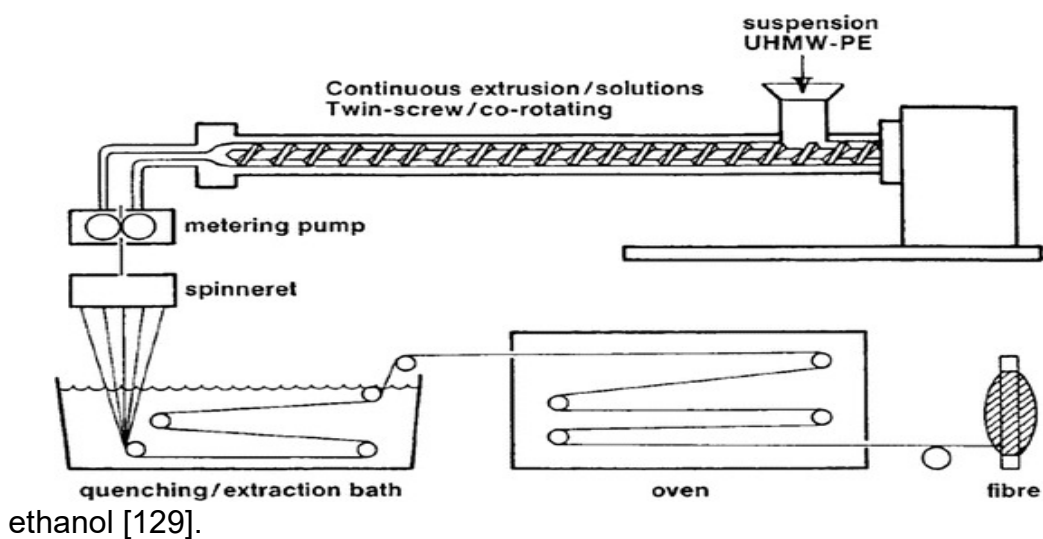


Figure 13: Diagram showing gel spinning of UHMWPE

2.3.7 Centrifugal spinning

A polymer solution is added to a metal container with orifices in the sides. This “pot” can be rotated at large speeds (200-13,000 rpm). Centrifugal forces exerted onto the solution cause it to eject out of the orifices. Once ejected it undergoes stretching and solidification as the solvent evaporates [130]. This method has been used to produce nerve guides by Amalorpavamary et al. PCL/PVP blends were made and spun using a device built in-house [131]. A variation of this, known as pressurised gyration, uses pressurised gas as well as gyration to overcome the surface tension to produce a range of structures including fibres [132].

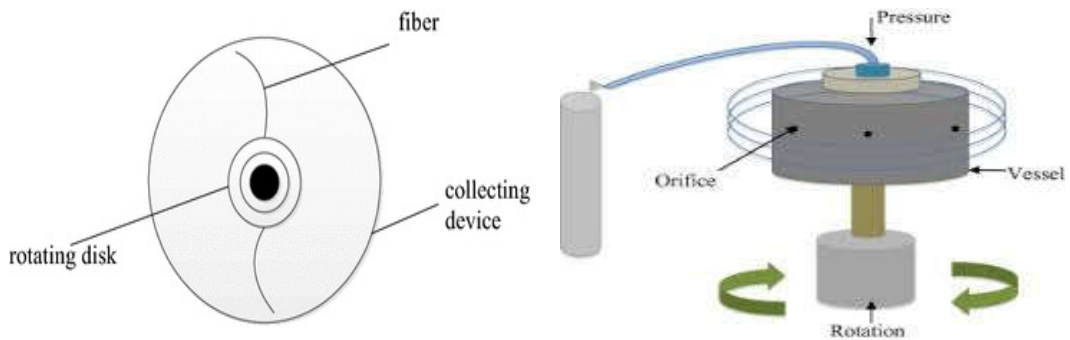


Figure 14: Image of centrifugal spinning (left) and pressurised gyration (right)

2.3.8 *Emulsion spinning*

This method is used for polymers that cannot be solvated or melted. Or, it can also be used to produce bi-component fibres. In the case of an insoluble material; it is mixed with another polymer which is soluble and will act as a spinning agent [121]. The spinning agent will then be removed post spinning either with a solvent or through heating. The spinning agent must not affect the properties of the “desired” material. In the case of bicomponent fibres the two polymers used will remain in the final fibre and the properties of both will be exploited [133]. The most popular use of this method is the production of polytetrafluoroethylene (PTFE), commonly known as Teflon™ produced by Chemours, a non stick coating used most famously on cooking utensils. A solution of 40% PTFE and 2.3% cellulose is spun into a bath of sulphuric acid, sodium sulphate and zinc sulphate. After drying the cellulose is removed via heating at 389 °C. The PTFE is then sintered to produce high strength fibres [134].

2.4 EHD Processing

Electrospinning is a top-down approach that is low cost [19, 135] compared to most bottom up techniques [121, 136]. The table below compares electrospinning to other spinning techniques.

Table 2: Various spinning methods [121].

Process	Micro/nano fibre	Feedstock	Solidification
Electrospinning	$\mu\text{m}/\text{nm}$	Melt, solution and emulsion	Cooling or evaporation or coagulation
Gel (dry-wet) spinning	μm	Solution (high solid content)	
Dry spinning	$\mu\text{m}/\text{nm}$	Solution	Heating or evaporation
Wet spinning	$\mu\text{m}/\text{nm}$	Solution	Coagulation
Emulsion spinning	No	Emulsion	Phase separation
Melt spinning	No	Melt	Cooling
Melt blowing	$\mu\text{m}/\text{nm}$	Melt	
Conjugate spinning	$\mu\text{m}/\text{nm}$	Melt	
Film splitting	μm	Melt	
Centrifugal spinning	$\mu\text{m}/\text{nm}$	Melt and solution	

Electrospinning is a top-down approach that is low cost [19, 135] compared to most bottom up techniques [121, 136]. The Table 2. compares electrospinning to other spinning techniques.

Electrospinning accepts the widest range of feedstock whilst being able to produce structures in the nanometre range. Cooling, evaporation or coagulation solidification regimes do not include heating which reduces energy consumption.

2.4.1 Brief history and Introduction

Historically, the interaction between a fluid and electrostatic charge was first observed in the 1600's when William Gilbert, who demonstrated the deformation of a water droplet in the presence of a charged piece of amber [137]. The first electrospinning patent applied for was by John Francis Cooley [138] in 1900. John Zeleny [139], began the process of mathematically modelling the behaviour of fluids under the influence of electrostatic forces, by observing the effect of an electromotive force on a droplet on the end of a capillary, and imaging the "jet" produced [140].

Anton Formhals also put forward 22 patents throughout the 1900's. Rozenblum and Petryanov-Sokolov of the USSR developed an electropsun cellulose acetate mat used as smoke filters in gas masks in 1938 [141]. The most notable contributor to the understanding of the process was Sir Geoffrey I. Taylor, who lent his name to the "Taylor" cone. He worked through 1964-69

laying the groundwork to mathematically describe the shape formed by fluids in the presence of an electric field [142]. In the past two decades, many university laboratories have retaken the interest in the EHD process.

The EHD process covers two production methods; electrospinning and electrospraying. The former is used to produce fibres and the latter, particles. The process involves pumping a solution (or melt) through a capillary, typically metal. A high voltage dc power supply connected to the capillary provides the electrostatic charge [143]. When a liquid droplet at the end of a metal capillary is subjected to an electric potential, the droplet lengthens and from the tip either droplets or fibres are ejected [144]. The difference between electrospraying and electrospinning are the solution parameters; primarily the polymer concentration. When this passes the polymer specific threshold, the polymer chains entangle preventing the jet to break up which occurs during electrospraying. The viscoelasticity of a high concentration solution is able to overcome instabilities that dominate electrospraying thereby producing fibres [145, 146]. These fibres are attracted to a grounded collector, where they are collected and observed. EHD processing uses an electric field to distort a polymeric droplet by charging the polymer chains inducing repulsion between them. This repulsive force overcomes the surface tension allowing a jet to be ejected. Depending on the solution properties either electrospinning or electrospraying will occur; producing fibres or particles respectively [147, 148].

2.4.2 Electrospinning

As the polymeric fluid, solution or melt, passes through a charged capillary, charges accumulate on the droplet surface as it emerges from the capillary end [149]. In the presence of the electric field formed between the capillary and the grounded collector, the charged polymer chains begin to repel one another, these repulsive forces between the polymer chains overcome the surface tension of the droplet and a jet is emitted from the deformed droplets tip, known as a Taylor cone [150]. As the jet traverses towards the collector both internal charges and the external electric field induce a whipping motion which works to stretch the polymer chains, reducing the fibre diameter [149], it is also at this point solvent evaporation occurs, again reducing the fibre size.

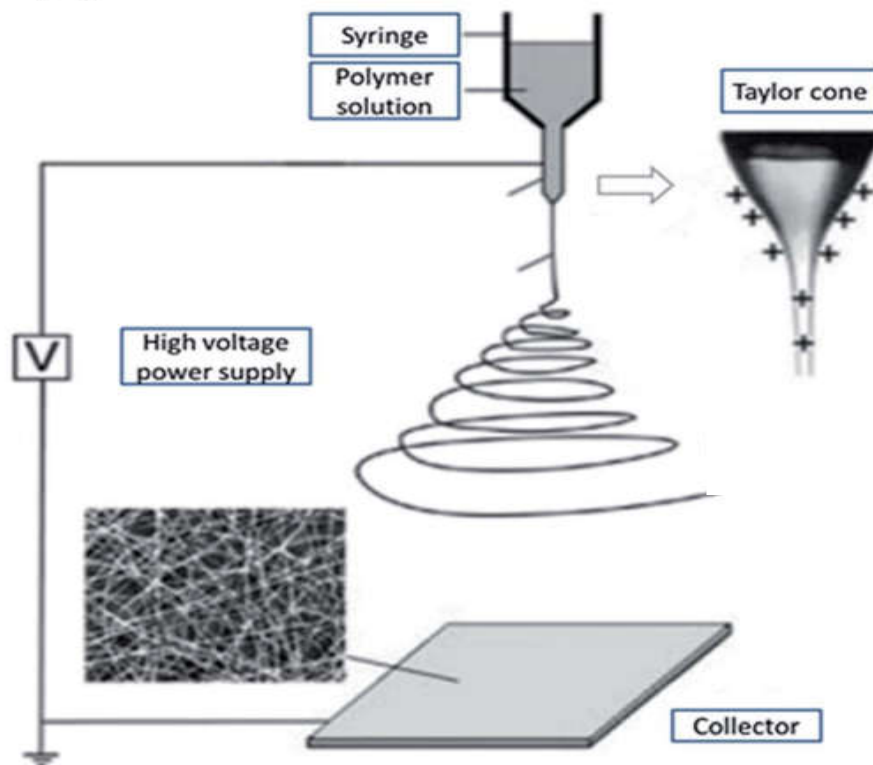


Figure 15: Schematic image of electrospinning set up with a magnified Taylor cone [151].

2.4.3 Solution parameters affecting electrospinning

The application of the electric field on the polymeric solution has the following effects:-

The electric field interacts with the ions present in the solution. There is an equal number of positive and negative ions in the solution, when the field is applied the ions move in the direction of the oppositely charge electrode. The difference in the amount of positive and negative ions in a given volume while the electric field is applied is known as the electric field.

Adding ionic salts will increase the amount of ions in the system but not the excess charge. This increase in conductivity can reduce the time it takes to establish the excess charge once the field is applied.

When the field is applied to the droplet at the capillary end the ions migrate to the droplet surface inducing a charge on the droplet surface. The instability takes effect when the potential difference is high enough for the electrical forces to overcome the surface tension; after which the jet emerges which acts to carry away the excess charge. Increasing the potential difference increases the charge on the jet.

Solutions with low conductivity solutions may need more time for sufficient charge accumulation at the droplet surface to initiate the jet. The external electric field, charge in space and air drag all cause the jet to traverse towards the collector [152]. The larger, thinner segments of the jet (closest to the

collector) are slower moving due to the air drag and disturbances to the electric field due to the presence of the charged jet and charged nanofibres collected nearby. Coiled and looped fibres can be collected; their curvature reflective of the pattern the jet takes, it is also dependent on the distance from the envelope apex at which the sample is collected. Also, Reneker hypothesises the jet (fibres) dries before hitting the collector and is therefore a direct indicator of the jets formation in space [153].

2.4.3.1 Concentration

Polymer concentration is the solution parameter that influences the EHD process greatest. In electrospinning the concentration must be high enough such that the molecular chains are able to entangle and prevent the jet to break up [150]. There is a critical value of entanglement C_e that must be met in order for electrospinning to occur. Solutions with entanglements below this value lead to jet break up and give rise to electrospaying, and the production of particles [154]. The gradual increase in the concentration of a polymer solution leads to the following transition; particles to bead-on-strings to smooth fibres to thick ribbon like fibres. An increase concentration with an increase in surface tension, reduces the likelihood of the jet breaking up to form droplets as [149]. A high concentration can block the needle tip and cause beaded fibres, as the flow is disrupted [150].

2.4.3.2 *Molecular weight*

The effect of molecular weight is analogous with solution concentration. Longer or more branched polymer chains will lead to greater chain entanglements, which will encourage electrospinning and fibre production. The greater molecular weight will help overcome the surface tension producing progressively smoother, more uniform fibres [149].

2.4.3.3 *Viscosity*

As the solution viscosity increases the bead size increases as does the distance between the beads on the fibres. An increase of viscosity also changes the shape of the beads from spherical to elliptical to spindle like until it smoothen out completely. This was shown by Lee et al, when electrospinning polystyrene [155]. Increasing the viscosity while lowering the surface tension which leads to smooth uniform fibres [156].

2.4.3.4 *Electrical Conductivity*

Solution conductivity is primarily controlled by the solvent used in the solution. The relationship between diameters of the fibres and conductivity is straight forward. Increasing the conductivity allows the solution to carry more charge, in the presence of an electric field this will lead to greater stresses being applied to the jet reducing the fibre size [143, 144].

2.4.3.5 *Surface Tension*

The effect of surface tension changes slightly with the viscosity of the solution used. Lower viscosity solutions are more susceptible to the effect of surface tensions which will promote electro spraying over electro spinning, as the jet will break up into droplets. At higher viscosities, surface tension plays a lesser role which allows for fibre formation [157]. Surface tension arises from the cohesive forces between the solution components and acts to maintain the droplet shape at the end of the capillary until the applied voltage provides enough columbic force to overcome the surface tension.

2.4.4 Processing parameters affecting electro spinning

2.4.4.1 *Voltage*

Once the threshold voltage has been reached, the electric field charges the molecular chains in the solution. The repulsive force overcomes the surface tension of the droplet distorting the shape to form the Taylor cone [150]. The effect of this parameter is polymer specific; research has shown both negative [158] and positive [159] correlations between the increase in fibre diameter and voltage.

2.4.4.2 *Flow rate*

The relationship between flow rate and fibre diameter is a straightforward one. Increasing the flow rate means a higher volume of solution flowing through the

EHD needle per unit time; this leads to an increase in fibre diameter. Flow rate must be a balance between the solution being replaced at the needle tip and minimum flow to ensure solvent evaporation to avoid beading [160].

2.4.4.3 *Collector Distance*

The distance between the collector and needle is what controls the flight time of the fibres produced by electrospinning. As the jet undergoes the whipping instability, solvent evaporates from the solution. The longer this phenomena is allowed to occur meaning the greater the distance between the tip and the collector, the smaller the diameters of the fibres collected will be [150].

2.5 Wound Healing Patches

A wound healing patch must have the following characteristics [34, 161]:-

- Provide a moist environment
- Removes excess wound exudate
- Allow gaseous exchange
- Large surface area
- Protect against pathogen infiltration
- Prevent necrosis
- Be biocompatible

The wound healing patch must also be able to mimic the role of skin as closely as possible in its capacity of keeping out microbes and preventing infection

[34], and also potentially to accelerate the wound healing process by maintaining the ideal conditions needed to allow the body to repair itself without interruption.

If a bandage is unable to control exudate it can cause tissue maceration. Managing the fluid level in a wound site can contribute to healing by reducing maceration [162].

2.5.1 Electrospun Wound Healing Patches

Electrospinning produces non-woven patches which are used widely in the healthcare and medical textiles. Non-woven fabrics are superior to typical knitted or woven textiles as they strongly resemble the extracellular, and costs are reduced due to shorter production times [162].

Due to the porous, non-woven nature of the electrospun fibres; they have the capacity to be excellent functional wound dressing materials. The porosity allows for the exudate to be absorbed and oxygen to permeate through whilst keeping out pathogens [163]. Electrospinning can produce nanosized fibres which maximises the surface to area ratio, enhances mechanical flexibility which leads to maximum conformability to the wound surface [51]. The large surface to volume ratio can be exploited to help in delivering drugs/active agents [164]. It is at this stage that these biomaterials become bioactive, and is able to interact with the physiological environment. The EHD process is an easy process that has the ability to be specialised for a number of industries [165].

Current dressings include cotton wool, natural cellulose gauze and bandages, these are involved in wound healing. Gauze or bandage do not absorb exudate very well, which means infection control is limited [31]. Most of those materials act as inert covers, not engaging in the in the healing process and only act as a physical cover/protection [166].

Electrospun collagen has been used to produce skin substitute scaffolds with superior properties compared to the more commonly used freeze dried scaffold; in homogeneity and similarity to natural extra cellular matrix, it was also found to elicit less wound contraction in wound healing than the freeze dried product [167].

Cellulose is classed as a bioactive material which is actively involved in the healing process. Most commonly carboxymethyl cellulose is use as a hydrocolloid which can readily absorb exudates [166].

The multi-symptomatic nature of diabetic wounds should to be addressed by its wound healing material. The excessive exudates produced should be absorbed, but the wound should not be left dry, as this is equally damaging to the healing process. Delivering active pharmaceutical agents to the wound site has been shown to help overcome arrested healing. A material capable of tackling multiple problems is necessary in such cases.

2.6 Drug release from electrospun fibres

Controlled drug delivery systems surpass conventional methods such as oral and parenteral by:-

- Control over the duration and type (i.e. quick-short term or sustained long-term) of delivery [168]
- Targeted delivery to specific structures or areas [169]
- Reduction of systemic drug delivered to the body, thereby reducing the likelihood of side effects [170]

In addition to these, conventional methods require a number of repeated doses in order to maintain a therapeutically relevant level of drug [171]. However, a biocompatible material doped with an active pharmaceutical ingredient (API) can have its properties tailored to deliver the API at the suitable site, level and duration, potentially with one application only [168]. These biomaterial based controlled drug delivery systems can be degradable or inert. Ideally, if a controlled drug delivery system is to be implanted into the body it should be biodegradable, and the products released as part of the degradation should be as non toxic as the parent material. This will remove the need for invasive procedures to remove the structures [168].

In terms of drug delivery systems produced using EHD, there is a vast array. Particles to non woven patches have been designed into drug delivery systems for many applications. Parhizkar *et al.* produced cisplatin encapsulated PLGA particles for the treatment of head and neck cancers The core shell particles containing the cisplatin were taken up by a greater degree

($EC_{50} = 6.2 \mu\text{m}$) compared to free drug ($EC_{50} = 9 \mu\text{m}$) [172]. Enayati *et al.* also investigated PLGA particles specifically, investigating parameters affecting the release profile of estradiol (a female hormone) by making changes to the particle size, coating material and thickness [103]. With even more sensitive materials like genetically engineered peptides, thermally responsive particles were electrosprayed to release doxorubicin (an anti cancer drug) [173].

Wound healing and cellular scaffolds are one of the most common uses for electrospun fibres. As previously mentioned, the similarity between electrospun fibres and the extra cellular matrix makes it an ideal match. The porosity allows for gaseous exchange to be maintained but the inter fibre porosity can stop the infiltration of bacteria into the wound site [174]. Fibres have been used to deliver growth factors, anti biotics and even supplements [88, 94, 95, 175, 176]. For wound healing dressings patches, certain substances can be added to enhance or aid the healing process. Sofokleous *et al.* loaded PLGA fibres with amoxicillin (an antibiotic) and charted the release behaviour through different media. When tested *in vitro* the fibres released the greatest amount of drug in simulated body fluid (81%) compared to phosphate buffered saline (22%) and distilled water (68%) [177]. Silver, a well known antimicrobial agent, was electrospun in its nitrate form (AgNO_3) with polyvinyl alcohol. Applying heat or UV radiation released the silver ions and work to kill bacteria [178].

2.7 Diabetic medication expand

Diabetes is the metabolic disease most associated with wound healing impairment [179]. As of November 2017, it is estimated 4.6 million people (3.7 million diagnosed and ~1 million undiagnosed) in the UK suffer from diabetes. Despite this, there has not been a large amount of research into the effect of anti-diabetic medications on wound healing. Non healing diabetic wounds maintain an elevated level of pro inflammatory cytokines, which disrupts the healing process [180]. Inflammation is a normal part of the healing process, but a hyperglycemic environment prevents progression of healing.

3 Chapter 3

Experimental Details

3.1 Introduction

This chapter describes the materials, procedures, methods and equipment used whilst producing the work described in this Thesis. This body of work was committed to incorporating cellulose materials of plant and bacterial origin into all the products produced. The cellulose derivatives were selected at the beginning of the PhD and what will be discussed are the polymers that have been used. All of these materials are already used in the biomedical field in one capacity or another, their suitability for medical applications has already been shown in literature. All materials were purchased from purchased from Sigma Aldrich (Poole, UK) unless otherwise stated.

3.2 Materials

The material selection is essentially in two sections. The first chapter of results involves plant derived cellulose polymers; ethyl cellulose (EC), cellulose acetate (CA) and carboxymethyl cellulose (CMC) blended with poly ethylene oxide (PEO). These were used with ethanol, acetone and water solvents, respectively.

The latter chapters used bacterial cellulose (BC) blended with polycaprolactone (PCL) dissolved in dimethylformamide (DMF) with tetrahydrofuran (THF) and bacterial cellulose blended with gelatin (Gel) with acetic acid (AA) with water, respectively. Some of the fibres were loaded with diabetic drugs glybenclamide (Gb) and metformin (Met) and their performance tested *in vitro*, using phosphate buffered saline (PBS).

3.2.1 Ethyl Cellulose

Ethyl cellulose (EC) is an off-white powder. The molecular weight used was $2.28 \times 10^4 \text{ g mol}^{-1}$ with 48% of the molecule labelled with ethoxy groups was used.

3.2.2 Cellulose Acetate

Cellulose acetate (CA) had a molecular number of $3 \times 10^4 \text{ g mol}^{-1}$ with 39.8wt% labelling of acetyl groups across the polymer chain.

3.2.3 Carboxymethyl Cellulose

Two types of sodium carboxymethyl cellulose (CMC) were used. CMC of molecular weight 2.5×10^5 and $7 \times 10^5 \text{ g mol}^{-1}$ were used, both with 0.9 carboxymethyl groups per cellulose monomer.

3.2.4 Polyethylene oxide

Polyethylene oxide (PEO) with a molecular weight of $2 \times 10^5 \text{ g mol}^{-1}$ was used in combination with CMC to act as a spinning agent.

3.2.5 Bacterial Cellulose

BC was provided by the Department of Medical Microbiology, Medipol University (Istanbul, Turkey). It was kept refrigerated in ultra-pure water until used.

3.2.6 Polycaprolactone

Polycaprolactone (PCL) with a molecular weight of $8 \times 10^4 \text{ g mol}^{-1}$ this was blended with bacterial cellulose as a “slow” degrading spinning agent. That is adding PCI facilitates degradation of the fibre.

3.2.7 Gelatin

Gelatin (Gel) derived from bovine skin with a molecular weight in the range of $4 \times 10^4 - 5 \times 10^4 \text{ g mol}^{-1}$ was used. This was used instead of the porcine type as it can be easily cross linked. This was blended with bacterial cellulose as a “fast” degrading spinning agent. The addition of Gel to the fibres speeds up the degradation of Gel-BC fibres compared to PCI-BC fibres.

3.2.8 Glybenclamide

Glybenclamide (Gb) (formula: $C_{23}H_{28}ClN_3O_5S$, molecular weight 494 g mol^{-1}). A common oral treatment for type II diabetes, from a class of drugs known as sulfonylureas. Mirza *et al.* demonstrated the application of Gb in pluronic gel to wounds excised on *db/db* mice accelerated re-epithelialisation and granulation tissue, along with reducing the level of inflammatory cytokines whilst increasing the pro healing cytokines [181]. Previous to this a number of studies showed the effect of the drug on inflammation. Whilst comparing glybenclamide to glimepiride (another sulfonylurea) within a group of diabetic patients (delivered orally), glybenclamide brought about a reduction in the levels of various inflammatory cytokines [182]. Equally, when Gb was tested against metformin, Gb was able to reduce the levels of c-reactive protein, a blood plasma protein whose level rises due to inflammation [183].

Gb has been shown to specifically inhibit the action of the nod like receptor inflammasome (NLRP-3), due to the presence of the sulfonyl and benzamido groups on the Gb molecule, they disrupt the biomolecular cascade that brings about NLRP secretion [184].

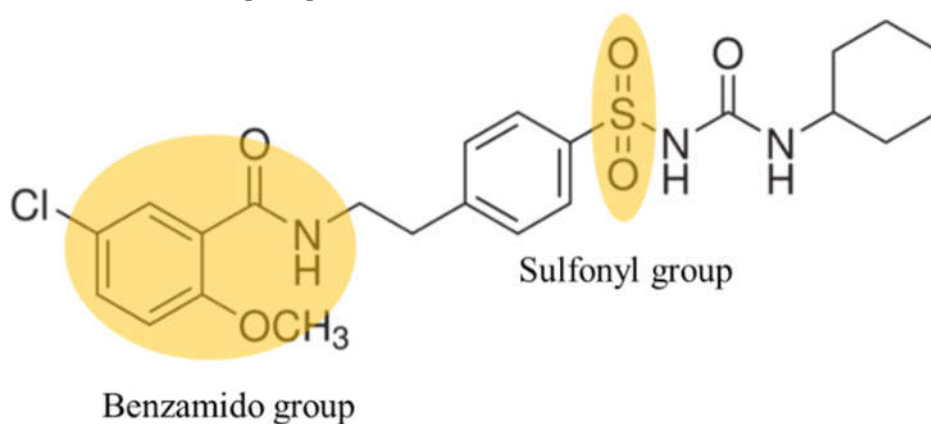


Figure 16: Image highlighting the benzamido and sulfonyl groups on the Gb molecule

3.2.9 Metformin

Metformin (Met) (formula: $C_4H_{11}N_5$, molecular weight: 129 g mol^{-1}). It is typically the first port of call in the treatment of type II diabetes, it belongs to a class of drugs known as biguanides. Metformin's effect on inflammation has not been tested on humans but its effect on murine macrophages has been described in the literature. Nath *et al.* showed the application of Met to RAW267.4 cells attenuated a number of pro inflammatory cytokines [185]. A more relevant example of Met used in wound healing was shown by Lee *et al.* Poly-lactide-glycolide (PLGA) and Met were electrospun and applied to diabetic induced rat wounds, these showed greater healing than wounds treated with virgin PLGA and the control treated with a conventional gauze [186]. Met was used to successfully reduce tumour necrosis factor and tissue factor, pro inflammatory cytokines present in atherosclerosis [187].

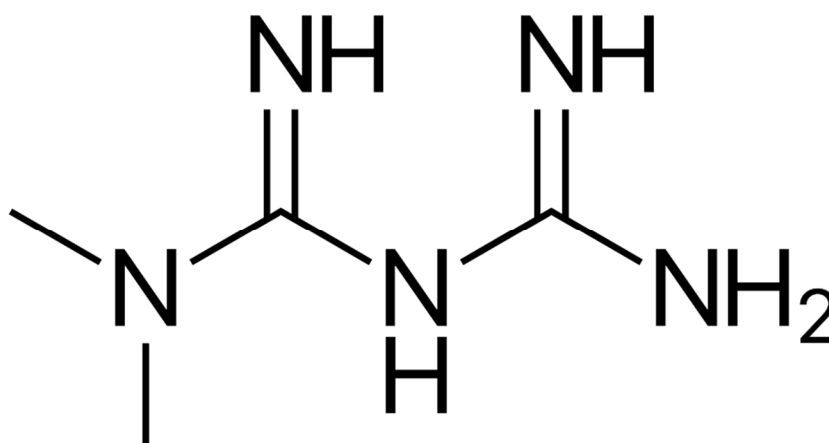


Figure 17: Image of metformin molecule

3.2.10 Solvents

Ethanol

Absolute ethanol (C_2H_6O , viscosity 1.08 cP, surface tension 22.3 mN m⁻¹, and electrical conductivity 1.4E-9 $\mu S m^{-1}$ [188]) was obtained from Fisher Scientific (Loughborough, UK).

Acetone

Acetone is a colourless solvent (C_3H_6O , viscosity 0.33 cP, surface tension 23.3 mN m⁻¹, and electrical conductivity 5E-9 $\mu S m^{-1}$ [188]).

Dimethylformamide

Dimethylformamide is a colourless solvent (C_3H_7NO , viscosity 0.82 cP, surface tension 35 mN m⁻¹, and electrical conductivity 6E-8 $\mu S m^{-1}$ [188]).

Tetrahydrofuran

Tetrahydrofuran is a colourless solvent (C_4H_8O , viscosity 0.55 cP, surface tension 28 mN m⁻¹, and electrical conductivity 4.5E-5 $\mu S m^{-1}$ [188]).

Acetic acid

Acetic acid is a colourless solvent ($C_2H_4O_2$, viscosity 1.13 cP, surface tension 27.4 mN m^{-1} , and electrical conductivity $6E-5 \mu S m^{-1}$ [188]).

3.2.11 Glutaraldehyde

Glutaraldehyde ($C_5H_8O_2$, M_w 100.12 g mol^{-1} , 50% in water) was used as a cross linking agent to cross link the gelatin samples in order to render the fibres insoluble in water reduce the degradation time and drug release. The aldehyde group, highlighted in Fig. 18 of the glutaraldehyde interacts with the lysine amino acids, found in the gelatin molecule resulted in links between the gelatin chains [189].

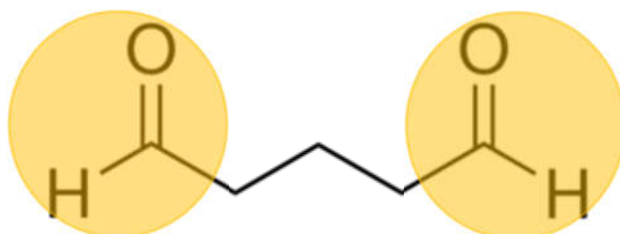


Figure 18: Image highlighting the aldehyde groups on the glutaraldehyde molecule

3.2.12 Phosphate buffered saline

Each tablet in 200 mL of deionized water yields 0.01 M phosphate buffer, 0.0027 M potassium chloride and 0.137 M sodium chloride, pH 7.4, at 25 °C.

3.3 Solution Characterisation

Each solution had viscosity, surface tension, electrical conductivity, and density characterised. Each characteristic was tested a minimum of 5 times.

3.3.1 Viscosity

Viscosity was measured using programmable rheometer (Brookfield DV-III ULTRA, Massachusetts, USA). The viscosity is measured by the resistance exerted on a rotating spindle (number 18) at a specific shear rate. To measure the viscosity 3 mL of solution was poured into the vessel and the spindle lowered into it until it is submerged. The shear rate was set where consistent viscosity readings are taken.

3.3.2 Surface Tension

Surface tension was measured using a tensiometer (Kruss K100SF, Kruss GmbH, Hamburg, Germany) using the Wilhelmy's plate method. The thin plate was lowered and submerged the test solution, by lowering the platform the beaker sits on a reading is taken as the plate leaves the interface of the solution and air.

3.3.3 Electrical Conductivity

The electrical conductivity was measured using a conductivity meter (Jenway 3450, Bibby Scientific Limited, Staffordshire, UK). The probe was submerged into the test solution until a stable reading is obtained.

3.4 Preparation of solutions

3.4.1 Cellulose derivatives solutions

Ethyl cellulose 5-30wt% and 17-25wt% in ethanol and water (80:20). Cellulose acetate 10, 12.5, 15 and 17.5wt% in acetone only. Cellulose acetate 10wt% in 100:0, 95:5, 90:10, 85:15, 80:20 acetone: water respectively. Carboxymethyl cellulose/PEO solutions were made at 25:75, 14:86 and 10:90 with M_w 250,000 and 14:86 with M_w 700,000 g mol⁻¹.

3.4.2 BC-PCL-Glybenclamide solutions

PCL solutions of 5 and 10wt% were produced with DMF:THF (50:50 weight ratio). The solutions were prepared under magnetic stirring for three hours at 50°C. Bacterial cellulose (BC) was made at 10 wt % in DMF only. A mixture was made using homogenisation (Branson Ultrasonic Sonifier SFX550, Fisher Scientific, UK) at 80% power output for 10 minutes. The solution and mixture were mixed (50:50 by weight). The drug, glybenclamide was later added at 10wt% of the PCI-BC mixture.

3.4.3 PB-Gel-Metformin suspension

A gelatin (Gel) solution 18wt% were produced with acetic acid:water (80:20 weight ratio). The solution were prepared under magnetic stirring overnight at room temperature (25 °C). BC was made as previously described. Again, the solution and mixture were mixed (50:50 by weight). The drug, metformin was later added at 10wt% of the Gel-BC mixture. As metformin does not dissolve a stable suspension was formed.

3.5 Experimental setup

3.5.1 Table top set up

Needle set up: For every test the solution was loaded into 10 mL syringes (Becton and Dickinson Company, Oxford, UK) attached with 0.76mm inner diameter capillary tubing (Sterilin, UK) to the steel needle (15 gauge, ID: 2.06mm, OD: 2.67mm, Stainless Tube & Needle Co Ltd, Staffordshire, UK).

Syringe pump: The solution flow rate was controlled by a syringe pump (PHD 4400, Harvard Apparatus, Edenbridge, UK).

High voltage power supply: The needle was attached to a high precision voltage generator (FC 120W, Glassman Europe Limited, Bramley, UK) with capability of 0 – 30kV. The ground electrode was attached to the metal collector.

The solutions were subjected to a range of voltages (0-20kV), the flow rates used were $50\mu\text{L min}^{-1}$ and $100\mu\text{L min}^{-1}$ and distance from collector to tip used were 100mm and 150mm for ethyl cellulose. Cellulose acetate was subjected to the same applied voltage range, 4mL/h and 6mL/h flow rate, all samples were collected at 100mm tip to collector distance. Carboxymethyl cellulose/PEO fibres were collected at 100mm from needle tip. Samples were collected on glass microscope slides. All experiments were carried out at ambient conditions (temperature 21°C and humidity 40-50% respectively).

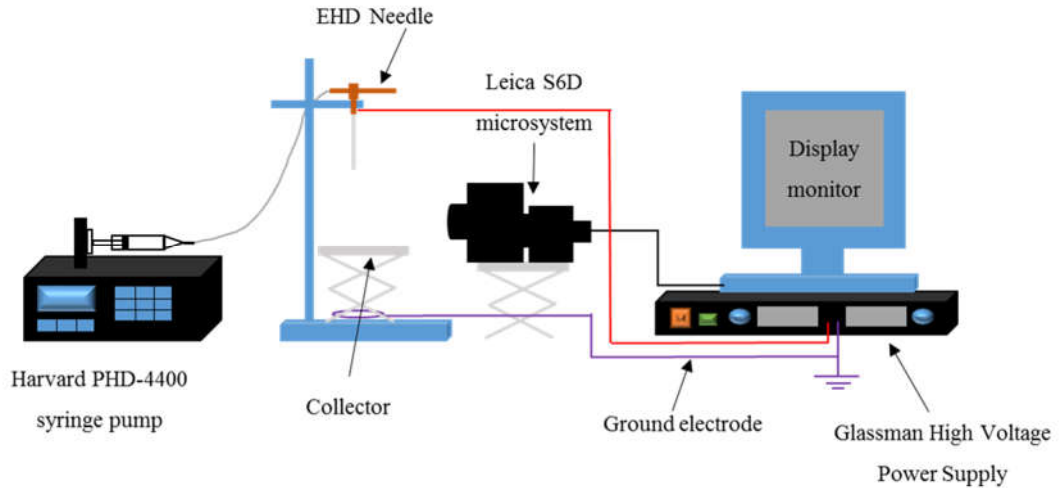


Figure 19: Schematic illustration showing electrospinning set-up

3.5.2 Portable EHD gun

The portable EHD gun, shown in Fig. 20, is functionally identical to the table top set up. The needle is encased in a repurposed gun was assembled with a single needle (ID: 0.69 mm, OD: 1.07 mm, Stainless tube & Needle Co. Ltd, Staffordshire, UK) and connected to 10 mL syringes (Becton and Dickinson Company, Oxford, UK) attached with 0.76mm inner diameter capillary tubing (Sterilin, UK). A strong potential difference was applied between the needle and a grounded collector using a high voltage supply (FC30 P4 12 W, Glassman Europe Limited, Bramley, UK). The working distance between the EHD gun needle exit and the grounded collector was set to 130 mm. The flow rates of the liquid were controlled using an ultra-high precision syringe pump (Infuse/Withdraw PHD 4400 Hpsi programmable syringe pump, Harvard Apparatus Ltd, Edenbridge, UK). When used to collect samples, a collected on stationary collector was used.

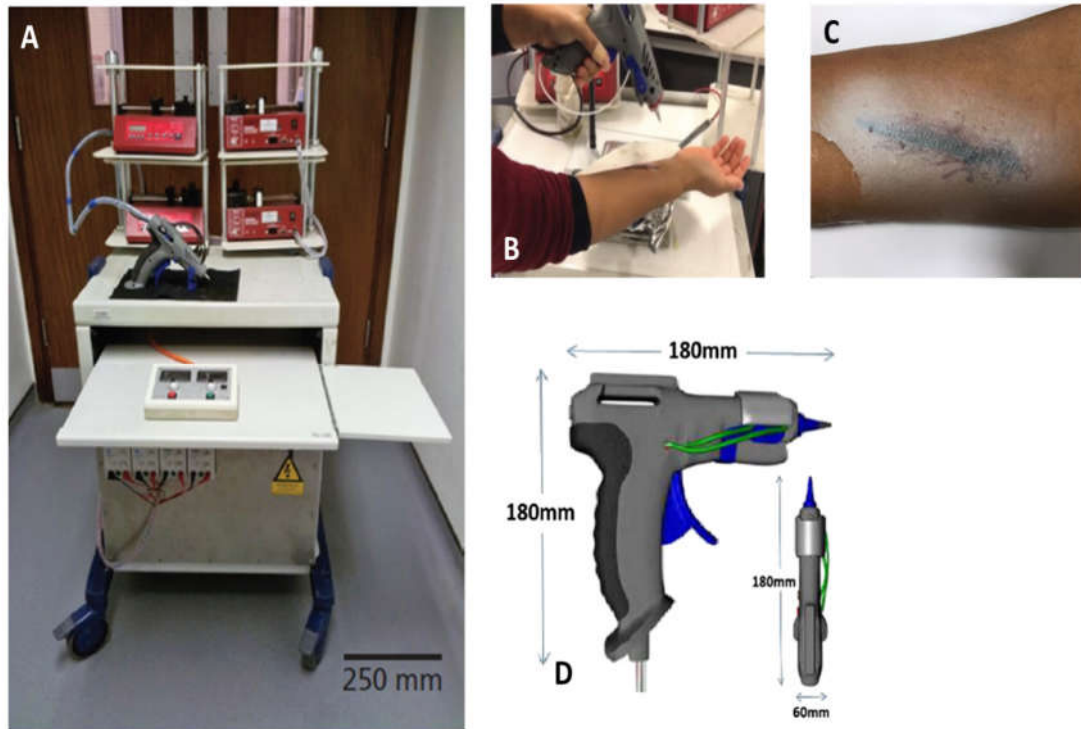


Figure 20: Image of A) portable EHD gun, B) gun in use, C) resulting patch produced in situ and, D) a detailed image of the applicator [190]

3.6 Characterisation of electrospun microstructures

3.6.1 Optical Microscopy

In order to observe the product shape, size and morphology samples were collected on glass microscope slides and were observed using an optical microscope (Zeiss AxioTech) fitted with a Q-imaging Micropublisher 3-3RTV camera.

3.6.1 Scanning electron microscopy

Scanning Electron Microscopy (Hitachi S-3400n) was used to observe the samples and determine the size distributions. The samples were mounted onto

metal stubs and were coated with gold for 90 seconds with Quorum Q150R pumped sputter coater (Quorum Technologies, UK) before observation.

3.6.2 Measurement of microstructures

All image analysis was carried out using ImageJ (public domain open source image processing software available online) to measure diameters of the microstructures produced. The error bars shown indicate the standard deviation of the measurements.

3.7 *In vitro* Testing

3.7.1 Release

A Branson Ultrasonics CPX Series Ultrasonic Cleaning Bath water bath was used to conduct the release tests. Each sample was suspended in PBS at the ratio of 1 mg of fibrous material to 3 ml of PBS. The sample and PBS were incubated at 35-36 °C in the water bath for the duration of the test, with a minimum of three test pieces per sample. Each test lasted 15 days with 1 ml of eluent collected every 24 hours and replaced with 1ml of fresh PBS.

3.7.2 UV Spectroscopy

An UV spectrophotometer, Jenway 7305 UV/Visible spectrophotometer, was used to determine the release profiles of metformin and glybenclamide. A calibration curve was constructed for both using standard solutions of known

concentrations of each drug. The amount of drug present in the fibrous patches made was determined as follows. Standards were made with known concentrations of drug dissolved in PBS and the absorbance measured

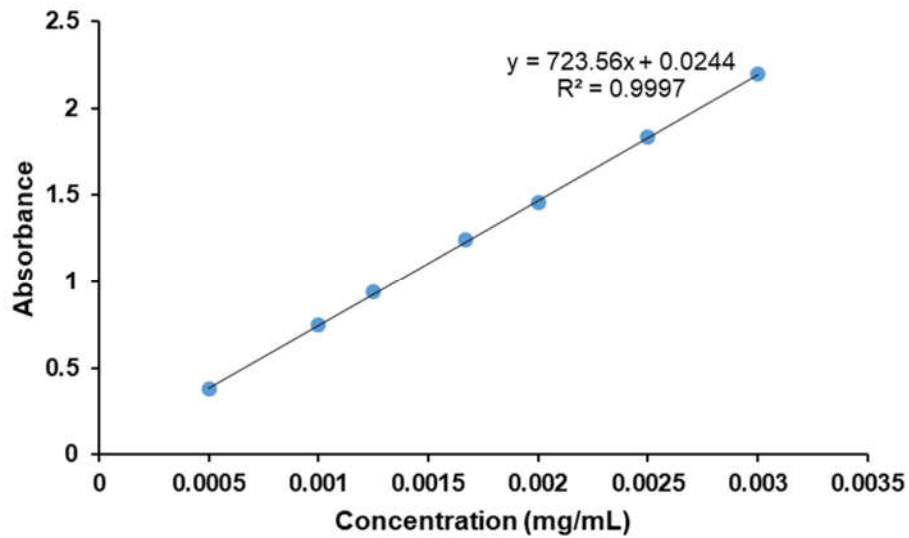


Figure 21: UV calibration curve of glybenclamide

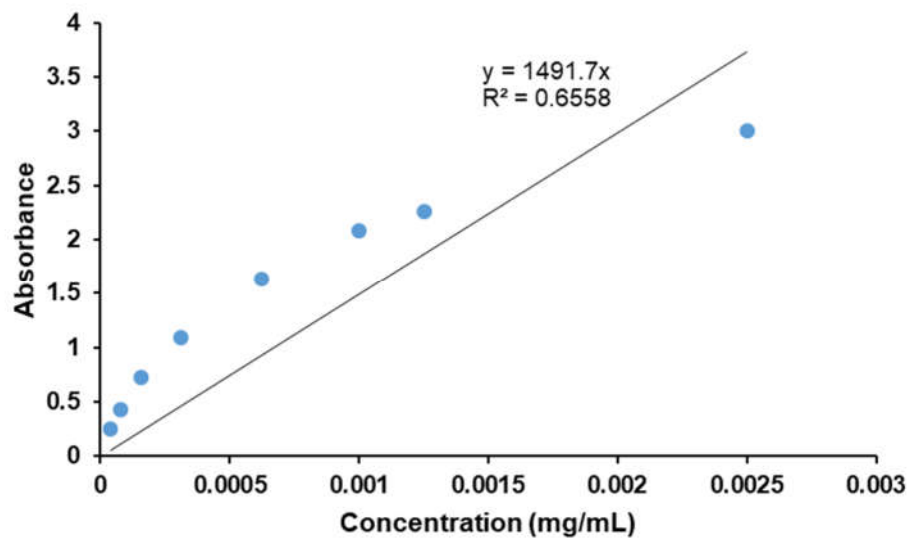


Figure 22: UV calibration curve of metformin

3.7.3 Swelling

To identify the absorption capacity of BC, plain polymer and polymer-BC blends their swelling ratios were measured. The electrospun fibres were immersed in PBS and incubated at 35-36 °C. They were removed at 1, 2, 3, 4 and 24 hours and weighed after the surface water was removed using filter paper. Their swelling capacity was calculated by:

$$\text{Swelling\%} = ((W - W_0)/W_0)100$$

where W_0 and W are the weights of the samples before and after immersion in water for various times, respectively [191].

4 Chapter 4

Results and Discussion

Ethyl cellulose, cellulose acetate and carboxymethyl cellulose microstructures prepared using electrohydrodynamics and green solvents

Overview

In allowing cellulose to be soluble in safe solvents, cellulose derivatives have made the polymer even more medically relevant, as it can now be processed without worry of the solvents used and the potentially harmful effects they could have *in vivo*. In this chapter, three different derivatives were used. Between the three; two ethers and an ester were used, of which one was hydrophilic and the others hydrophobic. This was done to cover the diversity of cellulose derivatives within this study. All three CDs were subject to changes in various parameters in order to identify their effects on the morphologies of the microstructures produced.

Table 3: Properties of the CDs used

Name	Type	Hydrophilicity/phobicity
Ethyl cellulose (Section 4.1)	Ether	Hydrophobic
Cellulose acetate (Section 4.2)	Ester	Hydrophobic
Carboxymethyl cellulose (Section 4.3)	Ether	Hydrophilic

Manipulating the morphology of an electrospun structure can be done through a number of ways; making changes to the processing parameters or changes to the solution itself, both were explored in this work.

4.1 Ethyl Cellulose

Electrospinning ethyl cellulose (EC) is well described in the literature, however, as listed in **Chap. 2**, this polymer is typically used with less than favourable solvents. This work used only water and ethanol whilst working EC. Water is the gold standard solvent, the safest to use, however, this is not possible to use alone with hydrophobic polymers like EC. But here water was used as part of a binary solvent system in order to reduce the proportion of ethanol used.

Processing and solution parameters: applied voltage, flow rate and collection distance and the polymer concentration were changed and with the effects on the morphology observed. These were all done whilst employing a safe and possibly, green solvent, in order to show the versatility of this solvent system despite it not being favoured amongst researchers.

4.1.1 Solution characterisation

Solution properties such as viscosity, surface tension and electrical conductivity all affect the electrospinning process, it is important to define these parameters and the resulting effect in the microstructures they will produce.

Table 4: Physical properties of ethyl cellulose solutions

Solution (wt%)	Density (kg m⁻³)	S. T. (mN m⁻¹)	Elec. Cond. (μS m⁻¹)
17	4450	53.70 \pm 1.09	64.42 \pm 0.33
18	4460	68.30 \pm 1.23	63.32 \pm 0.29
19	4510	76.12 \pm 2.87	62.00 \pm 1.24
20	4570	83.90 \pm 5.65	62.31 \pm 0.62
21	4550	107.42 \pm 1.99	62.52 \pm 0.71
22	4620	112.64 \pm 2.81	61.38 \pm 1.06
23	4640	132.03 \pm 2.77	61.02 \pm 0.87
24	4640	144.71 \pm 7.43	59.58 \pm 1.06
25	4740	163.60 \pm 3.97	57.84 \pm 0.4

4.1.2 Solvent selection

Despite its hydrophobic nature, the work conducted with EC used the binary solvent system of water and ethanol, at the ratio 20:80, developed by Luo et al. [192]. Decreasing the ethanol content, will reduce the amount of ethanol residue in the polymeric fibres/particles, which is a mild irritant [193]. In a wound dressing, keeping the ethanol content to a minimum would be preferable but this has to be balanced against solubilizing the polymer. It was found increasing the proportion of water above 20% (v/v) will form solid suspensions, and increasing the water content even further will show no solubility. Nevertheless, this solvent system is the least toxic and most biocompatible. Tetrahydrofuran (THF)/Dimethylacetamide (DMAc) binary solvent [45, 194], 2,2,2-Trifluoroethanol [111, 112], and Dimethylformamide (DMF)/acetone binary solvent [116] have all been used previously with ethyl cellulose. Ethanol and water has been demonstrated in the literature as well by Ahmad et al. [16]. Table 5. shows the ranking/desirability of the solvents

used with EC in the literature by major pharmaceutical companies; Pfizer, New York, USA [195], Sanofi, Gentilly, France [106] and GSK, London, UK [105], as well as data from a solvent guide published by American Chemical Society [196] in comparison to ethanol.

Table 5: Literature values of desirability/safety of solvents used with ethyl cellulose of all the solvents checked, only water and ethanol were given the “green light” across the board by ref. 105, 106, 193 and 194. The values listed correspond to the health score from American Chemistry Society (ACS), health (acute and chronic effects on human health and exposure potential) from GlaxoSmithKline (GSK), overall ranking from Sanofi and guide for medicinal chemistry from Pfizer.

Solvent	ACS Roundtable [196] 1-good, 10-poor	Sanofi [106]	Pfizer [195]	GSK [105] 1-bad, 10-poor
Tetrahydrofuran	-	Substitution advisable	-	6/10
Dimethylacetamide	7/10	Substitution requested	Undesirable	2/10
2,2,2-Trifluoroethanol	6/10	-	Usable	-
Dimethylformamide	7/10	Substitution requested	Undesirable	2/10
Acetone	4/10	Recommended	Preferred	8/10
Ethanol	3/10	Recommended	Preferred	8/10
Water	1/10	Recommended	Preferred	10/10

4.1.3 Concentration

Initial solutions of 5, 10, 15, 20, 25 and 30wt% were made and processed via EHD. 5 to 15wt% shows particle diameter increased, indicating electrospinning was occurring. At 20wt% there was an emergence of tails on the particles, but electrospinning was still occurring. With 25wt% fibres were being produced with spindle like beads, electrospinning had begun to occur. 30wt% gave rise to thick ribbon like fibres were being produced, this is again due to electrospinning. The solutions that resulted in producing particles, are a result of inadequate chain entanglement [156]. Coulomb fission is a phenomenon where a charged droplet reaches its Rayleigh limit, a value where the droplet is carrying the maximum charge for its mass. At this limit the droplet will eject some of its content in the form of “secondary” or “daughter” droplets, thereby reducing the charge of the droplet [197, 198], and giving a bimodal distribution in particle diameter. This can be seen clearly in Fig. 23.a. where the particles are clearly of non uniform size. When the chain entanglements between the polymer chains in solution reach a certain level the jet is not able to break up, this is prevented by the presence of the entanglements; these physical entanglements will bring about fibre formation during the EHD process [199]. The concentration of chain entanglements is controlled by polymer molecular chain length and solution polymer concentration, increasing both simultaneously or individually will lead to an increase in chain entanglements pushing electrospinning to electrospinning, continuing the increase will affect the diameter of the fibres produced, they will increase proportionally [198, 200]. From this selection of solutions only 20wt%

shows the chain entanglement approaching the critical chain entanglement value, at which electrospinning will occur, as shown by the presence of tails.

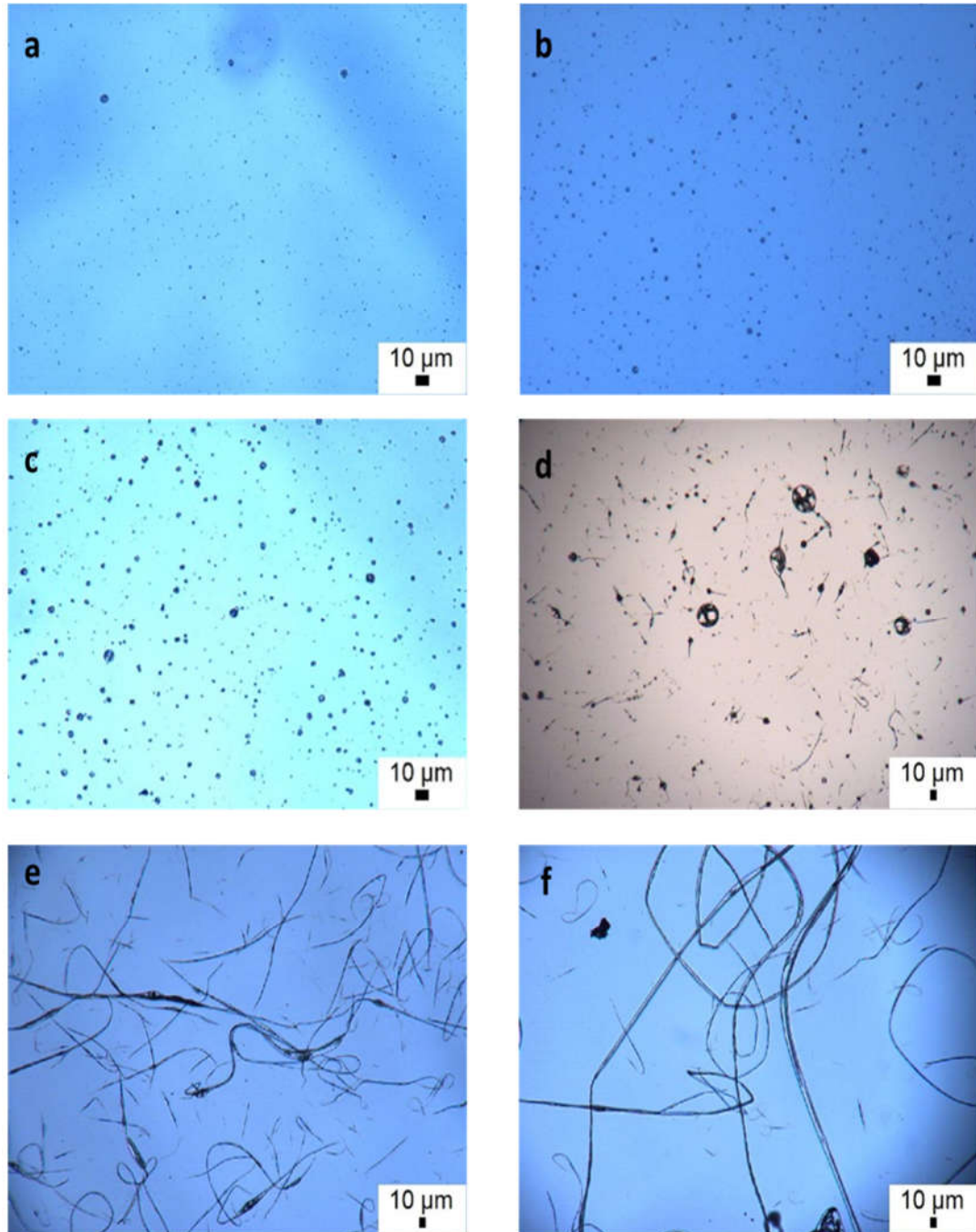


Figure 23: Optical micrographs of (a) 5wt% particles, (b) 10wt% particles, (c) 15wt% particles, (d) 20wt% beaded fibres, (e) 25wt% fibres and ribbons, (f) 30wt% ribbons, the flow rate, applied voltage and working distance were 100 μ L/min, 15kV and 100mm, respectively.

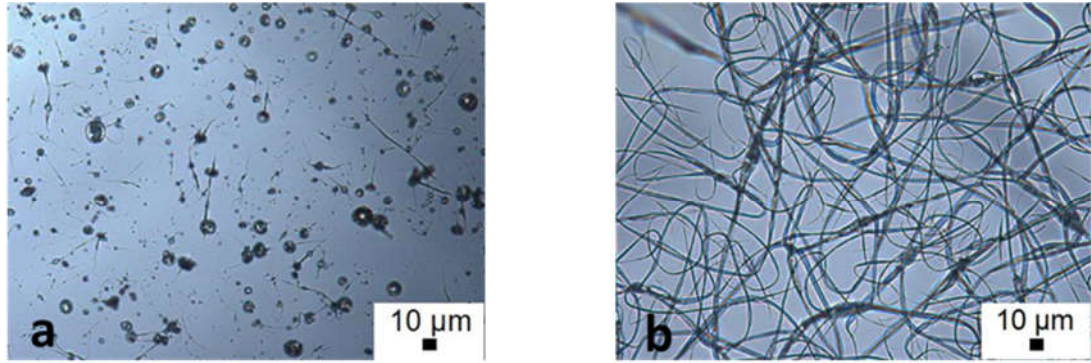


Figure 24: Optical micrographs showing the effect of concentration on microstructure morphology the flow rate, applied voltage and working distance were 50 μ L/min, 15kV and 100mm, respectively, a) 17wt%, b) 25wt%, respective microstructure distributions below.

Fig. 24 displays the two extremes of the 17-25wt% range and the very different morphologies produced as a result of change in concentration only. At 17wt% the chain entanglements are not sufficient enough to prevent the jet breaking up leading to particles with short tails.

The transition from particles with tails to almost smooth fibres shown in Fig. 24. is due to the increase in polymer chain entanglements, as the only parameter changed was the polymer concentration. At 25wt%, the Rayleigh instability has the least effect, this is evident as “electrospinning” rather than “electrospraying” has occurred. The Rayleigh instability is another phenomenon that occurs during EHD. In this case, when the electric field is applied, the force due to repulsion between polymer chains causing the droplet to expand is opposed by the surface tension of the droplet trying to maintain

the spherical shape in order to reduce the systems energy. As the charge builds the repulsion overcomes the surface tension, causing the well-known Taylor cone to form and a jet emitted [151]. However, the formation of beaded fibres shows the Rayleigh instability is present and has not been entirely overcome [201]. For high viscosity liquids the jet does not break up, but travels as a whipping jet to the grounded target [142]. Increasing the concentration shows a lengthening of the tails into fibres and also an elongated of the beads to spindle like to almost completely smooth fibres. As the concentration increases, the resistance to Rayleigh instabilities increases and the jet is less susceptible to break up (causing longer fibres) and disturbances (causing less beading). From these early experiments, it was clear there was an interesting region of transition between 15 to 25wt%, which required further investigating. In order to be able to chart the transition over smaller increments of concentration changes, solutions of 17, 18, 19, 20, 21, 22, 23 and 24wt% were also subjected to EHD and the gradual transition from particles to fibres was observed.

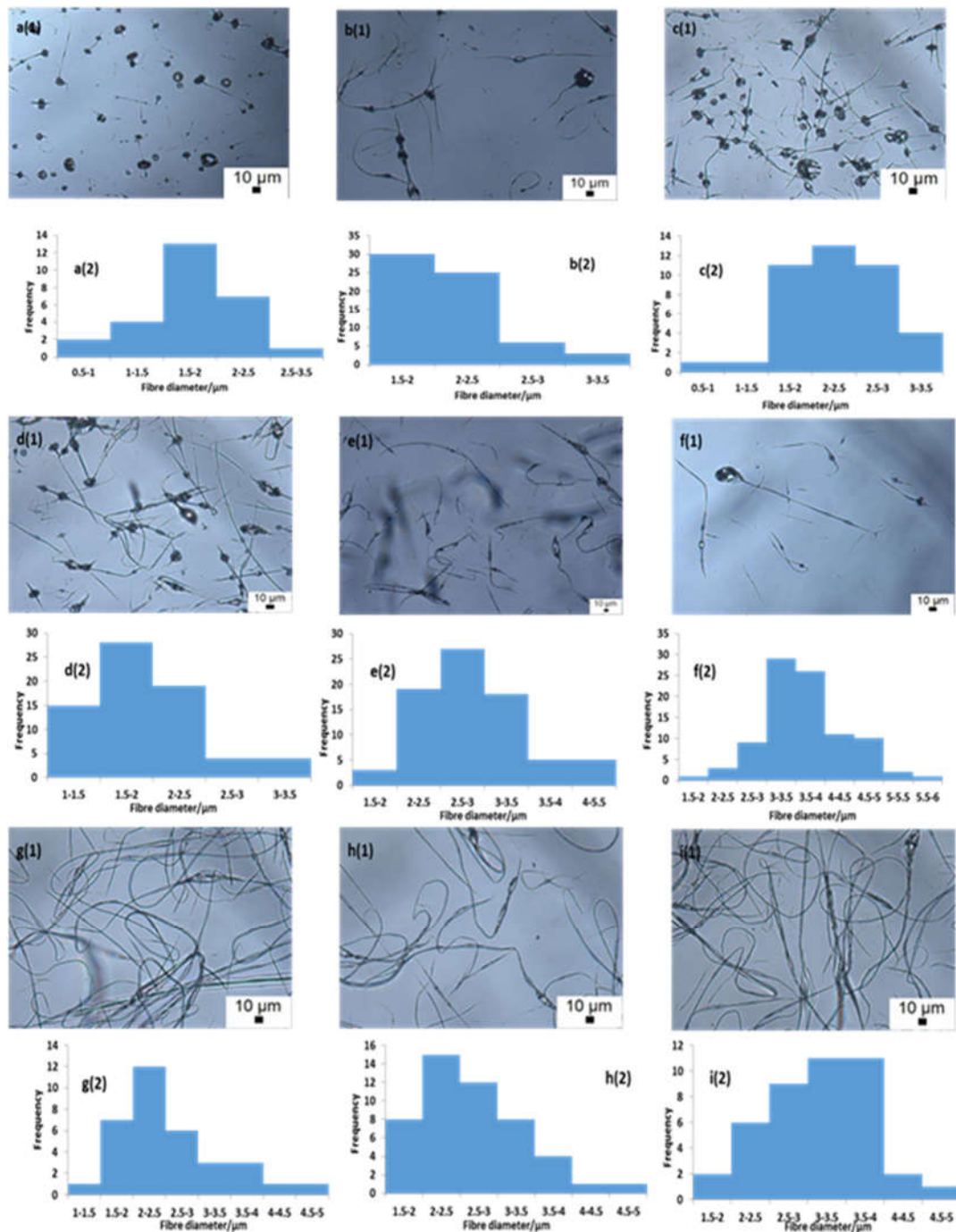


Figure 25: Effect of concentration on microstructure diameter at constant flow rate, applied voltage and working distance of 100 μ L/min, 19kV and 150mm, respectively a) 17wt%, b) 18wt%, c) 19wt%, d) 20wt%, e) 21wt%, f) 22wt%, g) 23wt%, h) 24wt% and i) 25wt%, each with their corresponding microstructure size distribution. A minimum of 100 structures per sample were measured to generate the distribution graphs.

4.1.4 Voltage

The effect of voltage on fibre diameter is disputed in the literature [116] and has been defined as material specific, however, theories have been suggested to support voltage increasing and decreasing fibre diameter. In the case of EC increasing the voltage has shown the general trend of reducing fibre diameter as shown by the graph in Fig. 26.

At 25wt%, it appears the intermediate voltages, 16-18kV, are the most stable, with minimum instabilities as shown by the lack of beading at these voltages. However, the overriding factor, at this concentration, pushing down the fibre diameter is increased repulsion. This high concentration has an increased number of polymer chains per unit solution, this means the effect of repulsion is greatest in these solutions. At 19kV, for the flow rate, (50 μ L/min) investigated, a stable cone jet is not formed, Rayleigh instabilities become a dominant factor and cause beaded structure. However, at 20kV, this small incremental increase in voltage, has increased the stretching, caused by the drawing stress of the jet to elongate the shape of the spherical beads (indicated with arrows) [18]. At 20kV the fusion of beads occurs, which brings down the fibre diameter [202]. At 19kV, there is a marked presence of circular beads at this voltage only. Changing the voltage independent of the flow rate increases the likelihood of beaded fibres forming; for each flow rate will have a "critical voltage" where a stable Taylor cone forms producing smooth fibres [203]. Higher electrical field strength, increases the repulsive forces acting on the polymer chain, thereby increasing the stretching leading to a reduction in fibre diameter [158].

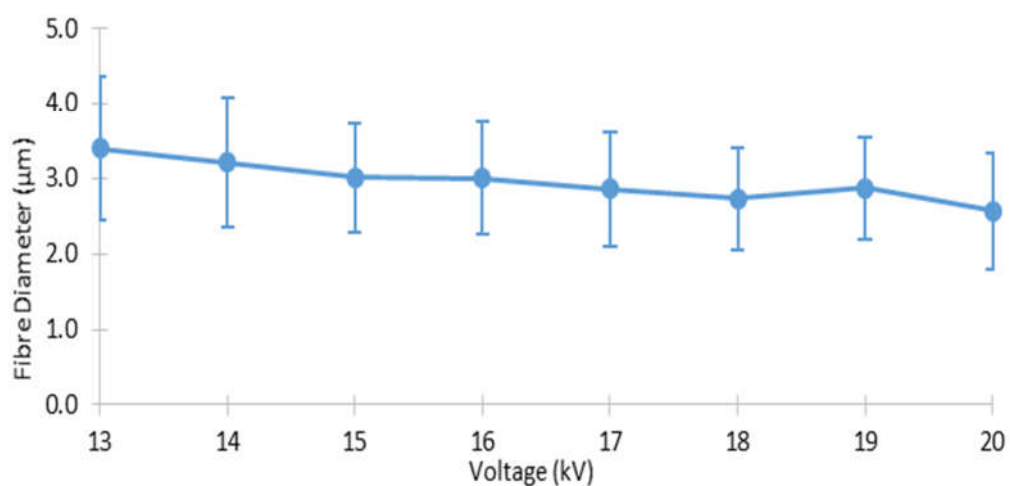
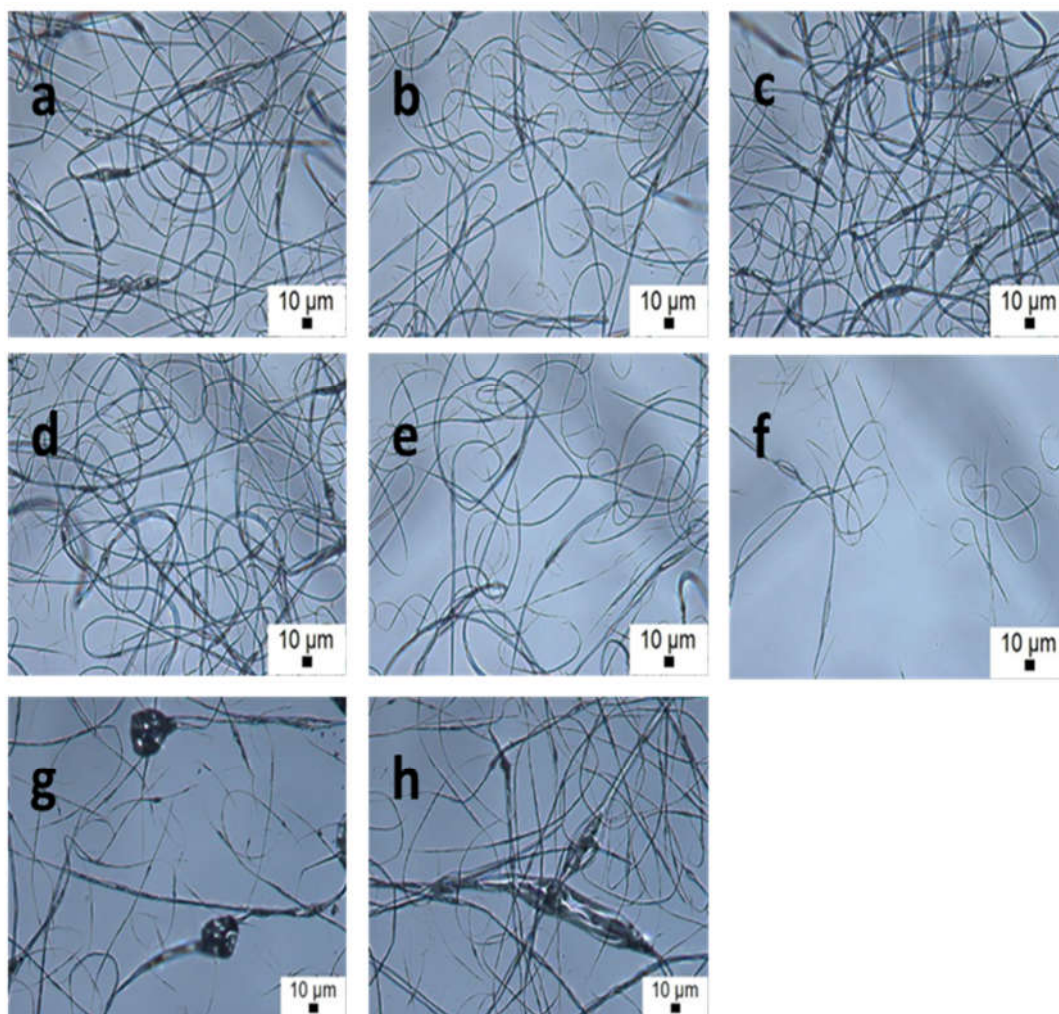
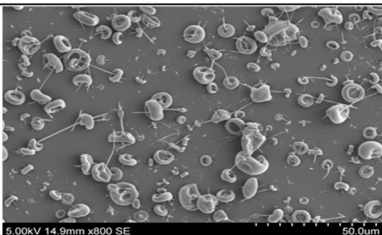
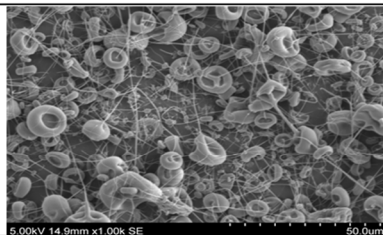
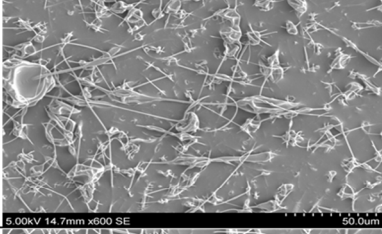
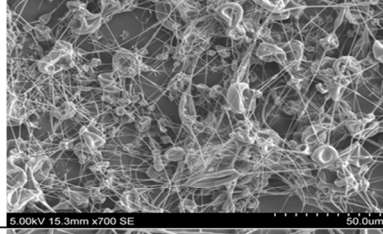
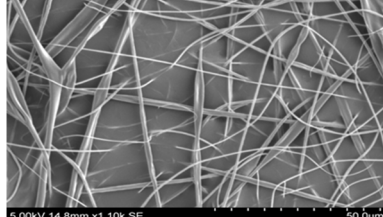


Figure 26: Effect of voltage on fibre diameter collected at flow rate, concentration and working distance used were 50 μ L/min, 25wt% and 100mm. a) 13kV, b)14kV, c)15kV, d)16kV, e)17kV, f)18kV, g)19kV and h)20kV, and graph showing the fibre diameter trend across the voltages. A minimum of 100 structures per sample were measured to generate the distribution graphs.

4.1.5 Flow rate

Changing the flow rate has a marked effect on the fibre morphology, especially at such high values. Doubling the flow rate increases fibre diameter and droplet/bead diameter. Having a larger volume of solution flowing from the needle tip per unit time i.e. 100 μ L/min reduces the solvent evaporation leading to larger fibres and beads as compared to microstructures produced at 50 μ L/min. The increased flow rate causes fewer stretching forces [116], as more solution flows per unit time, under the same voltage i.e. electrical field strength, the same amount of energy is competing to repel a greater number of polymer chains flowing through the needle tip. This same amount of energy cannot reproduce the same amount of repelling forces for a greater flow rate (i.e. greater volume), hence larger fibres are produced.

Table 6: Fibre diameter as a function of flow rate. Ethyl cellulose in EtOH:H₂O(80:20)

Concentration & Applied Voltage	Flow rate: 50 μ L/min	Flow rate: 100 μ L/min
17wt%, 20kV		
23wt%, 19kV		
25wt%, 17kV		

The four different concentrations shown in table 7. are 17, 20, 23 and 25wt% all follow the same process. At a lower flow rate the difference in fibre diameter is palpable, however, at 100 μ L/min the diameters converge, indicating the flow rate is limiting the extent the fibre diameter can be increased. Despite the slight variation in voltages, the flow rate appears to have greater impact in the fibre diameter than the voltages.

Table 7: Effect of flow rate on morphology; tip to collector distance: 100mm. A minimum of 100 structures per sample were measured to generate the distribution graphs.

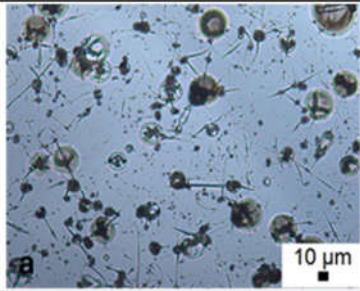
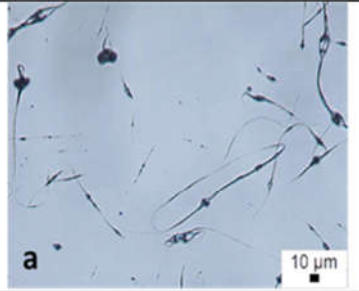
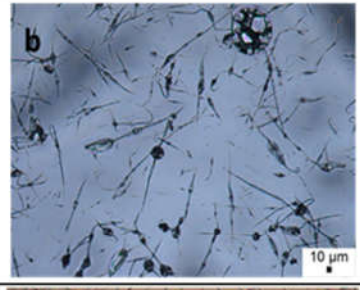
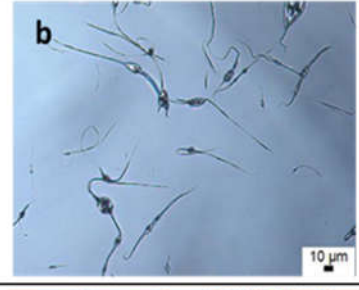
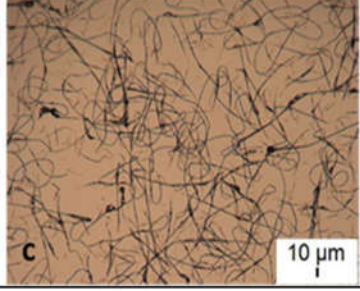
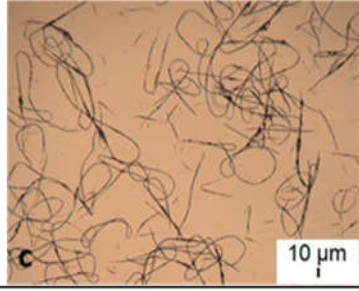
Sample parameter	Flow rate (μL min⁻¹)	Microstructure Diameter (μm)
Concentration: 17wt% Applied Voltage: 20kV Tip to Collector distance: 100mm	50	1.39
	100	2.03
Concentration: 20wt% Applied Voltage: 17kV Tip to Collector distance: 100mm	50	1.6
	100	2.08
Concentration: 23wt% Applied Voltage: 19kV Tip to Collector distance: 100mm	50	2.52
	100	3.2
Concentration: 25wt% Applied Voltage: 17kV Tip to Collector distance: 100mm	50	2.73
	100	3.21

4.1.6 Collector to tip distance

The dominant effect caused by changing the distance between the tip and the collector, is the time allowed for solvent evaporation. Increasing this distance, increases the time allowed for solvent evaporation to occur which decreases the fibre/bead diameter. Changing the tip to needle distance has a lesser effect on the higher concentrations. This could be because increasing the concentration reduces the percentage content of solvent. The reduced presence of solvent will be less affected by the time allowed or evaporation to occur so the diameter shrinkage at the higher weight percent solutions is less substantial, as shown by the images of fibres collected with 22wt%.

A reduction in the amount of solvent present in the system will prevent polymer diffusion occurring. As the solvent evaporates out of the system, the polymer diffuses in to occupy the space, these leads to a denser fibre with smaller fibre diameter [198].

Table 8: Effect of collector distance on morphology, voltage: 20kV, flow rate: 100 $\mu\text{L}/\text{min}$. A minimum of 100 structures per sample were measured to generate the distribution graphs.

Concentration	Tip to collector distance: 100mm	Tip to collector distance: 150mm
18wt%		
21wt%		
24wt%		

4.2 Cellulose Acetate

Cellulose acetate is mostly used for its film forming abilities, historically in water and chemical filtration, and more recently in as anti bacterial food packaging where [53], anti fouling filters [204]. Acetone is a popular solvent of CA, however, this is not the case when electrospinning CA. The high volatility of acetone commonly leads to blockages, stopping the fibre formation process. In this work, water was added to the acetone in order to bring down the

volatility and allow consistent spinning. The effect of water content of the solution on the morphology of the CA fibres, along with using a guard plate and concentration.

4.2.1 Solution characterisation

Table 10. displays the physical properties of CA solutions. Increasing the concentration leads to an increase across all the parameters including electrical conductivity, as the carboxylic groups of acetates are very conductive. This means the CA polymer is adding to the electrical property rather than hindering it, in this case the conductivity is not only attributed to the solvent but also the polymer.

Table 9: Physical properties of cellulose acetate solutions

Solution (wt%)	Solvent Acetone : water	Density (kg m⁻³)	Viscosity (mPa s)	S. T. (mN m⁻¹)	Elec. Cond. (μS m⁻¹)
10	100:0	823	25.8±0.1	33.2±2.9	3.75±0.05
12.5	100:0	832	33.9±0.3	34.6±2.2	3.79±0.03
15	100:0	839	65.2±0.4	42.0±4.1	3.96±0.03
17.5	100:0	848	154±7.4	47.1±3.3	3.94±0.03
10	80:20	896	65.8±2.6	44.5±2.2	8.60±0.41
10	85:15	874	42.7±1.1	40.3±2.0	8.40±0.01
10	90:10	856	36.0±0.8	39.0±1.9	8.73±0.03
10	95:5	838	27.4±1.0	34.0±0.8	6.72±0.07

4.2.2 Solvent Selection

There have been investigations into the effect solvent selection has on the *morphology* of electrospun CA fibres [54, 109, 110]. However, these were carried out without a specific application in mind therefore; toxicology was not taken into consideration.

Table 10: Literature values of desirability/safety of solvents used with cellulose acetate.

	ACS Roundtable [196] 1-good, 10-bad	Sanofi [106]	Pfizer [195]	GSK [105] 1-bad, 10-good
Chloroform	9/10	BANNED	Undesirable	3/10
DMAc	7/10	Substitution requested	Undesirable	2/10
Dichloromethane	7/10	Substitution advisable	Undesirable	4/10
DMF	7/10	Substitution requested	Undesirable	2/10
Acetone	4/10	Recommended	Preferred	8/10
Methanol	5/10	Recommended	Preferred	5/10
Formic acid	6/10	Substitution requested	-	-
Pyridine	6/10	Substitution advisable	Undesirable	4/10
Acetic acid	6/10	Substitution advisable	Usable	6/10
Trifluoroethylene	6/10	-	-	-
Water	1/10	Recommended	Preferred	10/10

Table 10. demonstrates the solvents used with CA in the literature and their desirability with regards to health. Some of these solvents are desirable in terms of functionality in electrospinning, they show; good solubility, good evaporation rates, produce smooth and uniform fibres. However, in this investigation *toxicity* must be deliberated, which in this case makes the production of smooth, uniform fibres more difficult.

Again water is the gold standard of solvents in biomedical terms, and in this work every attempt has been made to incorporate it into the solutions used. Solutions were made with a binary solvent; water and acetone in the ratios of 100:0, 95:5, 90:10, 85:15 and 80:20 (acetone/water v/v). Beyond this ratio, the polymer was no longer solubilised and would therefore be difficult to produce fibres. According to table 6. 3/4 sources approve acetone is a safe solvent with minimal risk to health. Coupled with water this binary solvent can be considered safe for biomedical use.

4.2.3 Solvent

The difference between the diameters of fibres made from an acetone only solution compared to those made up of the binary solvent with the greatest proportion of water, is due to the solvent conductivity. As acetone is more conductive than water, hence the acetone only solution have a greater charge carrying ability; the cause of its superior conductivity [143]. In an electric field,

a highly or more conductive solution is exposed to greater tensile force which will drive down the fibre diameter as demonstrated by Fig. 27 [144].

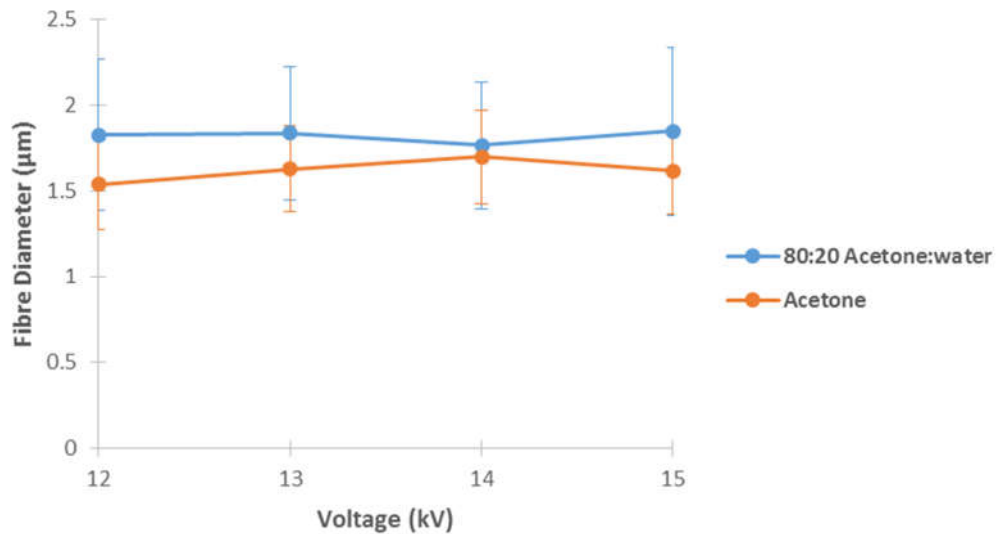


Figure 27: Graph showing fibre diameter with increase in applied voltage for 17.5wt% CA dissolved in 80:20 acetone/water and 100:0 acetone/water. A minimum of 100 fibres per sample were measured

This phenomenon also rings true with the solution made with different water to acetone ratios. As the proportion of water increases as does the fibre diameter as shown in Fig. 28, this is a directly attributable to the reduction of solution conductivity as the water proportion increases.

Alongside this, with the increase in the proportion of water the beading decreases, contributing to the increase in fibre diameter. The evaporation rate of acetone is high which lead to the needle becoming blocked after small durations of electrospinning [54]. The increase in water content reduces the surface tension of the solution which also favours thinner fibres [153].

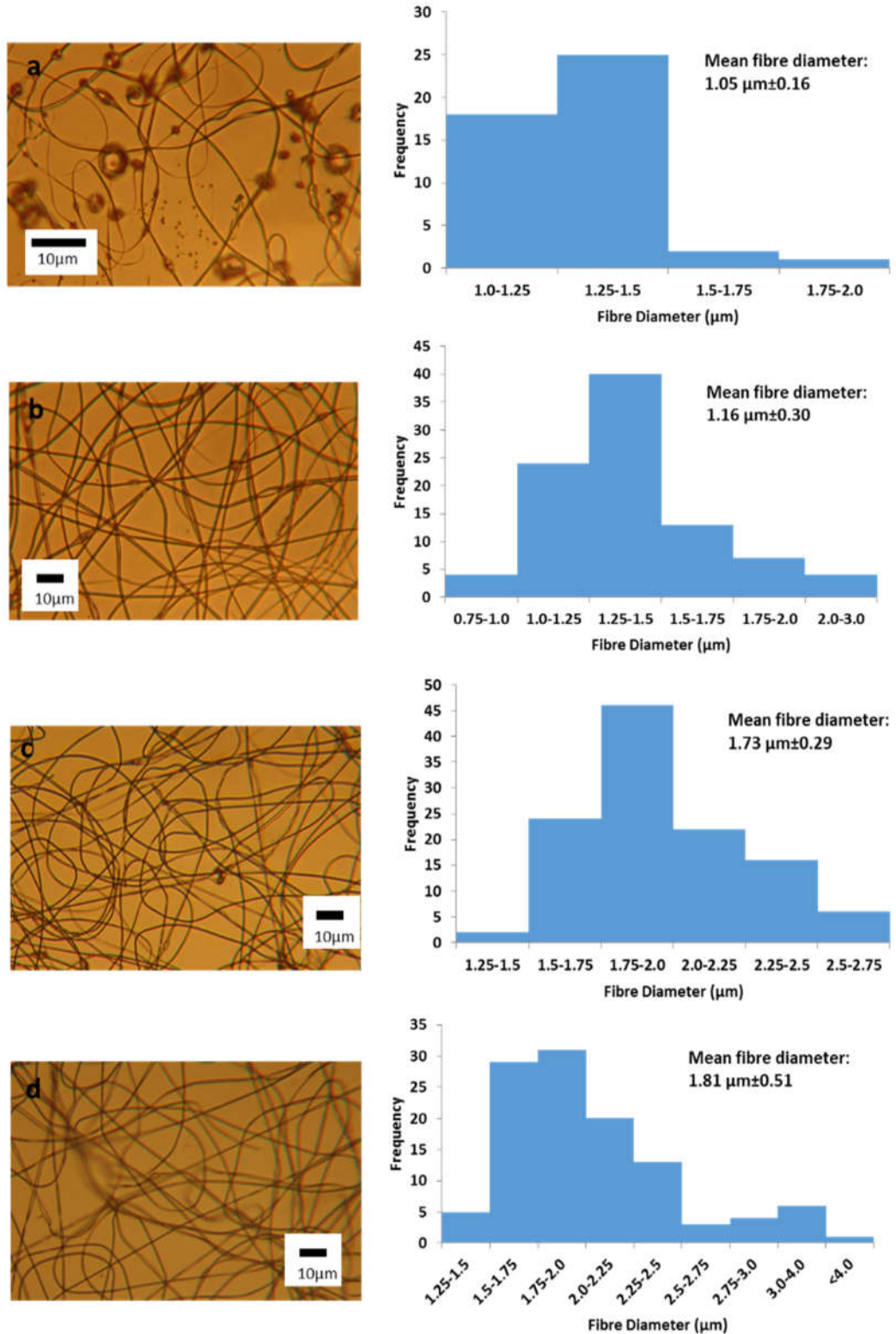


Figure 28: CA fibres electrospun from 10wt% solution at flow rate, voltage and working distance used were 4ml/h, 13kV and 100mm, respectively, with the following solvents; a) 95:5, b) 90:10, c) 85:15 and d) 80:20 (acetone: water). A minimum of 100 fibres per sample were measured.

4.2.4 Concentration

The effect of concentration on cellulose acetate is almost identical to the effect on ethyl cellulose (EC). Fig. 29 shows a positive correlation between the polymer concentration and fibre diameter. As with EC, the increase in polymer concentration increases the entanglement between the molecular chains. During EHD the jet is less likely to break up, fibre formation will occur as opposed to particles.

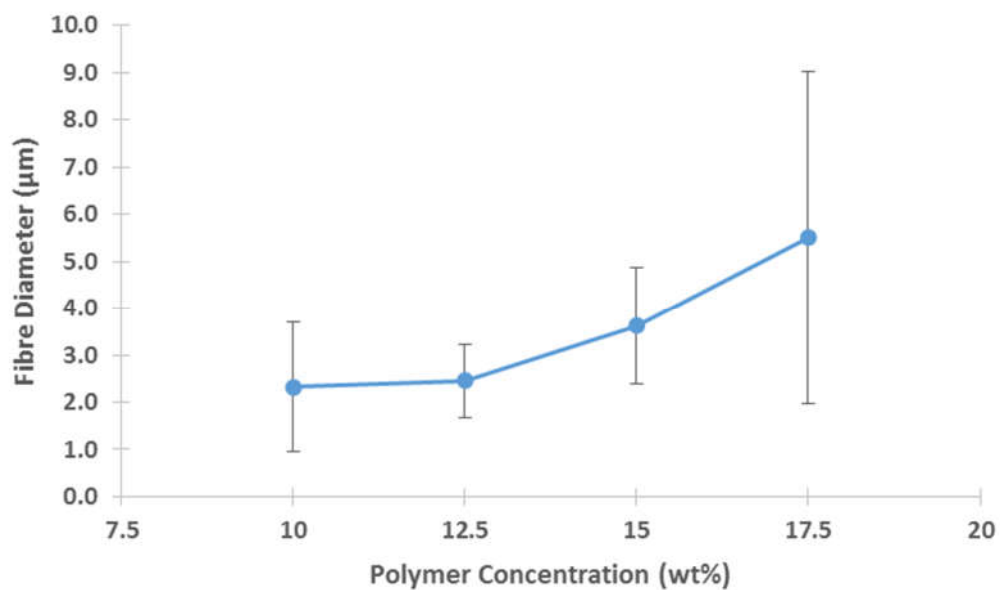


Figure 29: Correlation between fibre diameter and polymer concentration, the flow rate, applied voltage and working distance were 4ml/h, 12kV and 100mm, respectively.

Fig. 30 displays the change in morphology as the concentration increases. At 10wt%, the fibres are heavily beaded and have the smallest fibre diameter. Despite, the concentration being high enough to commence electrospinning the viscosity is not high enough to resist the instabilities allowing beads to form [102].

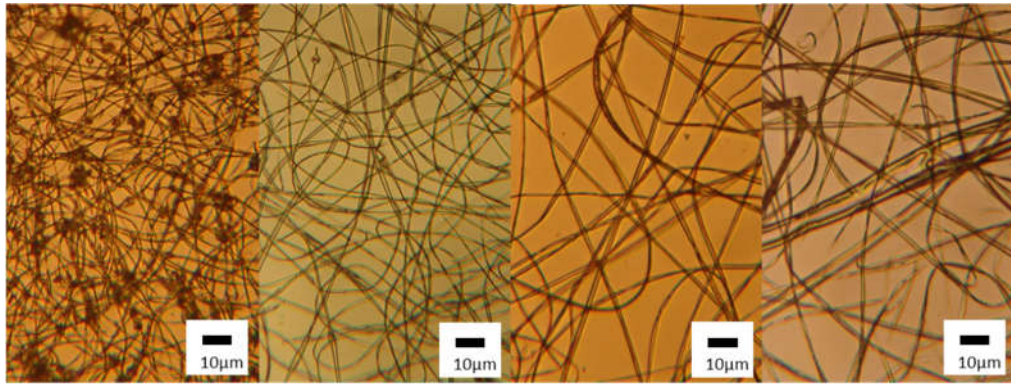


Figure 30: Optical micrographs of cellulose acetate fibres electrospun at 12kV, 6ml/h with the following solution concentrations L-R 10, 12.5, 15 and 17.5wt% (in acetone only)

Increasing the concentration to 12.5wt%, produces fibres with much less beading. The increased concentration strengthens the solution against the instabilities but the beads are now spindle like rather than spherical [205]. The reduction of spherical beading is also a source for the increased fibre diameter. As the beads smoothen out into the spindle morphology the polymer that would have made up the beads are now incorporated into the fibre driving up the diameter.

At 15wt%, the morphology has changed again to thick, flat fibres. The concentration is so great that the drawing process as the jet makes its way to the collector does not have a great effect, leading to this thickened morphology. As at 12.5wt% fibres with spindle-like beads were produced and at 15wt% flat ribbons were produced, it can be assumed the ideal concentration to produce smooth fibres lies between these two values; $12.5 <$

$C_{ideal} < 15\text{wt}\%$, which would have the highest surface to area ratio, if that was a required parameter.

17.5wt% produced the greatest fibre diameter, showing this concentration was least susceptible to the drawing process. It is also an indication that the solvent has not completely evaporated, that is the polymer is not completely dry [143].

4.2.5 Voltage

The effect of voltage on electrospun fibres has split authors, with some stating there is a relationship between fibre diameter and applied voltage be it a positive or negative correlation. Yuan et al. showed a reduction in fibre diameter with an increase in voltage with their polysulfone/dimethylacetamide/acetone system [159]. Whereas, Zhang et al. while working with polyethylene oxide/water system showed a negative correlation between high voltage and fibre diameter [158].

One mechanism to possibly cause a reduction in fibre diameter is the increased applied voltage causes an increase in the net charge of the jet, improving the whipping instability leading to thinner fibres. On the other hand, the increase in voltage causes a higher jet voltage, reducing the flight time of the jet and the time allowed for the solvent to evaporate, leading to thicker fibres [206, 207].

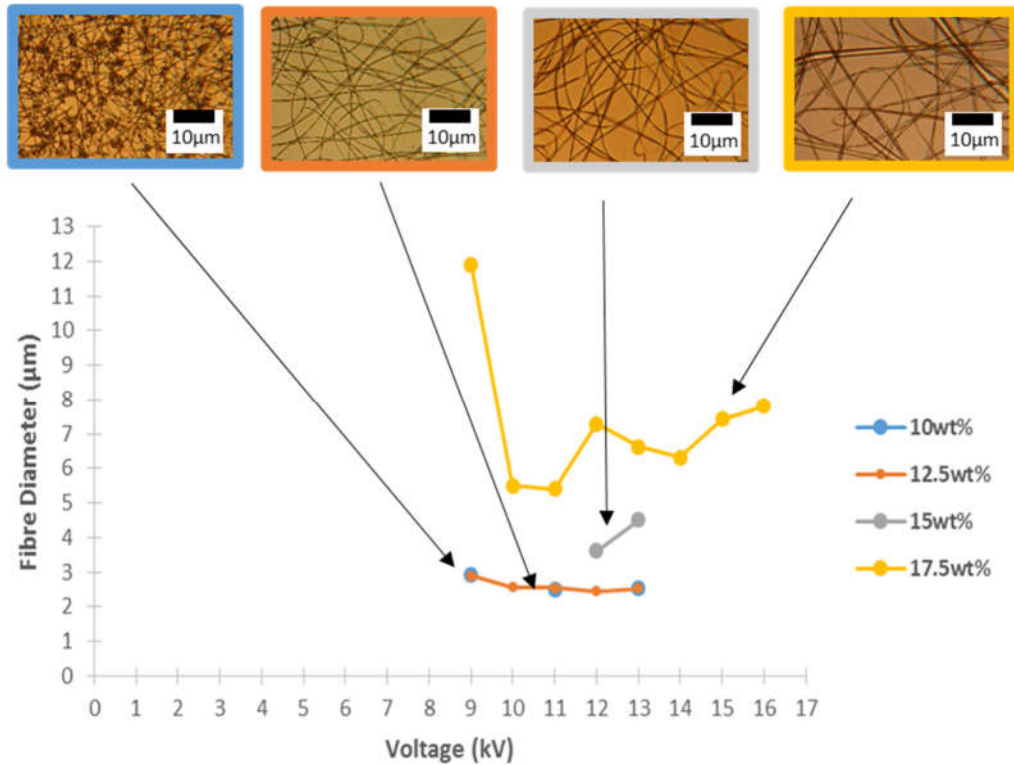


Figure 31: Graph representing the change in fibre diameter by increasing the applied voltage, fibres were collected at a constant flow rate; 6ml/h with a guard plate attached.

4.2.6 Guard Plate

The addition of the guard plate is another potential method to alter the structure size by strengthening the electric field. As shown in Fig. 32 the general trend shows that in the presence of the guard plate the fibre diameters were reduced. The guard plate strengthens the electric field, which affects the whipping instability, in that a larger force is exerted on the jet increasing the speed in turn increasing the stretching reducing fibre diameter [208].

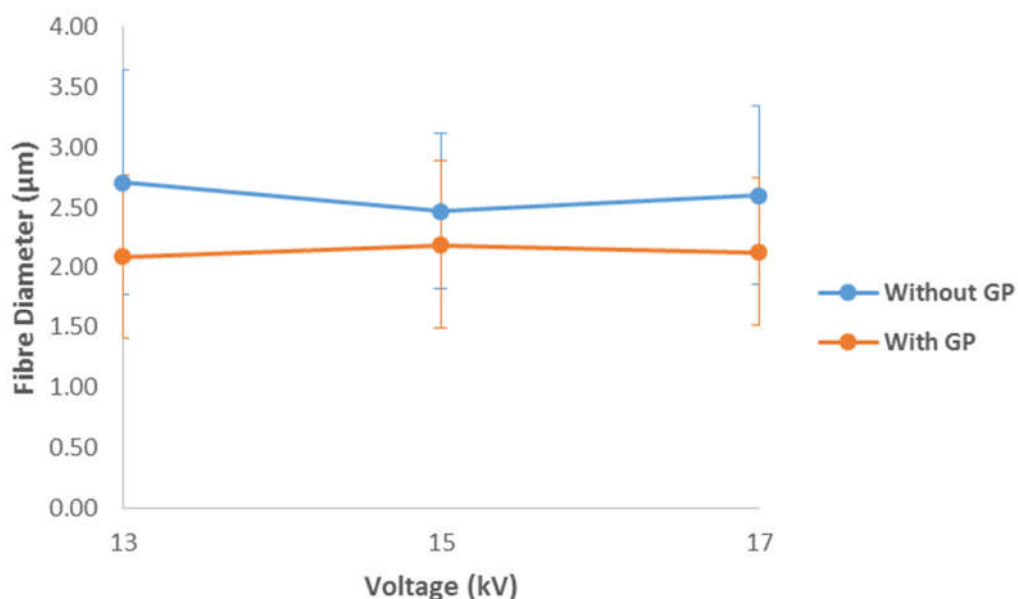


Figure 32: Graph showing the diameter of fibres at variable applied voltage with and without guard plate 80:20 (acetone/water) solvent at concentration, flow rate and working distance used were 10wt%, 6ml/h, and 100mm, respectively.

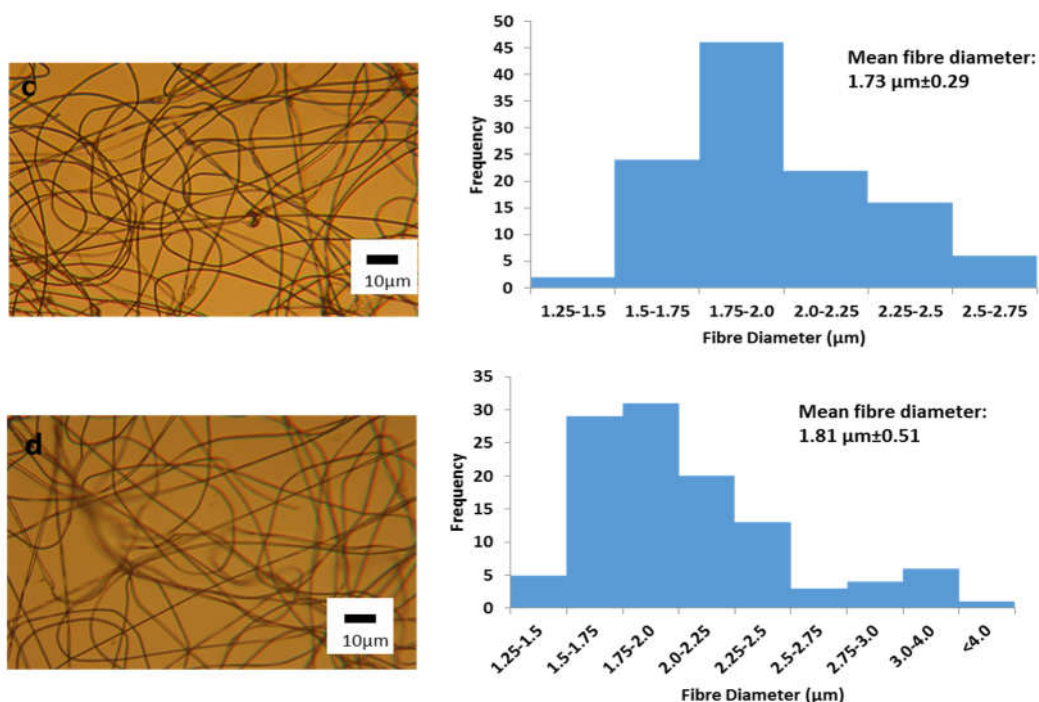


Figure 33: Optical microscope images and corresponding size distribution graphs for fibres produced from 80:20 (acetone: water) solvent, at concentration, flow rate, voltage and working distance used were 10wt%, 6ml/h, 15kV and 100mm, respectively. Top image: Without guard plate, bottom image: With guard plate.

4.3 Carboxymethyl Cellulose

PEO is added to the CMC solution to act as a spinning agent, on its own CMC cannot be electrospun [15]. This blend was made up of 4wt% carboxymethyl cellulose and 15wt% poly(ethylene oxide) at the following ratios 90:10, 86:14 and 75:25 as used by Brako et al [62] with two different molecular weights of carboxymethyl cellulose; 250,000 and 700,000 g mol⁻¹.

4.1.1 Solution characterisation

Table 11: Characteristics of carboxymethyl cellulose solutions

M_w	Solution (wt%)	Density (kg/m³)	S. T. (mN/m)	Elec. Cond. (μS/m)
250,000	25:75	1088	108.69±0.9	827.2±14.5
	14:86	1066	121.23±3.5	498.5±5.2
	10:90	1056	111.32±3.9	390.4±7.9
700,000	14:86	1034	92.1±1.9	371.2±5.2

4.1.2 Molecular weight

The effect of changing molecular weight in this experiment provided the expected result. The higher molecular weight increases the entanglements between polymer chains, not only leading to an increase in fibre diameter, as shown in table 12, but also strengthening the polymeric jet against the instabilities leading to smoother fibre deposition [116, 149].

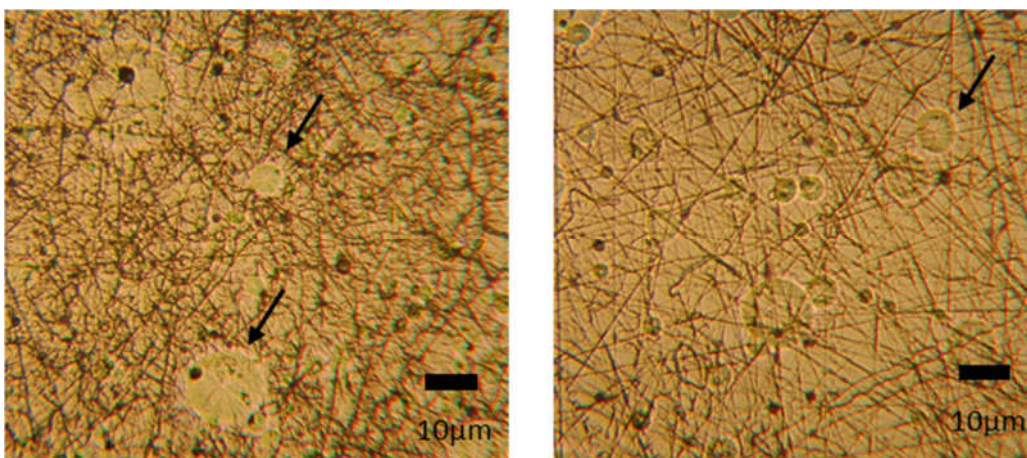


Figure 34: L-R Optical micrographs of carboxymethyl cellulose/poly(ethylene oxide) fibres electrospun at 16kV with $5\mu\text{L}/\text{min}$ flow rate with 100mm needle tip to collector distance, showing L-R $2.5 \times 10^5 \text{ g mol}^{-1}$ and $7 \times 10^5 \text{ g mol}^{-1}$.

The spots indicated by the arrows are small amounts of dried solution, which were not subjected to the whipping instabilities. This could potentially be overcome by reducing the flow rate or increasing the distance from the needle tip. However, previous experiments were conducted at $1\mu\text{L}/\text{min}$ where a receding jet formed. This occurs when the solution being ejected by the polymer jet is not being replenished quickly enough but the particular the flow rate.

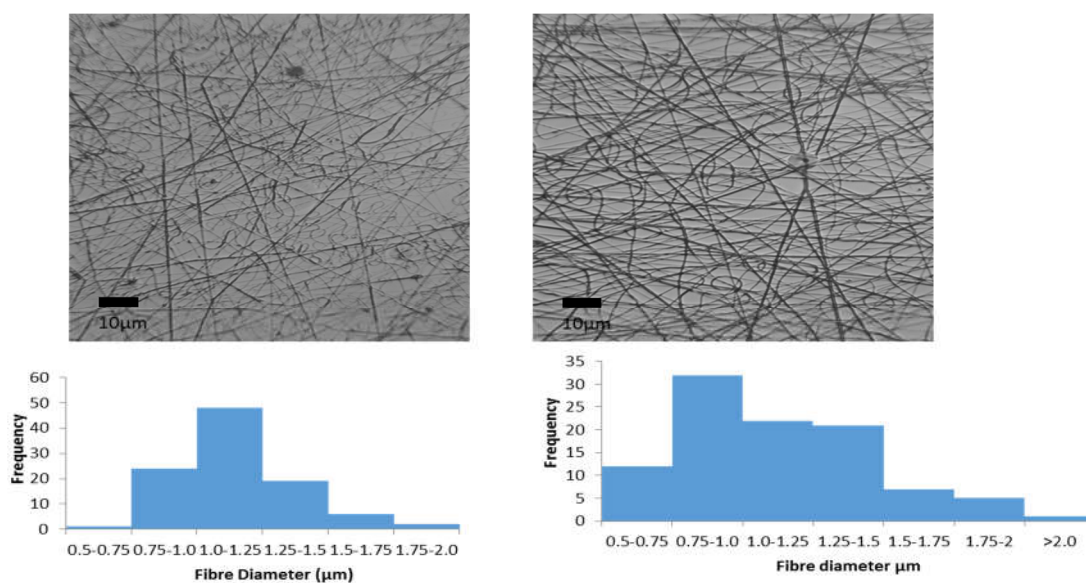


Figure 35: L-R Optical micrographs of carboxymethyl cellulose/poly(ethylene oxide) fibres electrospun at 15kV with 5µL/min flow rate with 100mm needle tip to collector distance, showing L-R 2.5×10^5 g mol⁻¹ and 7×10^5 g mol⁻¹.

Table 12: Fibre diameter as a function of molecular weight

Molecular weight (g mol ⁻¹)	Fibre diameter (µm)
250,000	0.89±0.35
700,000	1.12±0.23

Not only is the fibre diameter different but so is the morphology, as shown in Fig. 35. The fibres produced from M_w 250,000 have more kinks than the sample of M_w 700,000. As mentioned previously the higher molecular weight is less susceptible to the instabilities brought on by the electrical field, resulting in a smoother appearance. The kinks or “buckling” are caused molecular repulsion in the jet, the buckling forms as the whipping jet hits the collector [209].

4.8.2 CMC/PEO Content

An increase in carboxymethyl cellulose (CMC) content drives down the fibre diameter. Increasing the CMC is increasing the content of the longer polymer chain i.e. PEO M_w 200,000 against CMC M_w 250,000 or 700,000. This alone means the number of entanglements will increase being more susceptible to the stretching phase of the electrospinning process driving down the fibre diameter [200].

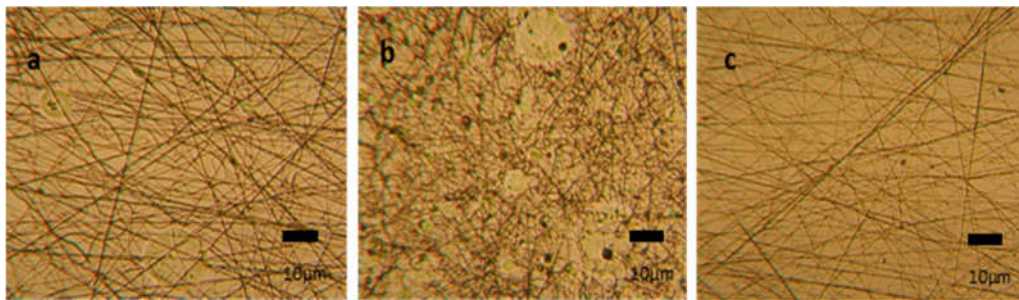


Figure 36: Optical micrographs of CMC (M_w 250,000)/PEO fibres electrospun at 16kV, 5 μ L/min at the following blends PEO:CMC a) 90:10, b) 86:14 and c) 75:25.

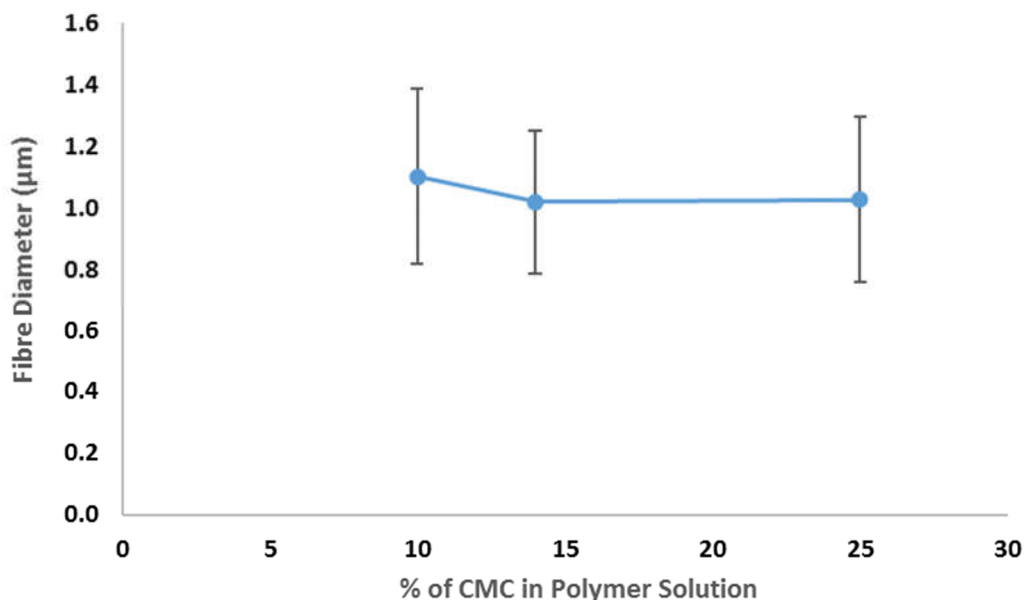


Figure 37: Graph showing effect of CMC proportion in solution on fibre diameter. Samples were collected at 15kV, with 5 μ L/min flow rate with 100mm needle tip to collector distance.

4.4 Summary

Despite cellulose derivatives being classed as a “family”, each type is different from the next and cannot be subjected to the same generalisations as ketones could be, for example. The inherently different chemistries of each functional group added to the polysaccharide, means each cellulose derivative must be investigated for its electrospinnability, material properties and eventually its role as a wound healing patch individually. Small variations such as solvent composition in the case of cellulose acetate, drastically change the fibre morphology, potentially broadening possible uses, along with allowing greater control over the morphologies produced.

Changing the various parameters for both ethyl cellulose and cellulose acetate, resulted in changes that agreed with principles described in the literature. Being able to control both solution and processing parameters to give rise to a range of morphologies from the same polymer and technique, EHD, is an important resource. Especially in the case of cellulose derivatives where more and more people are turning to renewable materials to replace non renewables; cellulose derivatives may be able to help fill that gap. Easy and simple manipulation of the products could make this even more attractive.

As the chemistry of each derivative is different, as will its niche as a biomedical material. In the context of wound healing, it may be that each derivative is suited to a particular wound, for example (hypothetically) ethyl cellulose for burns or cellulose acetate for grazes, but this will require further investigation.

5 Chapter 5

Results and Discussion

Electrohydrodynamic production of polycaprolactone and bacterial cellulose wound healing patches doped with Glybenclamide

Overview

The non-woven nature of electrospun patches makes them ideal for wound healing. The disorientated fibres are analogous to the extra cellular matrix. Therefore using this as a cover for an open wound whilst delivering a therapeutic agent, and absorbing the excess exudate produced by diabetic foot ulcers (DFU), is a desirable combination. In this chapter polycaprolactone and bacterial cellulose fibres were produced, with glybenclamide incorporated. Each constituent of this material plays a role in aiding the healing of DFU's; bacterial cellulose (BC) is essentially a sorbent material, glybenclamide (Gb) is an anti diabetic medication and polycaprolactone (PCL) is the spinning agent which also provides the matrix. The initial set of testing characterised the solutions used to electrospin and produce fibrous patches (**section 5.1**). The various non woven patches produced were interrogated to identify their surface morphologies and the presence of material constituents (**section 5.2**). Finally, the patches were subjected to *in vitro* testing; with their drug release and swelling behaviour assessed (**section 5.3**).

5.1 Solution characterisation and fibre production

The solutions used in this section of work were made up of a number of substances; including two solvents, two polymers (one synthetic and one natural) and an API. Each of these constituents have an effect on the characteristics of the solution, which would impact the nature i.e. size and morphology of the fibres made [210]. In turn, this could potentially impact the *in vitro* characteristics of the fibres.

Polycaprolactone has been electrospun extensively for biomedical purposes including drug delivery. In this work it is a backbone acting as a carrier or matrix for the BC and Gb, as bacterial cellulose is yet to be electrospun as is. PCL is non toxic, biocompatible and commonly used in this particular application [211]. Two concentrations of PCL solution were used; 10 and 15wt% in order to identify if the change in concentration had an effect on the *in vitro* behaviour.

Fibre diameter does not play a major role in wound healing, however, it is important to define the size of the fibres made in order to help determine the amount of drug being delivered to the body part. Although as spun electrospun meshes typically do not have pores wide enough to allow cells to infiltrate [212], it is possible, once it is immersed in a liquid, the mesh will swell enlarging the pores allowing infiltration [86].

5.1.1 Characterisation of PCI-BC-Glybenclamide solutions

The features of the fibres made are a result of both the characteristics of the solutions and the processing parameters applied to the solutions. The viscosity, electrical conductivity and surface tension of the solutions were determined. In order to identify the individual effect of each component (the designations are given in **Table 13**), the solutions were made in a step by step manner and tested as each component was added as shown in **Table 14**.

Table 13: Designations of polycaprolactone, bacterial cellulose and glybenclamide solutions.

Solution designation	PCI (wt%)	BC (wt%)	Gb (wt%)
PCI 10	10		
PCI 15	15		
PCIBC-10	10	10	
PCIBC-15	15	10	
PCIBCGb-10	10	10	10
PCIBCGb-15	15	10	10
PCIGb-10	10		10
PCIGb-15	15		10

Table 14: Characteristics of polycaprolactone, bacterial cellulose and glybenclamide solutions.

Solution	Surface tension (mN m⁻¹)	Electrical conductivity (μS m⁻¹)	Viscosity (mPa s)
PCI 10			
PCI 15			
PCIBC-10	44	25	545
PCIBC-15	55	20	16002
PCIBCGb-10			
PCIBCGb-15			
PCIGb-10			
PCIGb-15			

Increasing the PCI concentration increases the viscosity as expected along with the surface tension, but the electrical conductivity falls as a result of the higher polymer content. This difference will manifest as larger fibres produced by the PCI 15 solution compared to PCI 10. The PCI stock solutions used DMF and THF (50:50 weight.) as the solvent.

The BC solutions showed an interesting difference in viscosity. The BC stock solution was made up with DMF only, which has a lower electrical conductivity relative to THF [188]. Adding the BC solution to the PCI stock reduced the viscosity. The BC solution was made at 10wt%, weight for weight it has a similar polymer content to PCI 10 and less than the PCI 15, meaning the BC solution diluted the PCL stock solutions reducing viscosity. The increase in PCI concentration alone has a greater impact on the viscosity compared to the addition of BC, the difference in size between PCIBCGb-10 will not be as great as PCI 15 and PCI 10. The addition of Gb slightly increased the electrical conductivity. This could possibly be due to the release of ions from the drug molecule. Cl⁻, N⁻, S⁻ or H⁺ ions could be present in the solution triggering the increase in conductivity. A lower voltage would need to be applied to solutions with a higher conductivity. Gb powder was added directly to the PCI-BC blends, no added solvent was used to largely effect the viscosity.

5.1.2 Production of PCI-BC-Glybenclamide fibres

Using the portable EHD set up described in **Section 3.5.2**, the previously described solutions were processed and non woven wound healing patches were formed. Table 15 describes the processing parameters used to produce the various samples.

Table 15: Processing parameters used to electrospin polycaprolactone, bacterial cellulose and glybenclamide solutions.

Solution	Voltage (kV)	Flow rate ($\mu\text{L min}^{-1}$)	Collector distance (cm)
PCI 10	9	50	13
PCI 15	8.5	50	13
PCIBC-10	23	10	13
PCIBC-15	21.3	10	13
PCIBCGb-10	22	50	13
PCIBCGb-15	20.9	50	13
PCIGb-10	19.7	50	13
PCIGb-15	20.6	50	13

Plain PCI, PCI-BC, PCI-Gb and PCI-BC-Gb solutions were all electrospun to compare the different *in vitro* behaviours. As BC was primarily added for its absorption capacity, it was therefore necessary to compare the swelling/absorption capacity of plain PCI against PCI-BC blend.

This portable unit has featured in the literature [190] producing various fibrous patches for wound healing purposes [86, 213]. The first publication to

demonstrate this capability was Lau *et al.* where PLGA waterproof wound dressings were produced with the potential to be used *in situ* [190].

5.2 Characterisation of PCI-BC-Glybenclamide electrospun patches

Adding BC to PCI changes both the morphological and intrinsic characteristics such as swelling and more importantly, drug release behaviour. As PCI is a hydrophobic polymer, it releases encapsulated agents through the diffusion controlled method. This has been shown by Luong-Va *et al.* where heparin was released from electrospun PCL fibres, but no degradation of the polymer fibre was observed post *in vitro* testing [214], supporting the previous statement. The large water holding capacity of BC [215] will have an impact on the drug release rate, as more water is drawn into the fibre this could impact the amount of drug that diffuses out. In addition this PCI-BC blend has been tested beforehand with Saos-2 cell line (Homo sapiens bone osteosarcoma, ATCC HTB-85), where the cell viability test gave a result of 89% [86].

Blending the two polymers as opposed to using a co-axial set up is essential as BC cannot be electrospun alone. Even with a core-sheath arrangement, with the PCI on the outer sheath coating the BC, its hydrophobic property will shield the BC from water inactivating its swelling property this blend is trying to exploit. Inversely, using PCI as the core polymer to drive the spinning, the BC may not adhere to the core material and disperse into the system, rendering the bandage useless.

Elemental analysis, energy dispersive spectroscopy (EDS), was used to determine the presence of glybenclamide (Gb). Both the polymers used were

hydrocarbons, containing only carbon, hydrogen and oxygen. Gb, however, is a sulfonylurea, whilst atomically it is mostly made up of carbon and hydrogen, $C_{23}H_{28}ClN_3O_5S$, the presence of chlorine and sulphur make it distinguishable from the polymer matrix. Therefore EDS is the ideal technique to establish the presence of Gb in the fibres made.

5.2.1 Effect of concentration of PCI on morphology and diameter of fibres

Increasing the concentration of PCI within the blend gave rise to an increase in fibre diameter as expected. PCIBCGb-10 fibres had an average diameter of $0.57\ \mu\text{m}$ whereas, PCIBCGb-15 was larger at with an average of $1.30\ \mu\text{m}$. The presence of BC also had an effect on the size of the fibres shown in **Table 16**.

Comparing PCI 10 with PCI 15, there is an increase in the diameters produced. As shown in Fig. 37 increasing the concentration shows a complete omission of beads to almost completely smooth fibres, with PCI 15 having much thicker but bead free fibres. As previously described in **Chapter 4** the increase in polymer concentration buffers against instabilities which bring about beading. The loss of beading, contributes to the increase in fibre diameter, along with the greater level of entanglement brought about by the increase in concentration [201].

Table 16: Showing fibre diameters of BC and PCL-BC-Gb fibres

Type	Fibre diameter (μm)
PCI 10	0.24 ± 0.14
PCIBCGb-10	0.57 ± 0.2
PCI 15	2.16 ± 0.74
PCIBCGb-15	1.30 ± 0.5

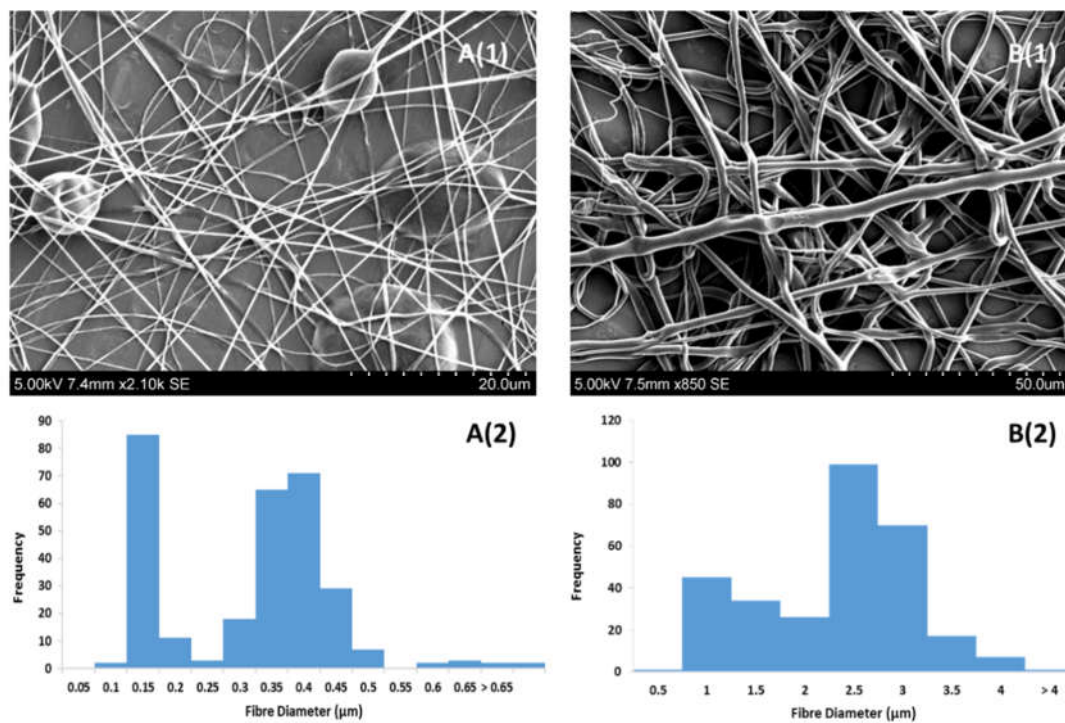


Figure 38: A(1) SEM image of 10wt% PCI fibres with A(2) accompanying histogram of fibre size. B(1) SEM image of 15wt% PCI fibres with B(2) accompanying histogram

Comparing plain 10wt% PCI fibres with PCIBCGb-10 (Fig. 38), the addition of BC and Gb appears to have pushed to fibre distribution from a near bimodal distribution to a standard distribution shape. The increase in conductivity and viscosity has reduced the beading almost completely, more than doubling the size

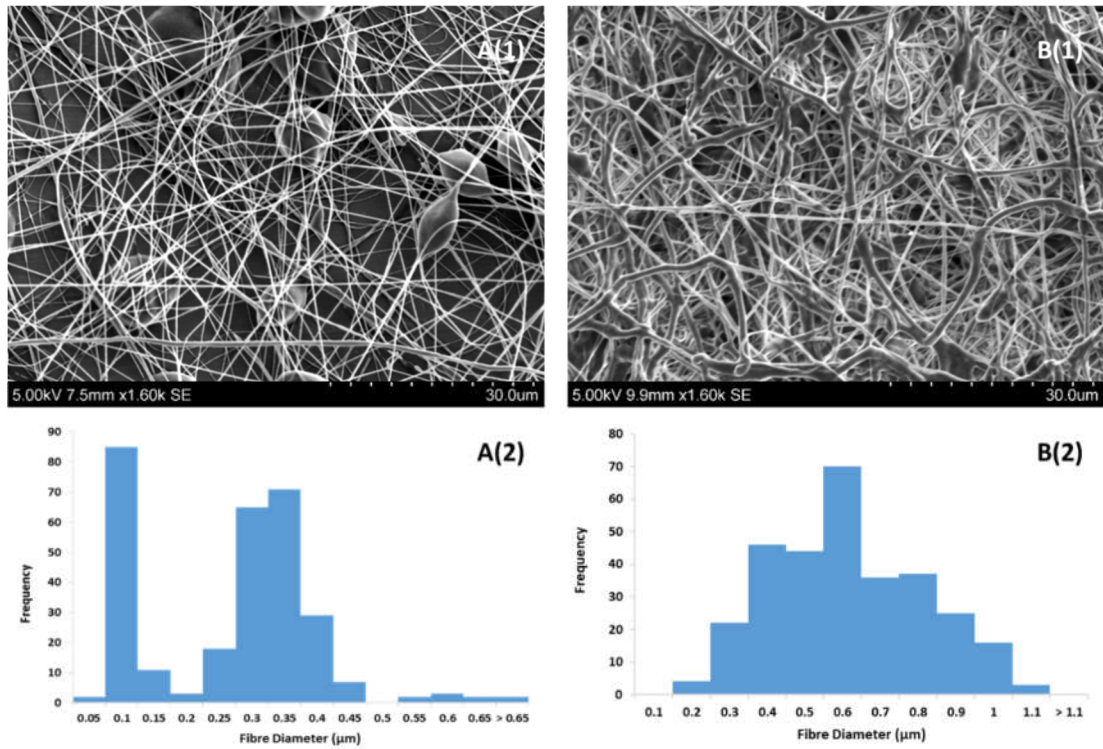


Figure 39: A(1) SEM image of 10wt% PCI fibres with A(2) accompanying histogram of fibre size. B(1) SEM image of PCIBCGb-10 fibres with B(2) accompanying histogram

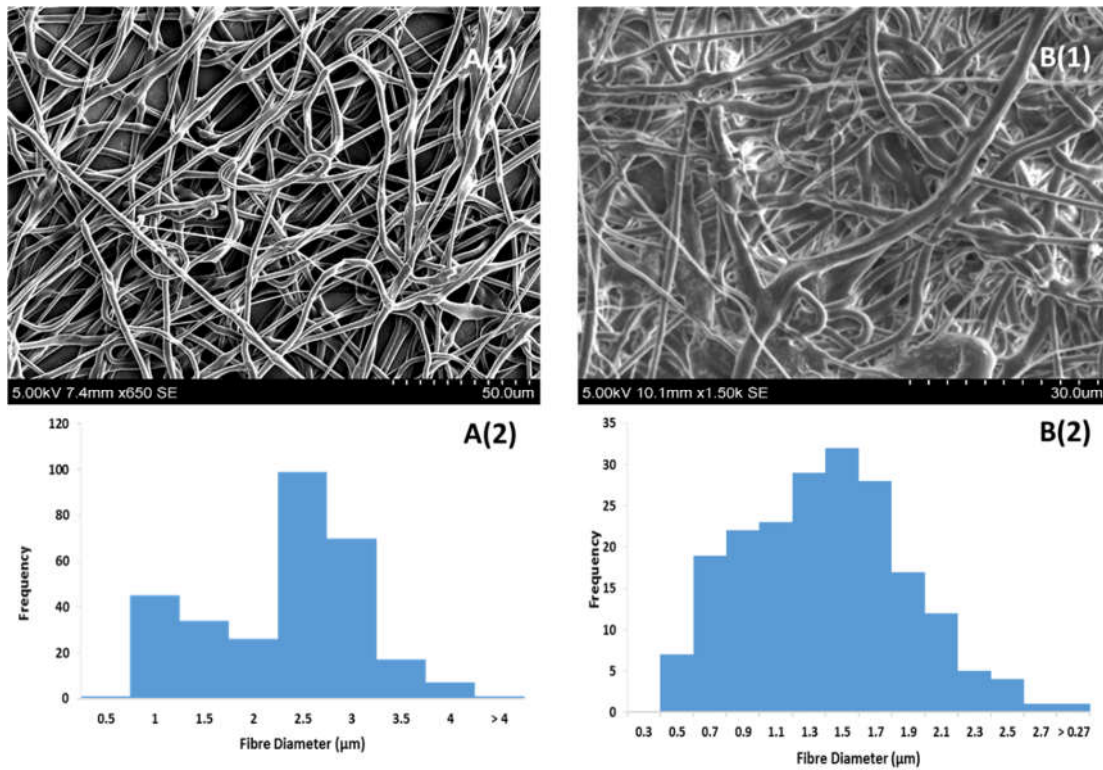


Figure 40: A(1) SEM image of 15wt% PCI fibres with A(2) accompanying histogram of fibre size. B(1) SEM image of PCIBCGb-15 fibres with B(2) accompanying histogram

The difference in morphology between PCI 15 and PCIBCGb-15, is not very obvious. However, the addition of BC and Gb in this instance has driven down the average fibre diameter from to 2.16 μm to 1.30 μm but as with PCIBCGb-15 has produced a more standard distribution of sizes.

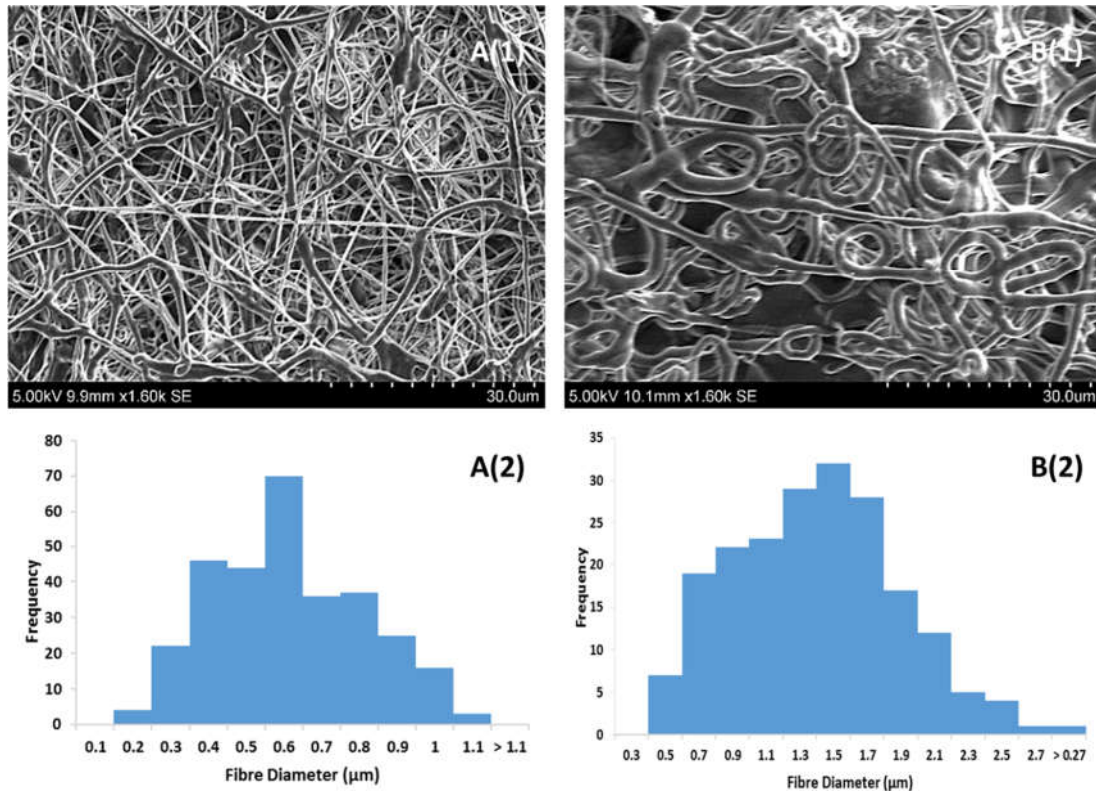


Figure 41: A(1) SEM image of PCIBCGb-15 fibres with A(2) accompanying histogram of fibre size. B(1) SEM image of PCIBCGb-10 fibres with B(2) accompanying histogram

PCIBCGb-10 PCIBCGb-15

5.2.2 Energy-dispersive X-ray spectroscopy

Elemental analysis was used to ensure the Gb incorporated into the solutions was present in the products made. Although, it was clear the drug dissolved in the solution, it could potentially have dropped out of suspension whilst being processed or the electric field could have brought about some separation

between the polymers and the drug. To begin with, the virgin drug was analysed to acquire a baseline, this is shown in Fig. 41, which showed sulphur present at 26.93% and chlorine at 28.3%.

As per the elemental composition of Gb, $C_{23}H_{28}ClN_3O_5S$, the most distinguishable atoms from the polymer matrix and natural atmosphere were chlorine and sulphur. These elements were used as confirmation that Gb was present in the fibres made. Fig. 42 shows the elemental spectrum for PCIBCGb-10, sulphur was present at 8.93% and chlorine was present at 7.55%.

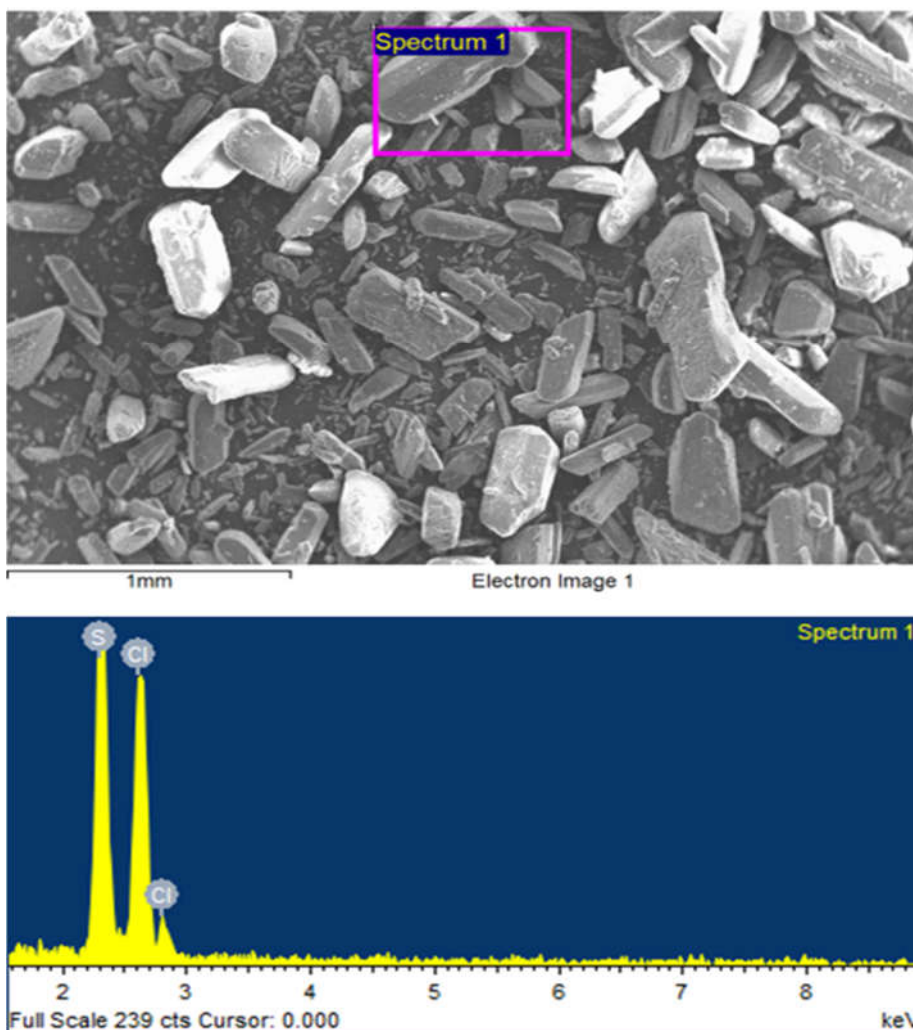


Figure 42: SEM image and elemental dispersive spectrum of glybenclamide drug

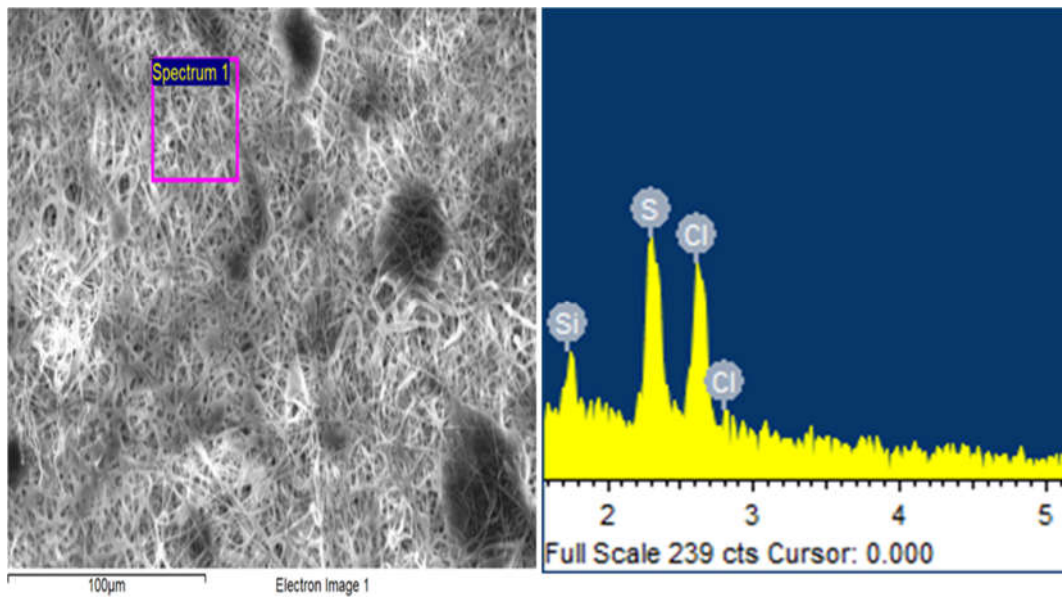


Figure 43: SEM image and elemental dispersive spectrum of PCIBCGb-10

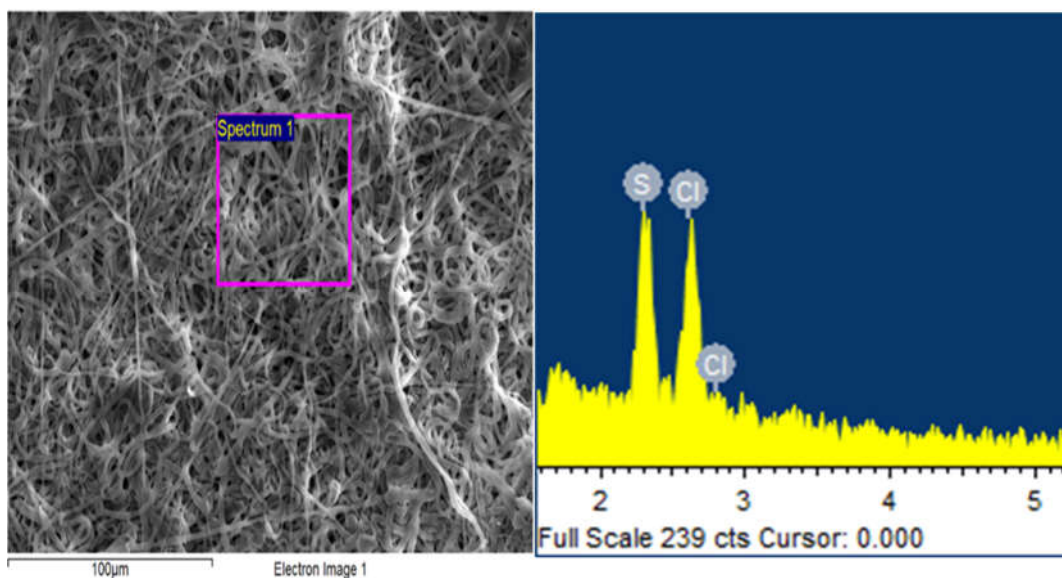


Figure 44: SEM image and elemental dispersive spectrum of PCIBCGb-15

The PCIBCGb-15 showed chlorine at 0.64% and sulphur at 0.81%. These lower values are representative of the higher polymer concentration used for PCI encapsulating the drug.

5.3 *In vitro* testing

PCI has good drug permeability and is used for long term drug delivery as it degrades slowly [216]. However, blending PCI with another polymer that interacts differently with water could possibly change this. The effect bacterial cellulose has on the drug release profile of PCI has yet to be investigated. As BC is hydrophilic, it will also have a great impact on the swelling properties of the composite.

5.3.1 Effect of BC on swelling characteristics

The excess exudate produced by diabetic foot ulcers is a problem this composite is trying to address. The nature of BC allows it large volumes of liquid to be absorbed and retained, this means the wound will be less susceptible to maceration and necrosis, allowing healing to progress normally.

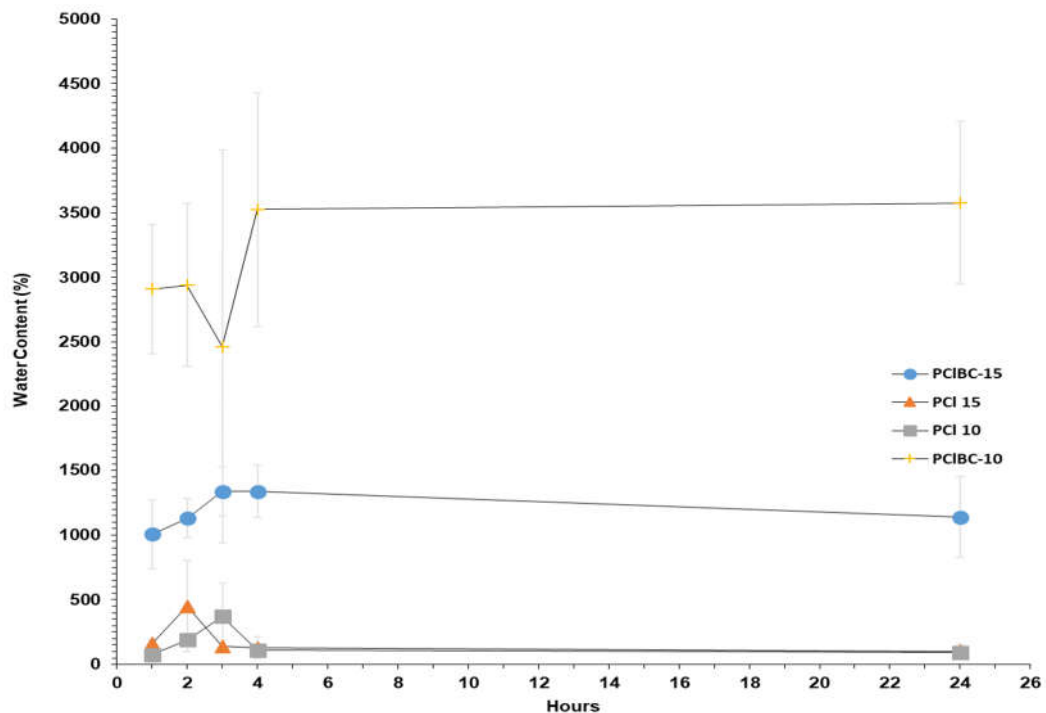


Figure 45: Graph showing swelling behaviours of PCI and PCL-BS patches over time

The effect of BC in the blend has a clear influence on the swelling behaviour. The PCI samples displayed a lesser degree of swelling compared to PCI-BC samples. Comparing the peak values for each sample; PCI 10 peaking at 369.47% at 3 h and PCI 15 peaking at 448.42% at 2 h. Whereas, PCIBC-10 peaked at 3575% at 24h and PCIBC-15 peaked at 1137.43% at 3 h.

Table 17: Showing swelling value over time with peak swelling values highlighted

Time point (h)	PCI 10 (%)	PCI 15 (%)	PCIBC-10 (%)	PCIBC-15 (%)
0	0	0	0	0
1	75.56	158.32	2908.33	1006.52
2	187.48	448.42	2937.50	1130.18
3	369.47	138.35	2462.50	1337.43
4	110.92	127.69	3525.00	1336.94
24	91.20	100.38	3575.00	1138.08

All samples showed an initial swell followed by a deswell, except PCIBC-10, which did not follow this trend. PCIBC-10 displays an incremental increase followed by a deswell and sharp increase. However, all showed little difference between 4 and 24h time points, the samples may have possibly reached an equilibrium point during this time. As the swelling test was carried out in a water bath set at 37 °C, the patches suspended in PBS heated up causing an initial infiltration into the polymer matrix. However, as the material equilibrates, some water is expelled and eventually an equilibrium state is found.

The difference between PCI 10 and PCI 15 is not substantial. However, PCL10 peaks an hour later than PCI 15. The difference in polymer concentration can result in differences in fibre density and porosity in the

patches made, leading to this variation. PCI 15 would have a higher fibre density as the fibres from this solution are larger, giving it greater porosity.

Comparing the PCI 10 with the PCIBC-10, from **Table 18**, the differences between the time points range from 6 times higher to 39 times greater. These are much greater than PCI 15 to PCIBC-15 comparison. The lower PCI concentration does not disrupt the BCs ability to take absorb the fluid, but it does appear to disrupt the swelling and deswelling progress the other samples follow. Perhaps PCI 15 stabilises this.

Table 18: Showing swelling value of PCL10 and PCI10BC10 and their ratio

Time point	PCIBC-10	PCI 10	PCIBC-10/PCI 10
0	0	0	0
1	2908.33	75.56	38.49
2	2937.50	187.48	15.67
3	2462.50	369.47	6.67
4	3525.00	110.92	31.78
24	3575.00	91.20	39.20

Looking at PCI 15 against PCIBC-15, shown in Table 18, the difference are less than the previous two, ranging from 2 times to 11 times higher. The higher concentration of PCI appears to restrict the absorption ability of BC, the higher concentration may give rise to a higher strength matrix that entraps the BC fragments physically stopping the BC taking on more liquid.

Table 19: Showing swelling value of PCL 15 and PCIBC-15 and their ratio

Time point	PCIBC-15	PCI 15	PCIBC-15/PCI 15
0	0	0	0
1	1006.52	158.32	6.36
2	1130.18	448.42	2.52
3	1337.43	138.35	9.67
4	1336.94	127.69	10.47
24	1138.08	100.38	11.34

5.3.2 Effect release of glybenclamide from PCI-BC

PCI degrades via a hydrolytic mechanism in *in vivo* conditions [217]. The ester groups within the chain are cleaved hydrolytically leading to random chain scission [218]. Other mechanisms include erosion (bulk or surface), diffusion, disintegration and desorption. As two different concentrations of PCI were used they could have affected the release profiles of the different patches. As the 15wt% PCI reduced the effect of BC on the swelling behaviour it would be reasonable to speculate it would also have an impact on the drug release profile.

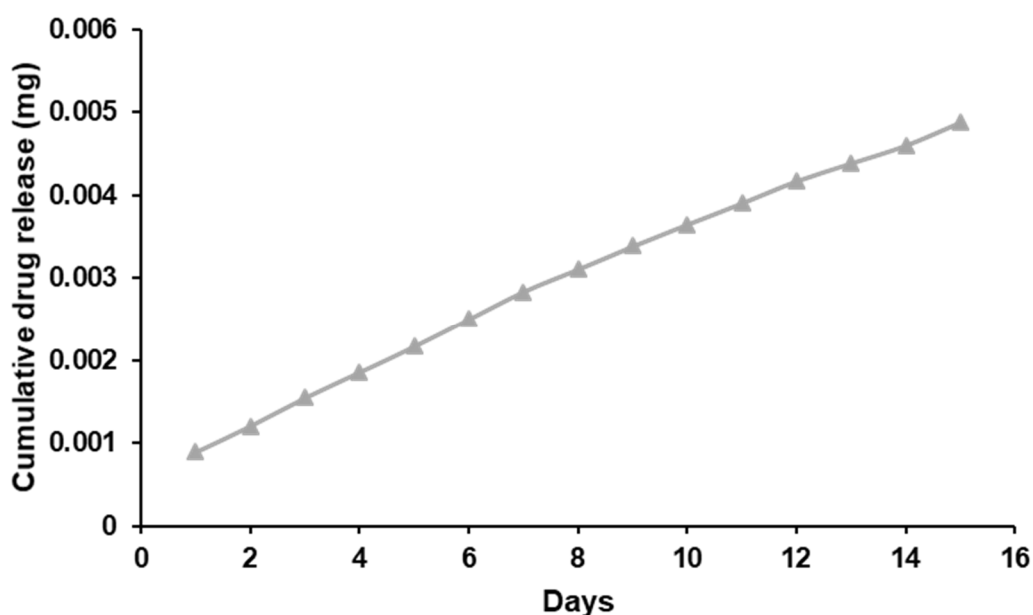


Figure 46: Drug release profile from PCIBCGb-10

This release follows a near linear pattern for the 15 days. PCI releases the glybenclamide (Gb) through a diffusion controlled mechanism, visually there was no changes to the fibres post release test indicating on polymer erosion or degradation occurred.

The release profile of PCIBCGb-15, Fig 46, is almost identical to the trace of PCIBCGb-10. A similar burst within the first 24 hours and near linear line for the entire 15 days. This is supported by Fig 47, which shows both release profiles overlaid and they are almost identical, with negligible differences.

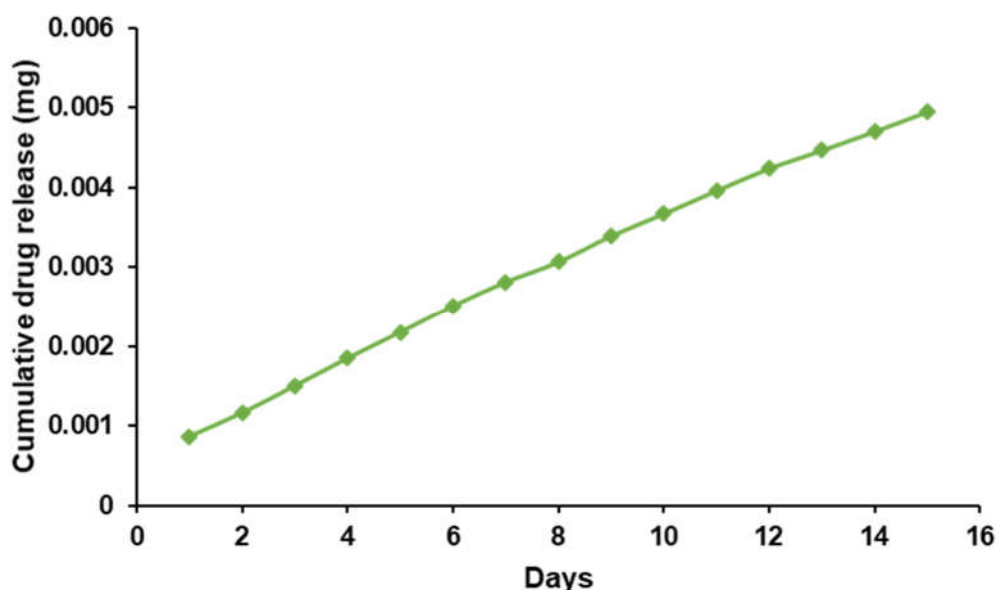


Figure 47: Drug release profile from PCIBCGb-15

Choosing between the two as the release profiles have no difference, PCIBCGb-10 would be the better choice simply because this option uses less polymeric material making it less consumptive.

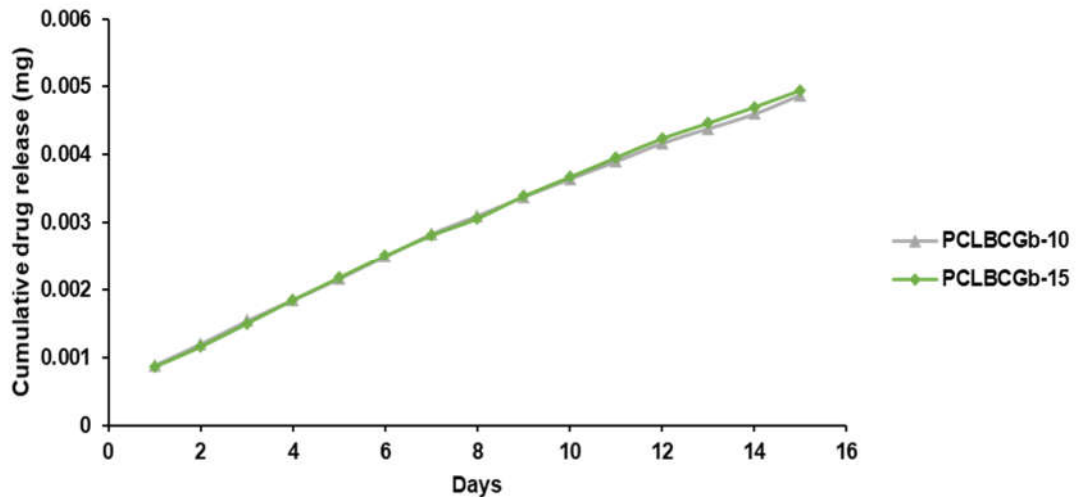


Figure 48: Comparison between PCIBCGb-10 and PCLBCGb-15

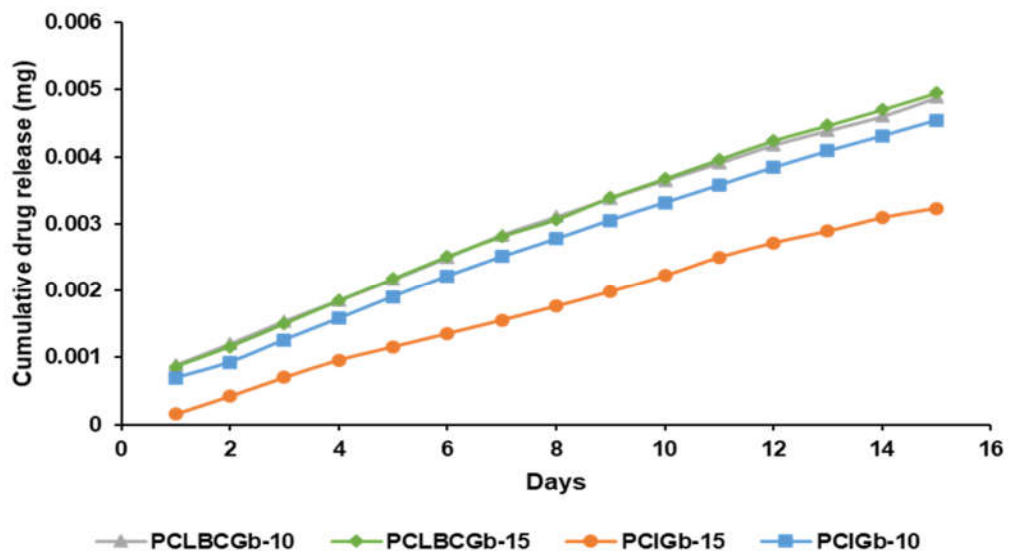


Figure 49: Release profiles of all four PCI based fibres

The presence of BC has a noticeable effect on the delivery of glybenclamide. Drug release was higher for all time points of the PCI-BC blends compared to the PCI only fibres. The increased swelling in PCI-BC fibres, demonstrated in **Section 5.3.1**, could have accelerated the hydrolytic degradation of the PCI, as more water infiltrated the fibre network due to the hydrophilic nature of BC. However, it is also possible some drug had been encapsulated in the BC fragments within the fibre, which again was released through the swelling of the fibre as water infiltrates.

6 Chapter 6

Results and Discussion

Production of gelatin and bacterial cellulose wound healing patches doped with Glybenclamide and Metformin using electrohydrodynamics

Overview

Wound dressings made from natural polymers are an important aspect of biomaterials. Protein based materials are less likely to instigate an immunogenic response and have the capacity to degrade *in vivo*, also without triggering an inflammatory response [219]. This combination, with bacterial cellulose, was produced in order to determine the validity of an all natural polymer construct. Gelatin and bacterial cellulose were electrospun with metformin (**section 6.1**) and glybenclamide (**section 6.2**). The surface morphologies and elemental constitutions were tested. Comparisons were made between the drug release profiles of cross linked and non cross linked fibres. Although there has not been many examples of metformin used in wound healing there has been some studies that have shown diabetic patients that have taken metformin have reduced the levels of pro inflammatory cytokines [185, 187, 220-224]. There is one example in the literature of drug eluting PLGA fibres doped with metformin for wound healing applications [186].

Solution	Voltage (kV)	Flow rate ($\mu\text{L min}^{-1}$)	Collector distance (cm)
Gel			13
Gel-BC			
Gel-Met	19.9	10	13
Gel-Gb	22.1	7	13
PCI(95)-BC(5)-Met	18	10	13
PCI(95)-BC(5)-Gb	19.7	10	13

6.1 Gelatin with Bacterial Cellulose and Metformin

Metformin is another commonly prescribed treatment for type 2 diabetes, one of its actions is to increase the sensitivity to insulin. This has been shown to indirectly help in wound healing as insulin resistance has been shown to hinder healing by affecting the contraction and re epithelialisation [225, 226]. The fibres were designed to release metformin with comparisons between the release mechanisms between gelatin only and gelatin blended with bacterial cellulose.

6.1.1 Fibres

Fibres produced from gelatin only

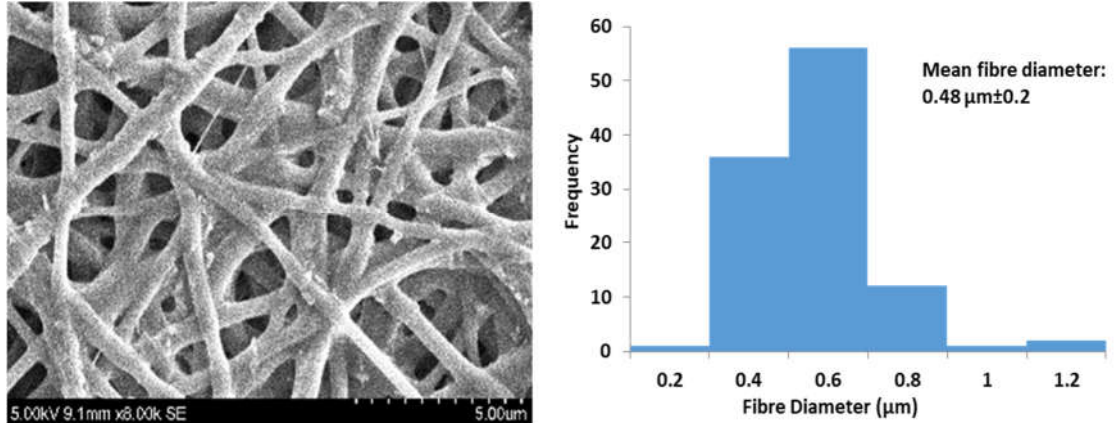


Figure 50: Gelatin and Met fibres with fibre diameter distribution

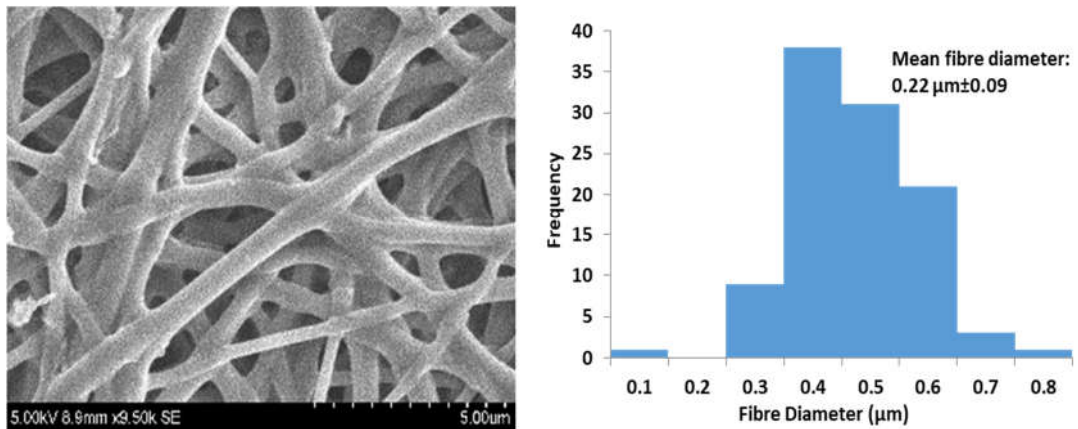


Figure 51: Gelatin, BC and Met fibres with fibre diameter distribution

6.1.1 Elemental analysis

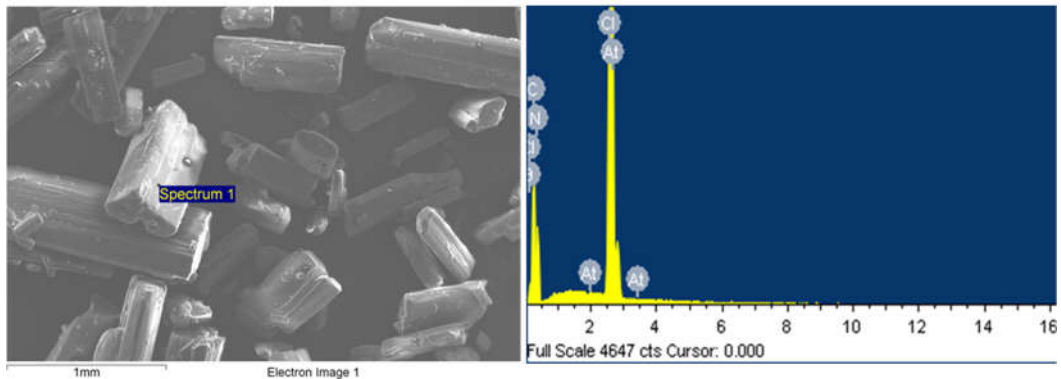


Figure 52: SEM image and elemental dispersive spectrum of metformin drug

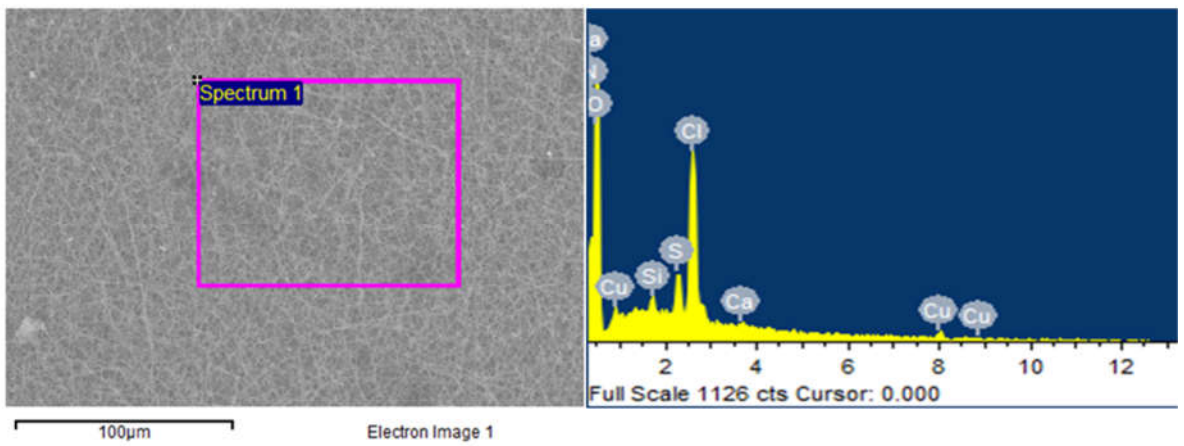


Figure 53: SEM image and elemental dispersive spectrum of Gel-Met

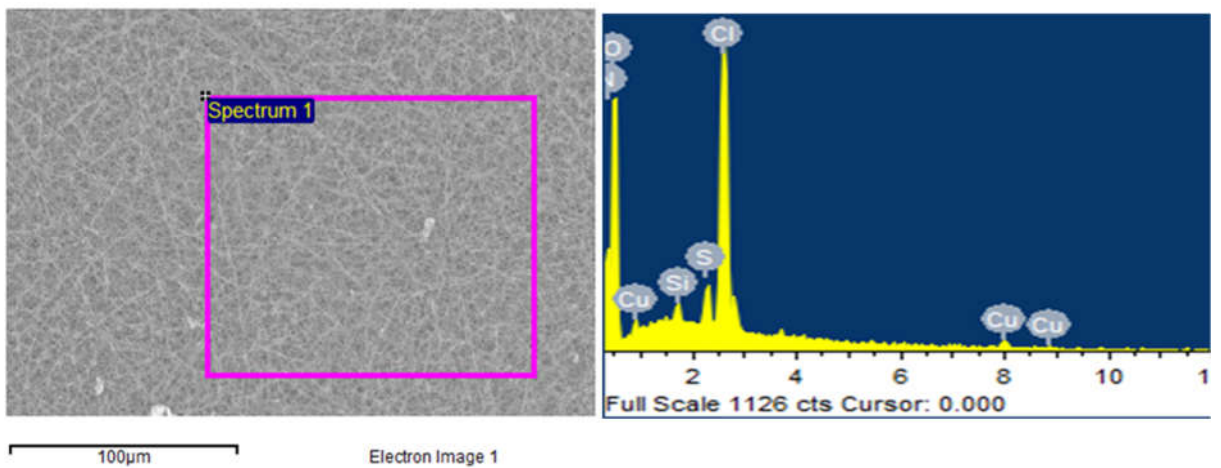


Figure 54: SEM image and elemental dispersive spectrum of Gel-BC-Met

6.1.2 Drug release

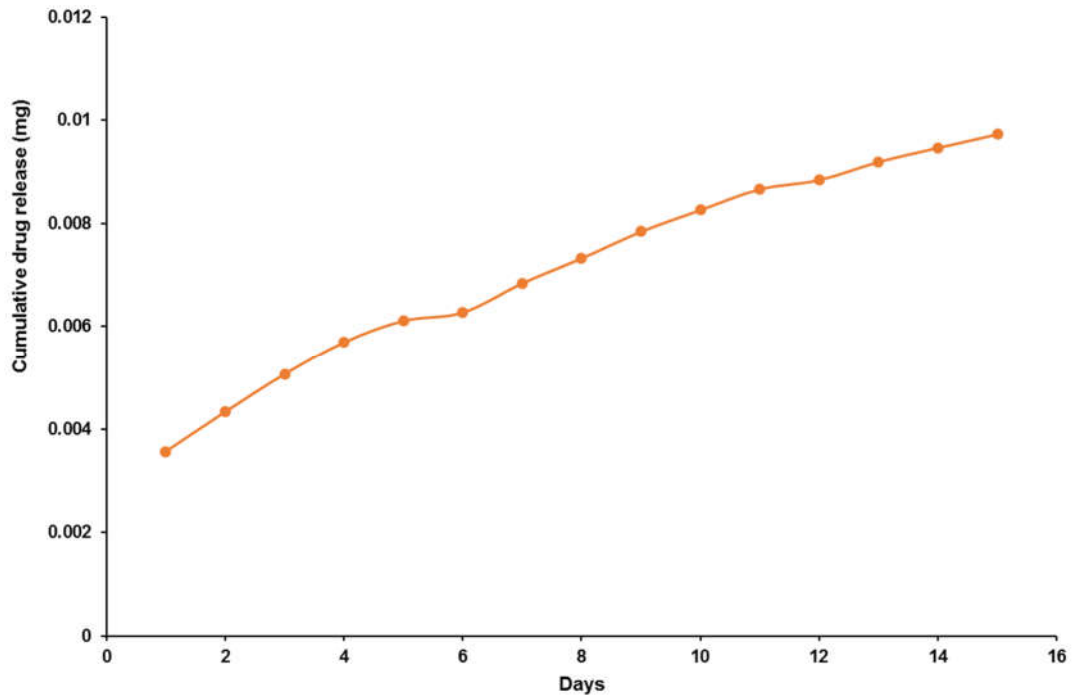


Figure 55: Release of Met from cross linked Gel only

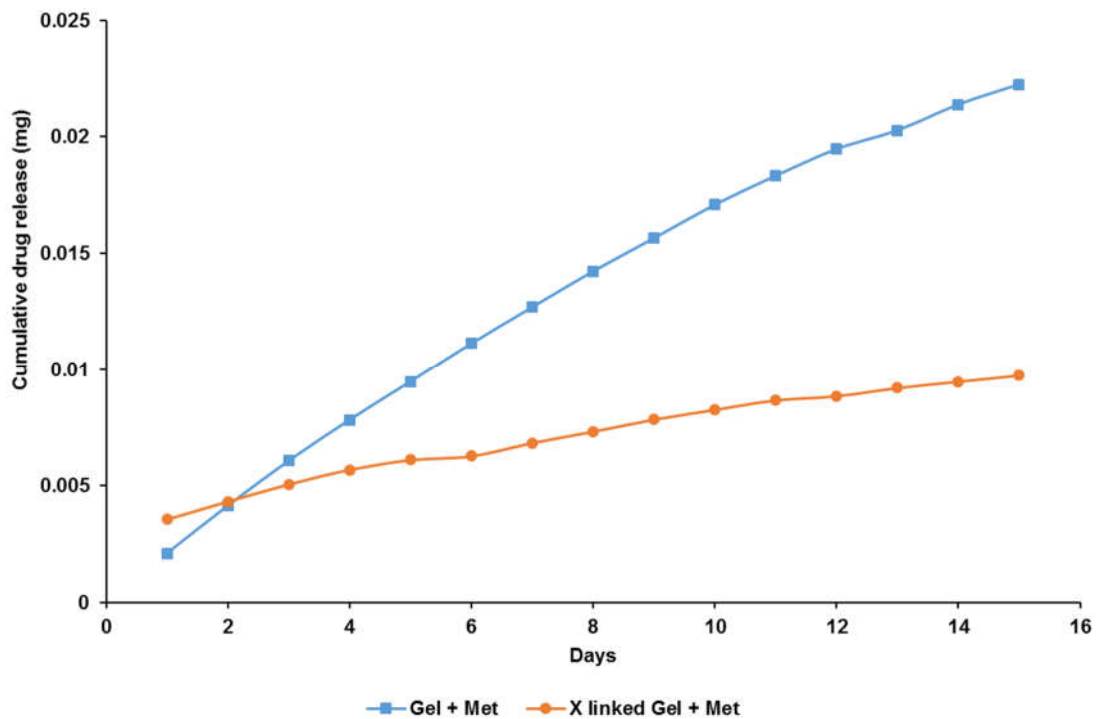


Figure 56: Release of Met from cross linked Gel compared to non cross linked Gel

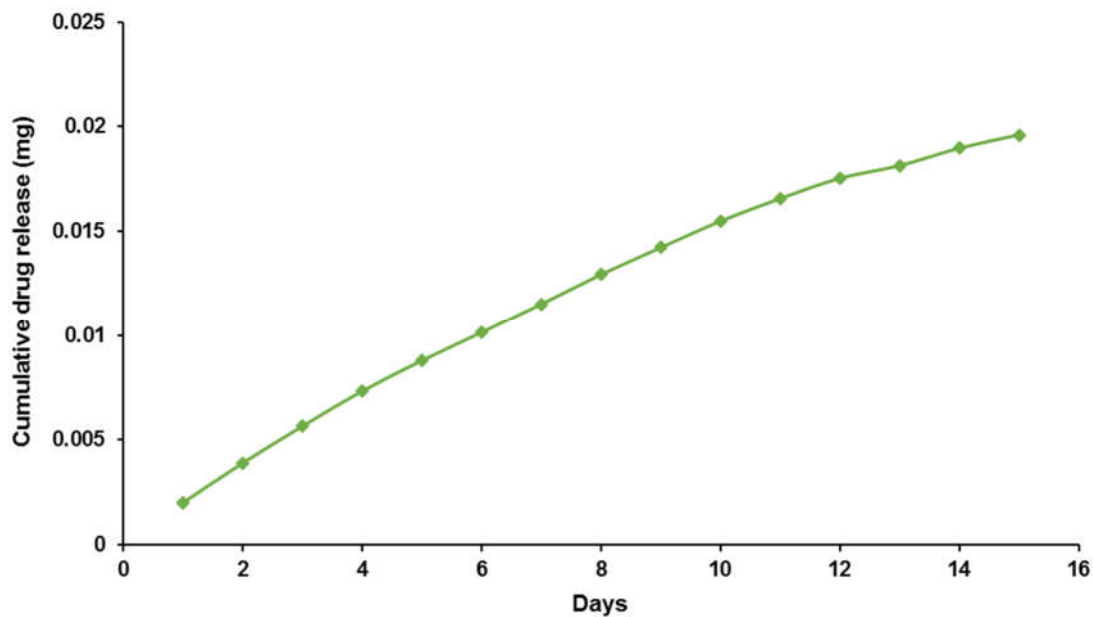


Figure 57: Release of Met from cross linked Gel-BC only

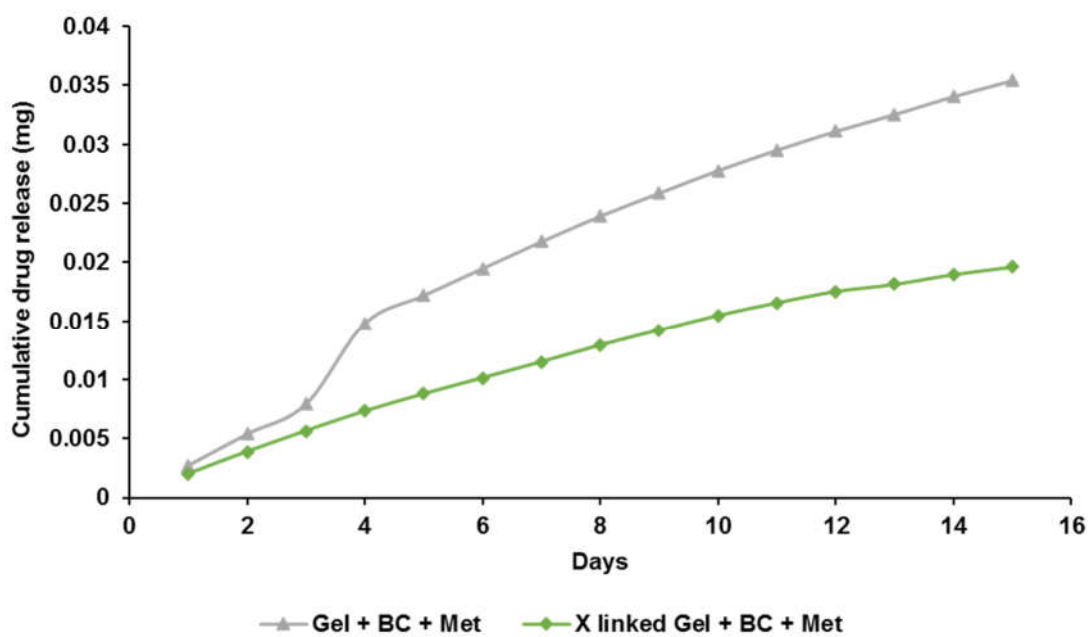


Figure 58: Release of Met from cross linked Gel-BC compared to non cross linked Gel-BC

6.2 Gelatin with Bacterial Cellulose and Metformin

6.2.1 Fibres

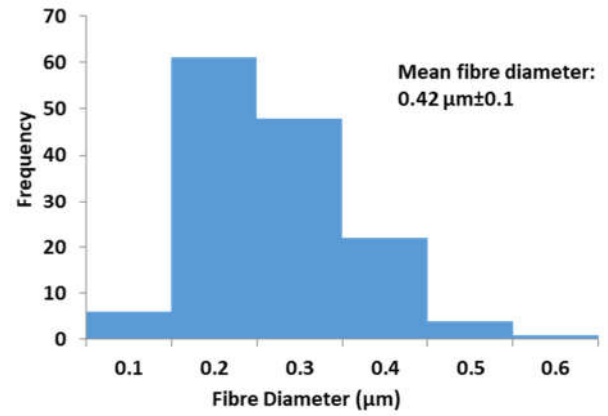
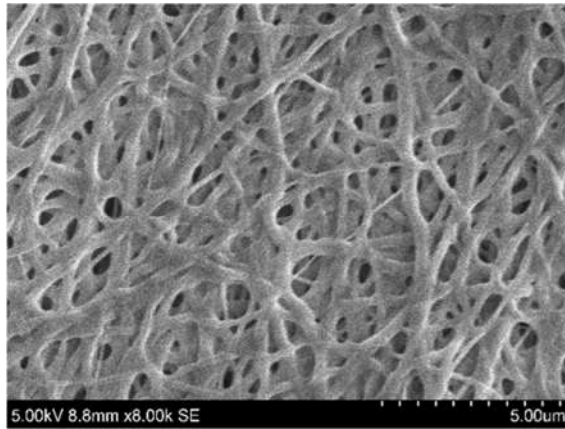


Figure 59: Gelatin and Gb fibres with fibre diameter distribution

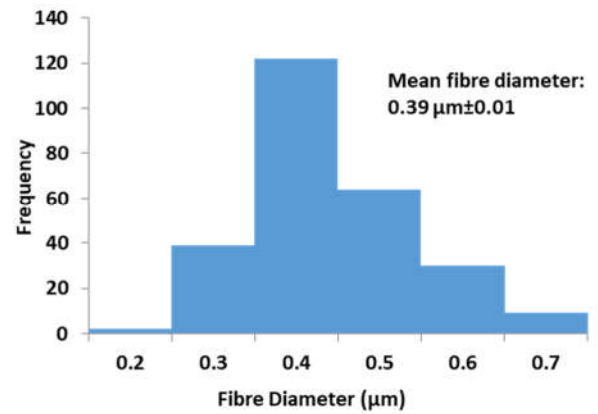
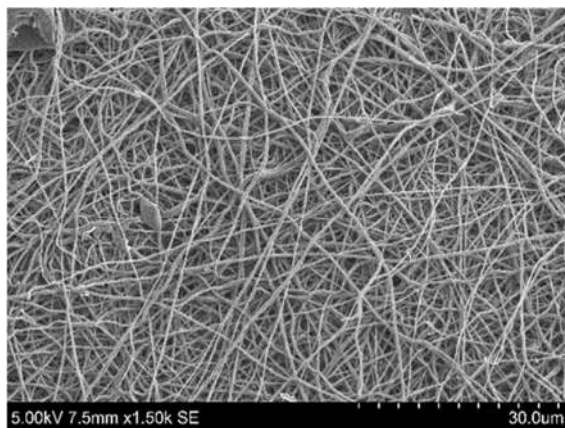


Figure 60: Gelatin-BC and Gb fibres with fibre diameter distribution

6.2.2 Elemental analysis

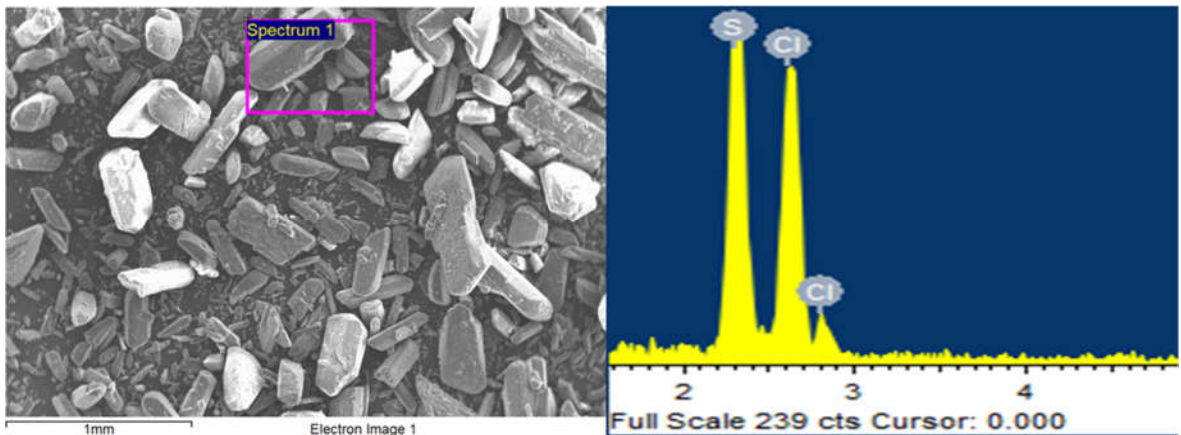


Figure 61: SEM image and elemental dispersive spectrum of glybenclamide drug

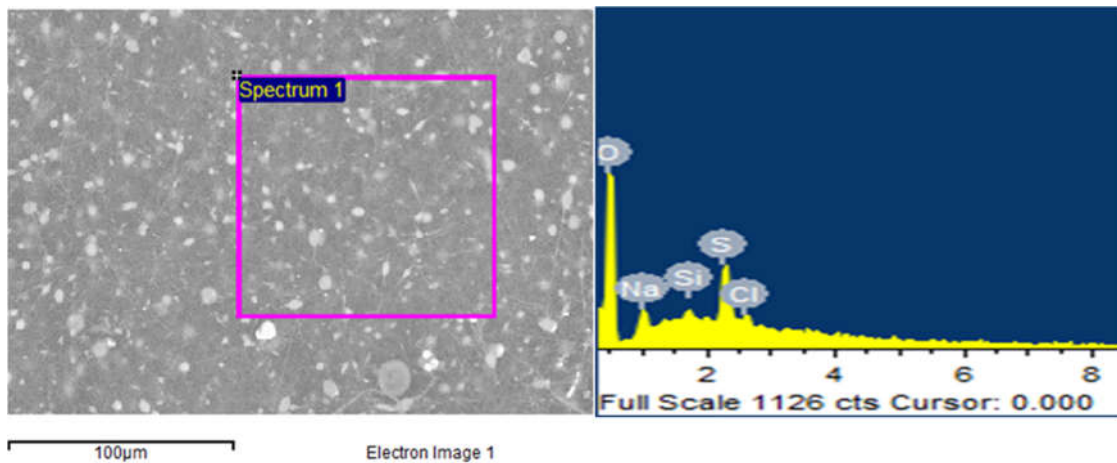


Figure 62: SEM image and elemental dispersive spectrum of Gel-Gb

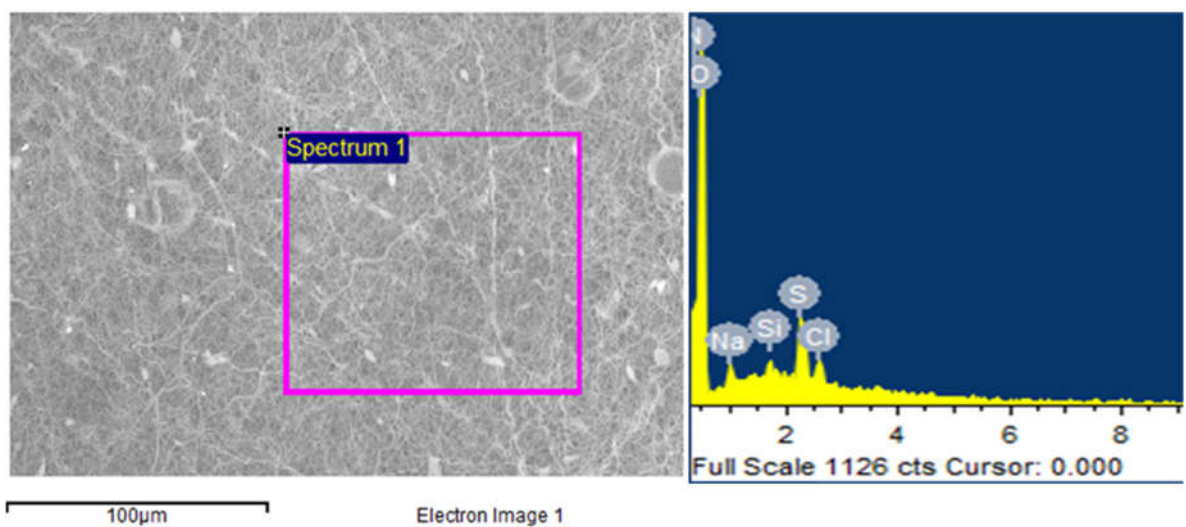


Figure 63: SEM image and elemental dispersive spectrum of Gel-BC-Gb

6.2.3 Drug release

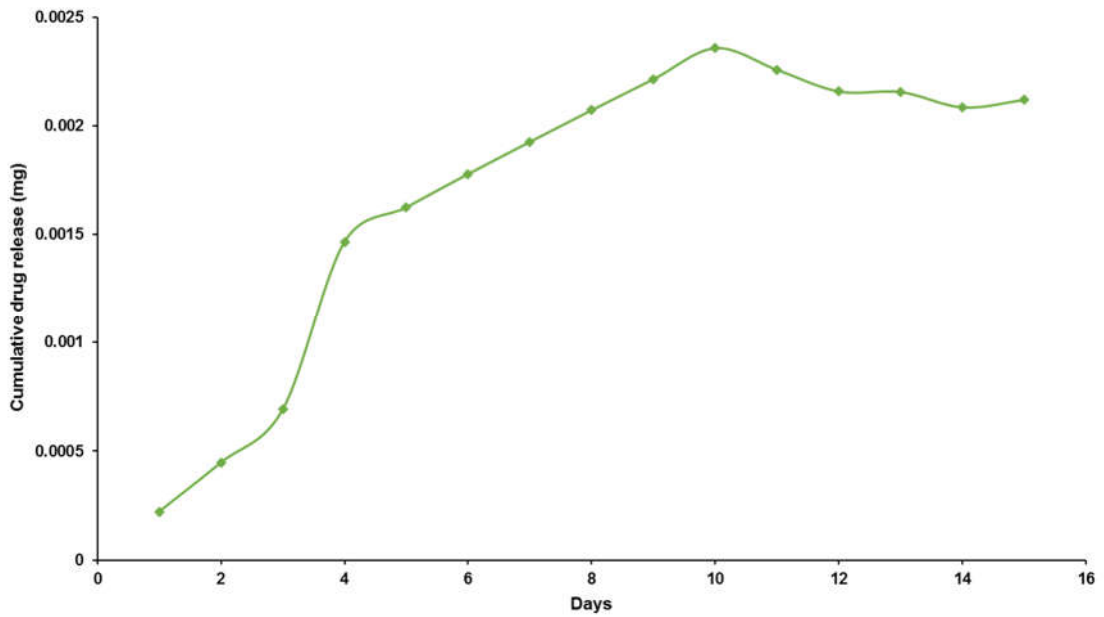


Figure 64: Release of Gb from cross linked Gel only

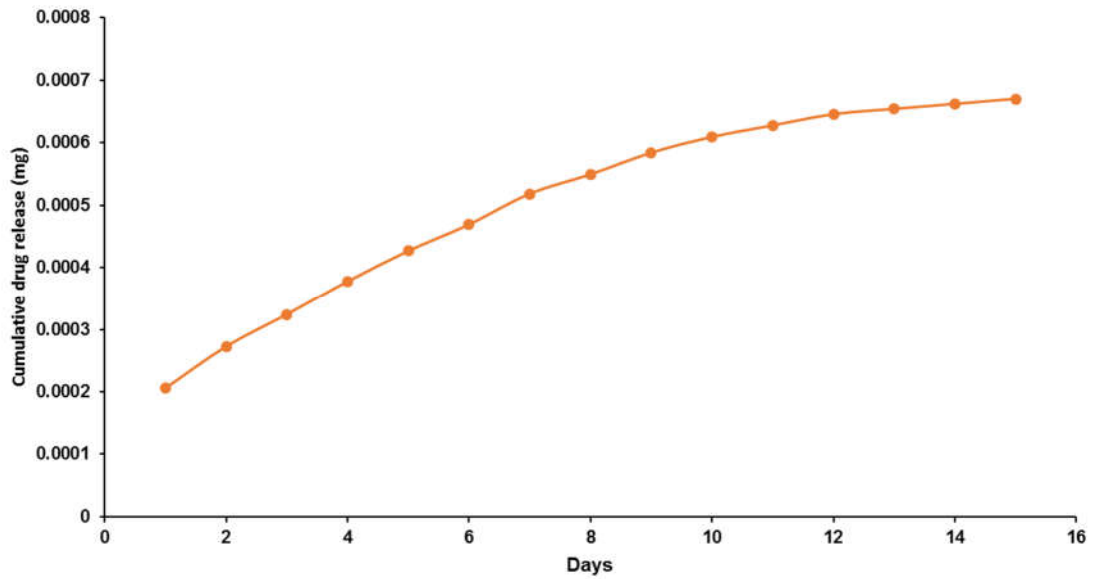


Figure 65: Release of Gb from cross linked Gel compared to non cross linked Gel

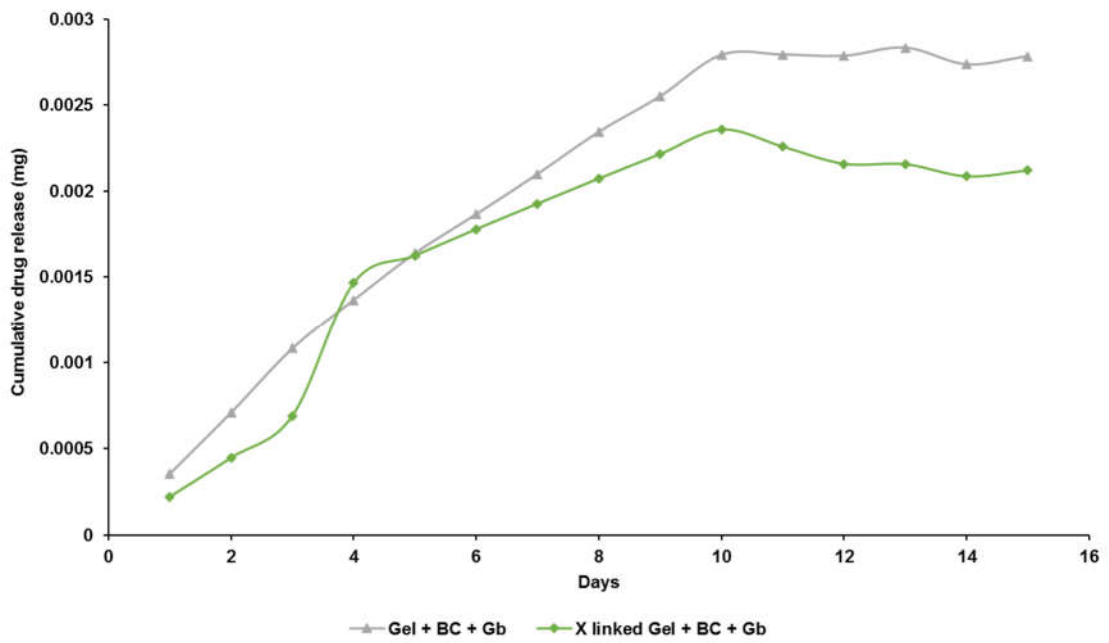


Figure 66: Release of Gb from cross linked Gel-BC only

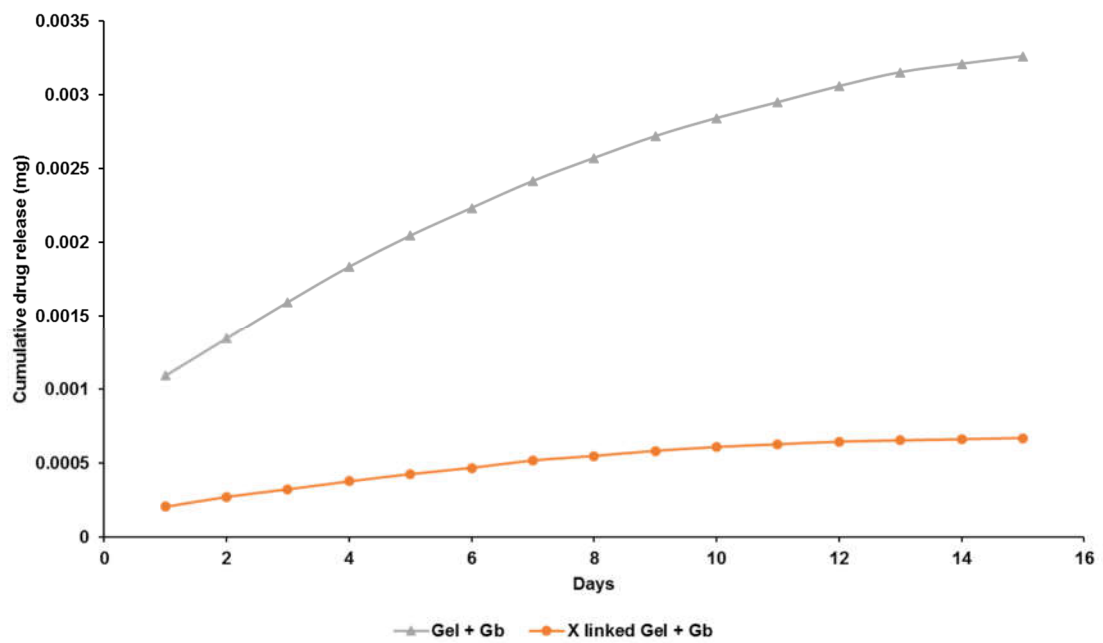


Figure 67: Release of Gb from cross linked Gel-BC compared to non cross linked Gel-BC

7 Chapter 7

Conclusions and future work

7.1 Conclusion

The overall theme of this work was to exploit the favourable properties of various cellulose derivatives in a way that was conscientious of safety. This was achieved through observing the effect various processing and solution parameters had on the morphology of the microstructures produced.

Secondly was, using the electrospinning method to make a biomedically relevant material more accessible. Bacterial cellulose's contribution to the healing process has been established. But the as-produced membrane is very inconvenient, and a more appropriate application method is required in order to bring the appeal to the masses. This was achieved by the addition of a spinning agent, and relevant API, a multi-faceted wound healing patch aimed to aid the healing of chronic diabetic foot ulcers.

7.1.1 Electrospinning ethyl cellulose derivatives with ethanol and water

A range of ethyl cellulose microstructures were produced as a result of manipulating solution (polymer concentration) and processing properties. Lower polymer concentrations 5-15wt% gave rise to particles, at 20wt% beaded fibres were formed, from 25 to 30wt% fibres of increasing diameters were made.

When higher voltages were applied, for the same concentration, instabilities came into play causes beading and irregular fibres to form. Across the different

concentrations this demonstrated a window for the ideal voltage to give rise to “smooth” fibres. The flow rate had a linear relationship. The higher flow rate (100 μ L) gave rise to thicker fibres, the opposite was true for fibres made at the lower flow rate (50 μ L). Inversely, the tip to collector distance had a contrary relationship with the fibre diameter, at the larger distance (150 mm) smaller structures formed and vice versa. Any combination of these parameters could be used to control the size of the structures.

7.1.2 Electrospinning of cellulose acetate

This work showed the morphology of the cellulose acetate fibres could be drastically changed by with changing the solvent proportions of water and acetone or polymer concentration. Increasing the water content of the binary solvent used smoothed the appearance of the fibres, as did increasing the polymer concentration.

Using an auxiliary plate, only affected the fibre diameter making no changes to the morphology itself.

Being able to use water in dissolving cellulose acetate makes its use even more favourable in biomedicine as residual solvent will be less of a problem.

7.1.3 Electrospinning of carboxymethyl cellulose

The effect of changing the CMC molecular weight had the expected effect in increasing the fibre diameter. As did changing the ratio between CMC and PEO spinning agent, a higher CMC content brought down the fibre size due its lower molecular weight.

7.1.4 Production of PCI-BC-Gb wound healing patches

The comparison between PCI10BC10Gb10 and PCI15BC10Gb10 ultimately only showed a difference in the swelling behaviour and not in their release profiles. The lower concentration of PCI gave the bacterial cellulose more flexibility to uptake a greater amount of fluid, which is an important aspect in treating diabetic foot ulcers. Also, using less material to produce it (10wt% as opposed to 15wt%) is also better.

7.2 Future work

7.2.1 Wound healing assays

The BC blend fibres were designed to address a number of issues caused by diabetic foot ulcers. There a number of tests to ensure the fibres were able to address them. In this work, *in vitro* testing such as drug release and swelling characteristics were profiled. To follow this and validate the efficacy of the fibre cellular testing is also necessary.

7.2.2 Cytotoxicity testing

The first interactions the fibres should have with cells should be to initially determine if the fibres are cytotoxic. This is done using cell models, in this case, as the fibres are designed to be used topically in direct contact with the skin, keratinocytes would be the most appropriate [227]. This involves culturing the cells in medium with fibres had been exposed to. The fibres are suspended in Dulbecco's modified Eagle's medium (DMEM) and stirred in order to collect eluents, to expose to cells through MTT.

7.2.3 MTT Assay

MTT [(4,5-Dimethylthiazol-2-yl)-2,5-diphenyltetrazolium bromide] assays are colorimetric assays which measure cell viability. Cells are seeded into the wells of a 96 well plate. These are incubated for 24 hours and a specified volume of eluent from the fibres are added to the wells containing cells, there are allowances made for a negative control where only media is added and a positive control where some diluted media with alcohol is added. These are incubated for another 24 hours after which the MTT reagent is added. The MTT reagent is blue and upon interactions with live cells exhibiting the nicotinamide adenine dinucleotide phosphate oxidase enzyme on the cell membrane surface, the reagent is reduced to formazan which purple. The level of MTT cleavage i.e. formation of formazan, is directly proportional to the number of living cells. UV spectroscopy is used to measure the absorption by formazan which can be used to measure the level of living cells [228].

8 References

1. Hon, D.N.-S., *Cellulose: a random walk along its historical path*. Cellulose, 1994. **1**: p. 1-25.
2. Smith, L.E. and D. Steele, *A history of materials and practices for wound management*. Wound Practice and Research, 2012. **20**(4).
3. Forrest, R., D. , *Early history of wound treatment*. Journal of the Royal Society of Medicine, 1982. **75**.
4. Shah, J.B., *The history of wound care*. Journal of the American College of Certified Wound Specialists, 2011. **3**(3): p. 65-6.
5. Klemm, D., B. Heublein, H.P. Fink, and A. Bohn, *Cellulose: fascinating biopolymer and sustainable raw material*. Angew Chem Int Ed Engl, 2005. **44**(22): p. 3358-93.
6. Hilton, J.R., D.T. Williams, B. Beuker, D.R. Miller, and K.G. Harding, *Wound Dressings in Diabetic Foot Disease*. Clinical Infectious Diseases, 2004. **39**(s100-3).
7. Sindhu, K.A., R. Prasanth, and V.K. Thakur, *Medical Applications of Cellulose and its Derivatives: Present and Future*, in *Nanocellulose Polymer Nanocomposites*. 2015.
8. Ulrich, D., R. Smeets, F. Unglaub, M. Woltje, and N. Pallua, *Effect of oxidized regenerated cellulose/collagen matrix on proteases in wound exudate of patients with diabetic foot ulcers*. J Wound Ostomy Contenance Nurs, 2011. **38**(5): p. 522-8.

9. Chicone, G., V.F. de Carvalho, and A.O. Paggiaro, *Use of Oxidized Regenerated Cellulose/Collagen Matrix in Chronic Diabetic Foot Ulcers: A Systematic Review*. *Advances in Skin & Wound Care*, 2018. **31**(2): p. 66-71.
10. Veves, A., P. Sheehan, H.T. Pham, and S. For the Promogran Diabetic Foot Ulcer, *A randomized, controlled trial of promogran (a collagen/oxidized regenerated cellulose dressing) vs standard treatment in the management of diabetic foot ulcers*. *Archives of Surgery*, 2002. **137**(7): p. 822-827.
11. Wu, S.C., V.R. Driver, J.S. Wrobel, and D.G. Armstrong, *Foot ulcers in the diabetic patient, prevention and treatment*. *Vascular health and risk management*, 2007. **3**(1): p. 65-76.
12. Moura, L.I.F., A.M.A. Dias, E. Carvalho, and H.C. de Sousa, *Recent advances on the development of wound dressings for diabetic foot ulcer treatment—A review*. *Acta Biomaterialia*, 2013. **9**(7): p. 7093-7114.
13. Frey, M.W., *Electrospinning Cellulose and Cellulose Derivatives*. *Polymer Reviews*, 2008. **48**(2): p. 378-391.
14. Son, W.K., J.H. Youk, and W.H. Park, *Antimicrobial cellulose acetate nanofibers containing silver nanoparticles*. *Carbohydrate Polymers*, 2006. **65**(4): p. 430-434.

15. Frenot, A., M.W. Henriksson, and P. Walkenström, *Electrospinning of cellulose-based nanofibers*. Journal of Applied Polymer Science, 2007. **103**(3): p. 1473-1482.
16. Ahmad, B., S. Stoyanov, E. Pelan, E. Stride, and M. Edirisinghe, *Electrospinning of ethyl cellulose fibres with glass and steel needle configurations*. Food Research International, 2013. **54**(2): p. 1761-1772.
17. Kim, C.-W., D.-S. Kim, S.-Y. Kang, M. Marquez, and Y.L. Joo, *Structural studies of electrospun cellulose nanofibers*. Polymer, 2006. **47**(14): p. 5097-5107.
18. Angamma, C.J. and S.H. Jayaram, *The Effects of Electric Field on the Multijet Electrospinning Process and Fiber Morphology*. IEEE Transactions on Industry Applications, 2011. **47**(2): p. 1028-1035.
19. Reneker, D.H. and A.L. Yarin, *Electrospinning jets and polymer nanofibers*. Polymer, 2008. **49**(10): p. 2387-2425.
20. Yarin, A.L., S. Koombhongse, and D.H. Reneker, *Taylor cone and jetting from liquid droplets in electrospinning of nanofibers*. Journal of Applied Physics, 2001. **90**(9): p. 4836.
21. Wustenberg, T., *Cellulose and Cellulose Derivatives in the Food Industry Fundamentals and Applications*. 2014, Germany: Wiley-VCH.
22. Kondo, T., *The Relationship between Intramolecular Hydrogen Bonds and Certain Physical Properties of Regioselectively Substituted Cellulose Derivatives*. Polymer Physics 1997. **35**(4).

23. Credou, J. and T. Berthelot, *Cellulose: from biocompatible to bioactive material*. Journal of Materials Chemistry B, 2014. **2**(30): p. 4767.
24. Schubert, M., *The manufacture of cellulose: A practical treatise for paper and cellulose technologists, managers and superintendents*. 1899, New Yor: A. Geyer.
25. Moon, R.J., A. Martini, J. Nairn, J. Simonsen, and J. Youngblood, *Cellulose nanomaterials review: structure, properties and nanocomposites*. Chem Soc Rev, 2011. **40**(7): p. 3941-94.
26. Gibson, L.J., *The hierarchical structure and mechanics of plant materials*. J R Soc Interface, 2012. **9**(76): p. 2749-66.
27. Cosgrove, D.J., *Growth of the plant cell wall*. Nat Rev Mol Cell Biol, 2005. **6**(11): p. 850-61.
28. Cummings, J.H., *Microbial Digestion of Complex Carbohydrates in Man*. Proceedings of the Nutrition Society, 2007. **43**(01): p. 35-44.
29. Pinkert, A., K.N. Marsh, and S. Pang, *Reflections on the Solubility of Cellulose*. Industrial & Engineering Chemistry Research 2010. **49**: p. 11121-11130.
30. Kalia, S., A. Dufresne, B.M. Cherian, B.S. Kaith, L. Avérous, J. Njuguna, and E. Nassiopoulou, *Cellulose-Based Bio- and Nanocomposites: A Review*. International Journal of Polymer Science, 2011. **2011**: p. 1-35.

31. Ye, D., Z. Zhong, H. Xu, C. Chang, Z. Yang, Y. Wang, Q. Ye, and L. Zhang, *Construction of cellulose/nanosilver sponge materials and their antibacterial activities for infected wounds healing*. *Cellulose*, 2015. **23**(1): p. 749-763.
32. Lin, S., L. Chen, L. Huang, S. Cao, X. Luo, and K. Liu, *Novel antimicrobial chitosan–cellulose composite films bioconjugated with silver nanoparticles*. *Industrial Crops and Products*, 2015. **70**: p. 395-403.
33. Franz, G., *Polysaccharides in Pharmacy: Current Applications and Future Concepts*. *Planta Medica* 1989. **55**: p. 493-497.
34. Fouda, M.M.G., R. Wittke, D. Knittel, and E. Schollmeyer, *Use of chitosan/polyamine biopolymers based cotton as a model system to prepare antimicrobial wound dressing*. *International Journal of Diabetes Mellitus*, 2009. **1**(1): p. 61-64.
35. Jayakumar, R., M. Prabakaran, P.T. Sudheesh Kumar, S.V. Nair, and H. Tamura, *Biomaterials based on chitin and chitosan in wound dressing applications*. *Biotechnol Adv*, 2011. **29**(3): p. 322-37.
36. Miyamoto, T., S.-i. Takahashi, H. Ito, and H. Inagaki, *Tissue biocompatibility of cellulose and its derivatives*. *Journal of Biomedical Materials Research*, 1989. **23**: p. 125-133.
37. Bruno, L., S. Kasapis, V. Chaudhary, K.T. Chow, P.W.S. Heng, and L.P. Leong, *Temperature and time effects on the structural properties*

- of a non-aqueous ethyl cellulose topical drug delivery system.*
Carbohydrate Polymers, 2011. **86**(2): p. 644-651.
38. Fink, H.P., P. Weigel, H.J. Purz, and J. Ganster, *Structure formation of regenerated cellulose materials from NMMO-solutions.* Progress in Polymer Science 2001. **26**: p. 1473-1524.
39. Han, S.O., J.H. Youk, K.D. Min, Y.O. Kang, and W.H. Park, *Electrospinning of cellulose acetate nanofibers using a mixed solvent of acetic acid/water: Effects of solvent composition on the fiber diameter.* Materials Letters, 2008. **62**(4-5): p. 759-762.
40. El-Kafry, A., *Investigation of the Cellulose/LiCl/Dimethylacetamide and Cellulose/LiCl/N-Methyl-2-Pyrrolidinone Solutions by ¹³C NMR Spectroscopy.* Journal of Applied Polymer Science, 1982. **27**: p. 2435-2443.
41. Verreck, G., I. Chun, J. Peeters, J. Rosenblatt, and M.E. Brewster, *Preparation and Characterization of Nanofibers Containing Amorphous Drug Dispersions Generated by Electrostatic Spinning.* Pharmaceutical Research, 2003. **20**(5).
42. Crowley, M.M., B. Schroeder, A. Fredersdorf, S. Obara, M. Talarico, S. Kucera, and J.W. McGinity, *Physicochemical properties and mechanism of drug release from ethyl cellulose matrix tablets prepared by direct compression and hot-melt extrusion.* International Journal of Pharmaceutics, 2004. **269**(2): p. 509-522.

43. Lin, W.J. and T.L. Wu, *Modification of the initial release of a highly water-soluble drug from ethyl cellulose microspheres*. J Microencapsul, 1999. **16**(5): p. 639-46.
44. Park, J.-Y., J.-I. Kim, and I.-H. Lee, *Fabrication and Characterization of Antimicrobial Ethyl Cellulose Nanofibers Using Electrospinning Techniques*. Journal of Nanoscience and Nanotechnology, 2015. **15**(8): p. 5672-5675.
45. Wu, X., L. Wang, H. Yu, and Y. Huang, *Effect of solvent on morphology of electrospinning ethyl cellulose fibers*. Journal of Applied Polymer Science, 2005. **97**(3): p. 1292-1297.
46. Al-Omran, M.F., S.A. Al-Suwayeh, A.M. El-Helw, and S.I. Saleh, *Taste masking of diclofenac sodium using microencapsulation*. J Microencapsul, 2002. **19**(1): p. 45-52.
47. Parikh, N.H., S.C. Porter, and B.D. Rohera, *Aqueous Ethylcellulose Dispersion of Ethylcellulose. I. Evaluation of Coating Process Variables*. Pharmaceutical Research, 1993. **10**(4): p. 525-534.
48. Kamel, S., *Pharmaceutical significance of cellulose: A review*. eXPRESS Polymer Letters, 2008. **2**(11): p. 758-778.
49. Gunduz, O., Z. Ahmad, E. Stride, and M. Edirisinghe, *Continuous generation of ethyl cellulose drug delivery nanocarriers from microbubbles*. Pharm Res, 2013. **30**(1): p. 225-37.
50. Arias, J.L., M. Lopez-Viota, M.A. Ruiz, J. Lopez-Viota, and A.V. Delgado, *Development of carbonyl iron/ethylcellulose core/shell*

- nanoparticles for biomedical applications*. Int J Pharm, 2007. **339**(1-2): p. 237-45.
51. Liakos, I., L. Rizzello, H. Hajiali, V. Brunetti, R. Carzino, P.P. Pompa, A. Athanassiou, and E. Mele, *Fibrous wound dressings encapsulating essential oils as natural antimicrobial agents*. J. Mater. Chem. B, 2015. **3**(8): p. 1583-1589.
52. Malm, C.J. and L.J. Tanghe, *Chemical Reactions in the Making of Cellulose Acetate*. Industrial and Engineering Chemistry, 1955. **47**(5): p. 995-999.
53. Gouvêa, D.M., R.C.S. Mendonça, M.L. Soto, and R.S. Cruz, *Acetate cellulose film with bacteriophages for potential antimicrobial use in food packaging*. LWT - Food Science and Technology, 2015. **63**(1): p. 85-91.
54. Son, W.K., J.H. Youk, T.S. Lee, and W.H. Park, *Electrospinning of Ultrafine Cellulose Acetate Fibers: Studies of a New Solvent System and Deacetylation of Ultrafine Cellulose Acetate Fibers*. Journal of Polymer Scienc: Polymer Physics, 2003. **42**: p. 5-11.
55. Cui, W., Y. Zhou, and J. Chang, *Electrospun nanofibrous materials for tissue engineering and drug delivery*. Science and Technology of Advanced Materials, 2016. **11**(1): p. 014108.

56. Konwarh, R., B. Gogoi, R. Philip, M.A. Laskar, and N. Karak, *Biomimetic preparation of polymer-supported free radical scavenging, cytocompatible and antimicrobial "green" silver nanoparticles using aqueous extract of Citrus sinensis peel*. *Colloids Surf B Biointerfaces*, 2011. **84**(2): p. 338-45.
57. Konwarh, R., J.P. Saikia, N. Karak, and B.K. Konwar, '*Poly(ethylene glycol)-magnetic nanoparticles-curcumin' trio: directed morphogenesis and synergistic free-radical scavenging*. *Colloids Surf B Biointerfaces*, 2010. **81**(2): p. 578-86.
58. Liu, X., T. Lin, Y. Gao, Z. Xu, C. Huang, G. Yao, L. Jiang, Y. Tang, and X. Wang, *Antimicrobial electrospun nanofibers of cellulose acetate and polyester urethane composite for wound dressing*. *J Biomed Mater Res B Appl Biomater*, 2012. **100**(6): p. 1556-65.
59. Suwantong, O., P. Opanasopit, U. Ruktanonchai, and P. Supaphol, *Electrospun cellulose acetate fiber mats containing curcumin and release characteristic of the herbal substance*. *Polymer*, 2007. **48**(26): p. 7546-7557.
60. Ogushi, Y., S. Sakai, and K. Kawakami, *Synthesis of enzymatically-gellable carboxymethylcellulose for biomedical applications*. *J Biosci Bioeng*, 2007. **104**(1): p. 30-3.
61. Zheng, W.J., J. Gao, Z. Wei, J. Zhou, and Y.M. Chen, *Facile fabrication of self-healing carboxymethyl cellulose hydrogels*. *European Polymer Journal*, 2015. **72**: p. 514-522.

62. Brako, F., B. Raimi-Abraham, S. Mahalingam, D.Q.M. Craig, and M. Edirisinghe, *Making nanofibres of mucoadhesive polymer blends for vaginal therapies*. *European Polymer Journal*, 2015. **70**: p. 186-196.
63. Biswal, D.R. and R.P. Singh, *Characterisation of carboxymethyl cellulose and polyacrylamide graft copolymer*. *Carbohydrate Polymers*, 2004. **57**(4): p. 379-387.
64. Ibrahim, M.M., A. Koschella, G. Kadry, and T. Heinze, *Evaluation of cellulose and carboxymethyl cellulose/poly(vinyl alcohol) membranes*. *Carbohydrate Polymers*, 2013. **95**(1): p. 414-420.
65. Lin, S.-P., I. Loira Calvar, J.M. Catchmark, J.-R. Liu, A. Demirci, and K.-C. Cheng, *Biosynthesis, production and applications of bacterial cellulose*. *Cellulose*, 2013. **20**(5): p. 2191-2219.
66. Brown, A.J., *XLIII.—On an acetic ferment which forms cellulose*. *Journal of the Chemical Society, Transactions*, 1886. **49**(0): p. 432-439.
67. Phillips, G.O. and P.A. Williams, *26. Bacterial Cellulose*, in *Handbook of Hydrocolloids (2nd Edition)*. Woodhead Publishing.
68. Yamanaka, S., K. Watanabe, N. Kitamura, M. Iguchi, S. Mitsuhashi, Y. Nishi, and M. Uryu, *The structure and mechanical properties of sheets prepared from bacterial cellulose*. *Journal of Materials Science*, 1989. **24**(9): p. 3141-3145.

69. Klemm, D., Heublein, H. P., Fink, H. P., Bohn, A., *Cellulose: fascinating biopolymer and sustainable raw material*. Angewandte Chemie International Edition, 2005. **44**: p. 3358-3393.
70. Brown, M., *Emerging technologies and future programming for industrialization of microbially derived cellulose*. American Chemical Society, 1992.
71. Klemm, D., Schumann, D., Udhardt, U., Marsch, S, *Bacterial synthesised cellulose-artificial blood vessels for microsurgery*. Progress in Polymer Science, 2001. **26**(9): p. 1561-1603.
72. George, J., Siddaramaiah, *High performance edible nanocomposite films containing bacterial cellulose nanocrystals*. Carbohydrate Polymers, 2012. **87**: p. 2031-2037.
73. Brown, R.M., Jr., J.H. Willison, and C.L. Richardson, *Cellulose biosynthesis in Acetobacter xylinum: visualization of the site of synthesis and direct measurement of the in vivo process*. Proceedings of the National Academy of Sciences of the United States of America, 1976. **73**(12): p. 4565-4569.
74. Zaar, K., *The biogenesis of cellulose by acetobacter xylinum*. Cytobiologie, 1977. **16**(1): p. 1-15.
75. Fontana, J.D., de Sousa, A. M., Fontana C. K., Torriani I. L., Moreschi, J. C., Galloti, B. J., de Sousa, S. J., Narcisco, G. P., Bichara, J. A., Farah, L. F., *Acetobacter cellulose pellicles as a*

- temporary skin substitute*. Applied Biotechnology and Biotechnology, 1990. **24**(25): p. 253-264.
76. Czaja, W., Krystynowicz, A., Bielecki, S., Brown, R. M., *Microbial cellulose--the natural power to heal wounds*. Biomaterials, 2006. **27**(2): p. 145-151.
77. Legeza, V.I., Galenko-Yaroshevskii, V. P., Zinov'ev, E. V., Paramonov, B. A., Kreichman, G. S., Karnovich, A. G., Khripunov, A. K., *Effects of new wound dressings on healing of thermal burns of the skin in acute radiation disease*. Bulletin of Experimental Biology and Medicine, 2004. **138**(3): p. 311-315.
78. Gayathry, G., Gopalawasmy, G., *Production and characterisation of microbial cellulosic fibre from Acetobacter xylinum*. Indian Journal of Fibre and Textile Research, 2012. **39**: p. 93-96.
79. Czaja, W., A. Krystynowicz, S. Bielecki, and R.M. Brown, Jr., *Microbial cellulose--the natural power to heal wounds*. Biomaterials, 2006. **27**(2): p. 145-51.
80. Czaja, W.K., D.J. Young, M. Kawecki, and R.M. Brown, *The Future Prospects of Microbial Cellulose in Biomedical Applications*. Biomacromolecules, 2007. **8**(1): p. 1-12.
81. Nishi, Y., M. Uryu, S. Yamanaka, K. Watanabe, N. Kitamura, M. Iguchi, and S. Mitsuhashi, *The structure and mechanical properties of sheets prepared from bacterial cellulose*. Journal of Materials Science, 1990. **25**(6): p. 2997-3001.

82. Khan, T., J.K. Park, and J.-H. Kwon, *Functional biopolymers produced by biochemical technology considering applications in food engineering*. Korean Journal of Chemical Engineering, 2007. **24**(5): p. 816-826.
83. Labet, M. and W. Thielemans, *Synthesis of polycaprolactone: a review*. Chemical Society Reviews, 2009. **38**(12): p. 3484-3504.
84. Azimi, B., P. Nourpanah, M. Rabiee, and S. Arbab, *Poly (ϵ -caprolactone) Fiber: An Overview*. Vol. 9. 2014. 74-90.
85. Deitzel, J.M., J. Kleinmeyer, D. Harris, and N.C. Beck Tan, *The effect of processing variables on the morphology of electrospun nanofibers and textiles*. Polymer, 2001. **42**: p. 261-272.
86. Aydogdu, M.O., E. Altun, M. Crabbe-Mann, F. Brako, F. Koc, G. Ozen, S.E. Kuruca, U. Edirisinghe, C.J. Luo, O. Gunduz, and M. Edirisinghe, *Cellular interactions with bacterial cellulose: Polycaprolactone nanofibrous scaffolds produced by a portable electrohydrodynamic gun for point-of-need wound dressing*. International Wound Journal, 2018. **15**(5): p. 789-797.
87. Shin, M., O. Ishii, T. Sueda, and J.P. Vacanti, *Contractile cardiac grafts using a novel nanofibrous mesh*. Biomaterials, 2004. **25**(17): p. 3717-23.
88. Huang, Z.-M., C.-L. He, A. Yang, Y. Zhang, X.-J. Han, J. Yin, and Q. Wu, *Encapsulating drugs in biodegradable ultrafine fibers through co-*

- axial electrospinning*. Journal of Biomedical Materials Research Part A, 2006. **77A**(1): p. 169-179.
89. Karuppuswamy, P., J. Reddy Venugopal, B. Navaneethan, A. Luwang Laiva, and S. Ramakrishna, *Polycaprolactone nanofibers for the controlled release of tetracycline hydrochloride*. Materials Letters, 2015. **141**: p. 180-186.
90. Labbaf, S., H. Ghanbar, E. Stride, and M. Edirisinghe, *Preparation of Multilayered Polymeric Structures Using a Novel Four-Needle Coaxial Electrohydrodynamic Device*. Macromolecular Rapid Communications, 2014. **35**(6): p. 618-623.
91. Venugopal, J., Y. Zhang, and S. Ramakrishna, *In Vitro Culture of Human Dermal Fibroblasts on Electrospun Polycaprolactone Collagen Nanofibrous Membrane*. Artificial Organs, 2006. **30**(6): p. 440-446.
92. Li, W.-J., K.G. Danielson, P.G. Alexander, and R.S. Tuan, *Biological response of chondrocytes cultured in three-dimensional nanofibrous poly(ϵ -caprolactone) scaffolds*. Journal of Biomedical Materials Research, 2003. **67A**: p. 1105-1114.
93. Pham, Q.P., U. Sharma, and A.G. Mikos, *Electrospun Poly(ϵ -caprolactone) Microfiber and Multilayer Nanofiber/Microfiber Scaffolds: Characterization of Scaffolds and Measurement of Cellular Infiltration*. Biomacromolecules, 2006. **7**: p. 2796-2805.

94. Choi, J.S., K.W. Leong, and H.S. Yoo, *In vivo wound healing of diabetic ulcers using electrospun nanofibers immobilized with human epidermal growth factor (EGF)*. *Biomaterials*, 2008. **29**(5): p. 587-596.
95. Bölgen, N., İ. Vargel, P. Korkusuz, Y.Z. Menceloğlu, and E. Pişkin, *In vivo performance of antibiotic embedded electrospun PCL membranes for prevention of abdominal adhesions*. *Journal of Biomedical Materials Research Part B: Applied Biomaterials*, 2006. **81B**(2): p. 530-543.
96. Zamani, M., M. Morshed, J. Varshosaz, and M. Jannesari, *Controlled release of metronidazole benzoate from poly epsilon-caprolactone electrospun nanofibers for periodontal diseases*. *Eur J Pharm Biopharm*, 2010. **75**(2): p. 179-85.
97. Ward, A.G., *The physical properties of gelatin solutions and gels*. *British Journal of Applied Physics*, 1954. **5**(3): p. 85-90.
98. *The Science and technology of gelatin / edited by A. G. Ward, A. Courts*. *Food science and technology*, ed. A.G. Ward and A. Courts. 1977, London ; New York: Academic Press.
99. Zhang, Y.Z., J. Venugopal, Z.M. Huang, C.T. Lim, and S. Ramakrishna, *Crosslinking of the electrospun gelatin nanofibers*. *Polymer*, 2006. **47**(8): p. 2911-2917.
100. Powell, H.M. and S.T. Boyce, *Fiber density of electrospun gelatin scaffolds regulates morphogenesis of dermal–epidermal skin*

- substitutes*. Journal of Biomedical Materials Research Part A, 2008. **84A**(4): p. 1078-1086.
101. Vatankhah, E., M.P. Prabhakaran, G. Jin, L.G. Mobarakeh, and S. Ramakrishna, *Development of nanofibrous cellulose acetate/gelatin skin substitutes for variety wound treatment applications*. J Biomater Appl, 2014. **28**(6): p. 909-21.
102. Somvipart, S., S. Kanokpanont, R. Rangkupan, J. Ratanavaraporn, and S. Damrongsakkul, *Development of electrospun beaded fibers from Thai silk fibroin and gelatin for controlled release application*. International Journal of Biological Macromolecules, 2013. **55**: p. 176-184.
103. Enayati, M., E. Stride, M. Edirisinghe, and W. Bonfield, *Modification of the release characteristics of estradiol encapsulated in PLGA particles via surface coating*. Therapeutic Delivery, 2012. **3**(2): p. 209-226.
104. Lu, C., P. Chen, J. Li, and Y. Zhang, *Computer simulation of electrospinning. Part I. Effect of solvent in electrospinning*. Polymer, 2006. **47**(3): p. 915-921.
105. Henderson, R.K., C. Jiménez-González, D.J.C. Constable, S.R. Alston, G.G.A. Inglis, G. Fisher, J. Sherwood, S.P. Binks, and A.D. Curzons, *Expanding GSK's solvent selection guide – embedding sustainability into solvent selection starting at medicinal chemistry*. Green Chemistry, 2011. **13**(4): p. 854.

106. Prat, D., O. Pardigon, H.-W. Flemming, S. Letestu, V. Ducandas, P. Isnard, E. Guntrum, T. Senac, S. Ruisseau, P. Cruciani, and P. Hosek, *Sanofi's Solvent Selection Guide: A Step Toward More Sustainable Processes*. Organic Process Research & Development, 2013. **17**(12): p. 1517-1525.
107. Haas, H.C., L. Farney, and C. Valle Jr, *SOME PROPERTIES OF ETHYL CELLULOSE FILMS*. 1952.
108. Huff, J., *Benzene-induced Cancers Abridged History and Occupational Health Impact*. International Journal of Occupational and Environmental Health, 2007. **13**(2): p. 213-221.
109. Tungprapa, S., T. Puangparn, M. Weerasombut, I. Jangchud, P. Fakum, S. Semongkhol, C. Meechaisue, and P. Supaphol, *Electrospun cellulose acetate fibers: effect of solvent system on morphology and fiber diameter*. Cellulose, 2007. **14**(6): p. 563-575.
110. Liu, H. and Y.-L. Hsieh, *Ultrafine fibrous cellulose membranes from electrospinning of cellulose acetate*. Journal of Polymer Science Part B: Polymer Physics, 2002. **40**(18): p. 2119-2129.
111. Jeun, J.P., Y.M. Lim, J.H. Choi, H.S. La, P.H. Kang, and Y.C. Nho, *Preparation of Ethyl-Cellulose Nanofibers via An Electrospinning*. Solid State Phenomena, 2007. **119**: p. 255-258.
112. Lim, Y.-M., H.-J. Gwon, J.P. Jeun, and Y.-C. Nho, *Preparation of Cellulose-based Nanofibers Using Electrospinning*. Nanofibers. 2010, Kumar, Ashok: InTech.

113. Duarte, A.R., M.D. Gordillo, M.M. Cardoso, A.L. Simplicio, and C.M. Duarte, *Preparation of ethyl cellulose/methyl cellulose blends by supercritical antisolvent precipitation*. Int J Pharm, 2006. **311**(1-2): p. 50-4.
114. Li, W., X. Li, W. Li, T. Wang, X. Li, S. Pan, and H. Deng, *Nanofibrous mats layer-by-layer assembled via electrospun cellulose acetate and electrospayed chitosan for cell culture*. European Polymer Journal, 2012. **48**(11): p. 1846-1853.
115. Wu, S., X. Qin, and M. Li, *The structure and properties of cellulose acetate materials: A comparative study on electrospun membranes and casted films*. Journal of Industrial Textiles, 2013. **44**(1): p. 85-98.
116. Wang, X., G. He, G. Liu, and D. Sun, *Fabrication and Morphological Control of Electrospun Ethyl Cellulose Nanofibers*, in *Nano/Micro Engineered Molecular Systems*. 2013: Suzhou.
117. Kessick, R. and G. Tepper, *Microscale electrospinning of polymer nanofiber interconnections*. Applied Physics Letters, 2003. **83**(3): p. 557.
118. Ma, Z., M. Kotaki, and S. Ramakrishna, *Electrospun cellulose nanofiber as affinity membrane*. Journal of Membrane Science, 2005. **265**(1-2): p. 115-123.
119. De Silva, R., K. Vongsanga, X. Wang, and N. Byrne, *Understanding key wet spinning parameters in an ionic liquid spun regenerated cellulosic fibre*. Cellulose, 2016. **23**(4): p. 2741-2751.

120. Lee, S.-H., S.-M. Park, and Y. Kim, *Effect of the concentration of sodium acetate (SA) on crosslinking of chitosan fiber by epichlorohydrin (ECH) in a wet spinning system*. Carbohydrate Polymers, 2007. **70**(1): p. 53-60.
121. Luo, C.J., S.D. Stoyanov, E. Stride, E. Pelan, and M. Edirisinghe, *Electrospinning versus fibre production methods: from specifics to technological convergence*. Chem Soc Rev, 2012. **41**(13): p. 4708-35.
122. Mather, R.R. and R.H. Wardman, *High-Performance Fibres in Chemistry of Textile Fibres* R.S.o. Chemistry, Editor. 2015, Royal Society of Chemistry: Cambridge
123. Hauru, L.K.J., M. Hummel, A. Michud, and H. Sixta, *Dry jet-wet spinning of strong cellulose filaments from ionic liquid solution*. Cellulose, 2014. **21**(6): p. 4471-4481.
124. Koombhongse, S., W. Liu, and D.H. Reneker, *Flat Polymer Ribbons and Other Shapes by Electrospinning*. Journal of Polymer Science: Part B: Polymer Physics, 2001. **39**: p. 2598-2606.
125. Chaochai, T., Y. Imai, T. Furuike, and H. Tamura, *Preparation and Properties of Gelatin Fibers Fabricated by Dry Spinning*. Fibers, 2016. **4**(1): p. 2.
126. Gupta, V.B., *Melt Spinning Processes*, in *Manufactured fibre technology* V.B. Gupta and V.K. Kothari, Editors. 1997, Chapman & Hall: London.

127. Xia, L., P. Xi, and B. Cheng, *A comparative study of UHMWPE fibers prepared by flash-spinning and gel-spinning*. *Materials Letters*, 2015. **147**: p. 79-81.
128. Hearle, J.W.S., *Gel-Spun High-Performance Polyethylene Fibres* in *High-performance fibres*. 2001, Woodhead Publishing: Cambridge.
129. Fang, X., T. Wyatt, Y. Hong, and D. Yao, *Gel spinning of UHMWPE fibers with polybutene as a new spin solvent*. *Polymer Engineering & Science*, 2016. **56**(6): p. 697-706.
130. Marano, S., S.A. Barker, B.T. Raimi-Abraham, S. Missaghi, A. Rajabi-Siahboomi, and D.Q. Craig, *Development of micro-fibrous solid dispersions of poorly water-soluble drugs in sucrose using temperature-controlled centrifugal spinning*. *Eur J Pharm Biopharm*, 2016. **103**: p. 84-94.
131. Amalorpavamary, L. and V. Giri Dev, *Development of biocomposites by a facile fiber spinning technique for nerve tissue engineering applications*. *Journal of Industrial Textiles*, 2015. **46**(2): p. 372-387.
132. Amir, A., S. Mahalingam, X. Wu, H. Porwal, P. Colombo, M.J. Reece, and M. Edirisinghe, *Graphene nanoplatelets loaded polyurethane and phenolic resin fibres by combination of pressure and gyration*. *Composites Science and Technology*, 2016. **129**: p. 173-182.
133. Koshiro, T., *A New Flame Retardant Synthetic Fiber Made by an Emulsion Spinning Process*. *Die Angewandte Makromolekulare Chemie* 1974. **40/41**: p. 277-290.

134. Sakurada, I. and T. Okaya, *Vinyl Fibers*, in *Handbook of Fiber Chemistry, Second Edition, Revised and Expanded*, M. Lewin and E.M. Pearce, Editors. 1998, Taylor & Francis.
135. Cadafalch Gazquez, G., S. Lei, A. George, H. Gullapalli, B.A. Boukamp, P.M. Ajayan, and J.E. Ten Elshof, *Low-Cost, Large-Area, Facile, and Rapid Fabrication of Aligned ZnO Nanowire Device Arrays*. ACS Appl Mater Interfaces, 2016. **8**(21): p. 13466-71.
136. Dzenis, Y., *Spinning Continuous Fibers for Nanotechnology*. Science, 2004. **304**: p. 1917-1919.
137. Gilbert, W., *On the loadstone and magnetic bodies and the great magnet the earth. A new physiology demonstrated with many arguments and experiments*. . 1893, New York: Ferris Bros.
138. Cooley, J.F., *Apparatus for electrically dispersing fluids*. 1899, Eastman, A., Farquhar, C. S. : USA.
139. Zeleny, J., *THE ELECTRICAL DISCHARGE FROM LIQUID POINTS, AND A HYDROSTATIC METHOD OF MEASURING THE ELECTRIC INTENSITY AT THEIR SURFACES*. Physical Review, 1914 a. **3**(2).
140. Zeleny, J., *Instability of Electrified Liquid Surfaces*. Physical Review, 1917. **10**(1): p. 1-6.
141. Tucker, N., J.J. Stanger, M.P. Staiger, H. Razzaq, and K. Hofman, *The History of the Science and Technology of Electrospinning from 1600 to 1995*. Journal of Engineered Fibers and Fabrics, 2012.

142. Taylor, G. *Disintegration of Water Drops in an Electric Field*. in *Proceedings of the Royal Society of London*. 1964. London: The Royal Society.
143. Sill, T.J. and H.A. von Recum, *Electrospinning: applications in drug delivery and tissue engineering*. *Biomaterials*, 2008. **29**(13): p. 1989-2006.
144. Baumgarten, P.K., *Electrostatic Spinning of Acrylic Microfibers* *Journal of Colloid and Interface Science*, 1971. **36**(1).
145. Zander, N., *Hierarchically Structured Electrospun Fibers*. *Polymers*, 2013. **5**(1): p. 19-44.
146. Oliveira, M.n.S.N. and G.H. McKinley, *Iterated stretching and multiple beads-on-a-string phenomena in dilute solutions of highly extensible flexible polymers*. *Physics of Fluids*, 2005. **17**(7): p. 071704.
147. Pillay, V., C. Dott, Y.E. Choonara, C. Tyagi, L. Tomar, P. Kumar, L.C. du Toit, and V.M.K. Ndesendo, *A Review of the Effect of Processing Variables on the Fabrication of Electrospun Nanofibers for Drug Delivery Applications*. *Journal of Nanomaterials*, 2013. **2013**: p. 1-22.
148. Ago, M., K. Okajima, J.E. Jakes, S. Park, and O.J. Rojas, *Lignin-based electrospun nanofibers reinforced with cellulose nanocrystals*. *Biomacromolecules*, 2012. **13**(3): p. 918-26.
149. Haider, A., S. Haider, and I.-K. Kang, *A comprehensive review summarizing the effect of electrospinning parameters and potential*

applications of nanofibers in biomedical and biotechnology. Arabian Journal of Chemistry, 2015.

150. Bhardwaj, N. and S.C. Kundu, *Electrospinning: a fascinating fiber fabrication technique*. Biotechnol Adv, 2010. **28**(3): p. 325-47.
151. Garg, K. and G.L. Bowlin, *Electrospinning jets and nanofibrous structures*. Biomicrofluidics, 2011. **5**(1): p. 13403.
152. Reneker, D. and I. Chun, *Nanometre diameter fibres of polymer, produced by electrospinning*. Nanotechnology, 1996. **7**: p. 216-223.
153. Fong, H., I. Chun, and D.H. Reneker, *Beaded nanofibers formed during electrospinning*. Polymer, 1999. **40**: p. 4585-4592.
154. McKee, M.G., G.L. Wilkes, R.H. Colby, and T.E. Long, *Correlations of Solution Rheology with Electrospun Fiber Formation of Linear and Branched Polyesters*. Macromolecules, 2004. **37**: p. 1760-1767.
155. Lee, K.Y., L. Jeong, Y.O. Kang, S.J. Lee, and W.H. Park, *Electrospinning of polysaccharides for regenerative medicine*. Adv Drug Deliv Rev, 2009. **61**(12): p. 1020-32.
156. Gupta, P., C. Elkins, T.E. Long, and G.L. Wilkes, *Electrospinning of linear homopolymers of poly(methyl methacrylate): exploring relationships between fiber formation, viscosity, molecular weight and concentration in a good solvent*. Polymer, 2005. **46**(13): p. 4799-4810.

157. Deitzel, J.M., J. Kleinmeyer, D. Harris, and N.C. Beck Tan, *The effect of processing variables on the morphology of electrospun nanofibers and textiles*. Polymer 2001. **42**.
158. Zhang, C., X. Yuan, L. Wu, Y. Han, and J. Sheng, *Study on morphology of electrospun poly(vinyl alcohol) mats*. European Polymer Journal, 2005. **41**(3): p. 423-432.
159. Yuan, X., Y. Zhang, C. Dong, and J. Sheng, *Morphology of ultrafine polysulfone fibers prepared by electrospinning*. Polymer International, 2004. **53**(11): p. 1704-1710.
160. Megelski, S., J.S. Stephens, D.B. Chase, and J.F. Rabolt, *Micro- and nanostructured surface morphology on electrospun polymer fibres*. Macromolecules, 2005. **35**: p. 8456-8466.
161. Agrawal, P., S. Soni, G. Mittal, and A. Bhatnagar, *Role of polymeric biomaterials as wound healing agents*. Int J Low Extrem Wounds, 2014. **13**(3): p. 180-90.
162. Uzun, M., S.C. Anand, and T. Shah, *A novel approach for designing nonwoven hybrid wound dressings: Processing and characterisation*. Journal of Industrial Textiles, 2014. **45**(6): p. 1383-1398.
163. Khil, M.S., S.R. Bhattarai, H.Y. Kim, S.Z. Kim, and K.H. Lee, *Novel fabricated matrix via electrospinning for tissue engineering*. J Biomed Mater Res B Appl Biomater, 2005. **72**(1): p. 117-24.
164. Panichpakdee, J., P. Pavasant, and P. Supaphol, *Electrospun Cellulose Acetate Fiber Mats Containing Emodin with Potential for*

- Use as Wound Dressing*. Chiang Mai Journal of Science, 2016. **43**(1): p. 195-205.
165. Agarwal, S., J.H. Wendorff, and A. Greiner, *Use of electrospinning technique for biomedical applications*. Polymer, 2008. **49**(26): p. 5603-5621.
166. Zahedi, P., I. Rezaeian, S.-O. Ranaei-Siadat, S.-H. Jafari, and P. Supaphol, *A review on wound dressings with an emphasis on electrospun nanofibrous polymeric bandages*. Polymers for Advanced Technologies, 2009: p. n/a-n/a.
167. Powell, H.M., D.M. Supp, and S.T. Boyce, *Influence of electrospun collagen on wound contraction of engineered skin substitutes*. Biomaterials, 2008. **29**(7): p. 834-43.
168. Griffith, L.G., *Polymeric biomaterials*. Acta Materialia, 2000. **48**(1): p. 263-277.
169. Huang, X. and C.S. Brazel, *On the importance and mechanisms of burst release in matrix-controlled drug delivery systems*. Journal of Controlled Release, 2001. **73**(2): p. 121-136.
170. Soppimath, K.S., T.M. Aminabhavi, A.R. Kulkarni, and W.E. Rudzinski, *Biodegradable polymeric nanoparticles as drug delivery devices*. Journal of Controlled Release, 2001. **70**(1): p. 1-20.
171. Cohen, S., T. Yoshioka, M. Lucarelli, L.H. Hwang, and R. Langer, *Controlled Delivery Systems for Proteins Based on*

- Poly(Lactic/Glycolic Acid) Microspheres*. *Pharmaceutical Research*, 1991. **8**(6): p. 713-720.
172. Reardon, P.J., M. Parhizkar, A.H. Harker, R.J. Browning, V. Vassileva, E. Stride, R.B. Pedley, M. Edirisinghe, and J.C. Knowles, *Electrohydrodynamic fabrication of core-shell PLGA nanoparticles with controlled release of cisplatin for enhanced cancer treatment*. *Int J Nanomedicine*, 2017. **12**: p. 3913-3926.
173. Wu, Y., J.A. MacKay, J. R. McDaniel, A. Chilkoti, and R.L. Clark, *Fabrication of Elastin-Like Polypeptide Nanoparticles for Drug Delivery by Electrospraying*. *Biomacromolecules*, 2009. **10**(1): p. 19-24.
174. Khil, M.-S., D.-I. Cha, H.-Y. Kim, I.-S. Kim, and N. Bhattarai, *Electrospun nanofibrous polyurethane membrane as wound dressing*. *Journal of Biomedical Materials Research Part B: Applied Biomaterials*, 2003. **67B**(2): p. 675-679.
175. Kim, K., Y.K. Luu, C. Chang, D. Fang, B.S. Hsiao, B. Chu, and M. Hadjiargyrou, *Incorporation and controlled release of a hydrophilic antibiotic using poly(lactide-co-glycolide)-based electrospun nanofibrous scaffolds*. *Journal of Controlled Release*, 2004. **98**(1): p. 47-56.
176. Katti, D.S., K.W. Robinson, F.K. Ko, and C.T. Laurencin, *Bioresorbable nanofiber-based systems for wound healing and drug*

- delivery: optimization of fabrication parameters.* J Biomed Mater Res B Appl Biomater, 2004. **70**(2): p. 286-96.
177. Sofokleous, P., E. Stride, and M. Edirisinghe, *Preparation, characterization, and release of amoxicillin from electrospun fibrous wound dressing patches.* Pharm Res, 2013. **30**(7): p. 1926-38.
178. Hong, K.H., *Preparation and properties of electrospun poly(vinyl alcohol)/silver fiber web as wound dressings.* Polymer Engineering & Science, 2006. **47**(1): p. 43-49.
179. Eming, S.A., P. Martin, and M. Tomic-Canic, *Wound repair and regeneration: Mechanisms, signaling, and translation.* Science Translational Medicine, 2014. **6**(265): p. 265sr6.
180. Salazar, J.J., W.J. Ennis, and T.J. Koh, *Diabetes medications: Impact on inflammation and wound healing.* J Diabetes Complications, 2016. **30**(4): p. 746-52.
181. Mirza, R.E., M.M. Fang, E.M. Weinheimer-Haus, W.J. Ennis, and T.J. Koh, *Sustained Inflammasome Activity in Macrophages Impairs Wound Healing in Type 2 Diabetic Humans and Mice.* Diabetes, 2014. **63**: p. 1103-1114.
182. Koshiha, K., M. Nomura, Y. Nakaya, and S. Ito, *Efficacy of glimepiride on insulin resistance, adipocytokines, and atherosclerosis.* The Journal of Medical Investigation, 2006. **53**(1,2): p. 87-94.

183. Putz, D.M., W.S. Goldner, R.S. Bar, W.G. Haynes, and W.I. Sivitz, *Adiponectin and C-reactive protein in obesity, type 2 diabetes, and monodrug therapy*. *Metabolism*, 2004. **53**(11): p. 1454-1461.
184. Lamkanfi, M., J.L. Mueller, A.C. Vitari, S. Misaghi, A. Fedorova, K. Deshayes, W.P. Lee, H.M. Hoffman, and V.M. Dixit, *Glyburide inhibits the Cryopyrin/Nalp3 inflammasome*. *The Journal of Cell Biology*, 2009. **187**: p. 61-70.
185. Nath, N., M. Khan, M.K. Paintlia, M.N. Hoda, and S. Giri, *Metformin Attenuated the Autoimmune Disease of the Central Nervous System in Animal Models of Multiple Sclerosis*. *The Journal of Immunology*, 2009. **182**: p. 8005-8014.
186. Lee, C.H., M.J. Hsieh, S.H. Chang, Y.H. Lin, S.J. Liu, T.Y. Lin, K.C. Hung, J.H. Pang, and J.H. Juang, *Enhancement of diabetic wound repair using biodegradable nanofibrous metformin-eluting membranes: in vitro and in vivo*. *ACS Appl Mater Interfaces*, 2014. **6**(6): p. 3979-86.
187. Arai, M., M. Uchiba, H. Komura, Y. Mizuochi, N. Harada, and K. Okajima, *Metformin, an Antidiabetic Agent, Suppresses the Production of Tumor Necrosis Factor and Tissue Factor by Inhibiting Early Growth Response Factor-1 Expression in Human Monocytes in Vitro*. *Journal of Pharmacology and Experimental Therapeutics*, 2010. **334**: p. 206-213.

188. Smallwood, I.M., *Handbook of organic solvent properties*. Organic solvent properties. 1996, London : New York: London : Arnold New York : Halsted Press.
189. Olde Damink, L.H.H., P.J. Dijkstra, M.J.A. Van Luyn, P.B. Van Wachem, P. Nieuwenhuis, and J. Feijen, *Glutaraldehyde as a crosslinking agent for collagen-based biomaterials*. Journal of Materials Science: Materials in Medicine, 1995. **6**(8): p. 460-472.
190. Sofokleous, P., E. Stride, W. Bonfield, and M. Edirisinghe, *Design, construction and performance of a portable handheld electrohydrodynamic multi-needle spray gun for biomedical applications*. Mater Sci Eng C Mater Biol Appl, 2013. **33**(1): p. 213-23.
191. Lee, C.H., S.H. Chang, W.J. Chen, K.C. Hung, Y.H. Lin, S.J. Liu, M.J. Hsieh, J.H. Pang, and J.H. Juang, *Augmentation of diabetic wound healing and enhancement of collagen content using nanofibrous glucophage-loaded collagen/PLGA scaffold membranes*. J Colloid Interface Sci, 2015. **439**: p. 88-97.
192. Luo, C., M. Nangrejo, and M. Edirisinghe, *A novel method of selecting solvents for polymer electrospinning*. Polymer, 2010. **51**(7): p. 1654-1662.
193. Loffler, H., G. Kampf, D. Schmermund, and H.I. Maibach, *How irritant is alcohol?* Br J Dermatol, 2007. **157**(1): p. 74-81.
194. Park, J.-Y. and I.-H. Lee, *Preparation of Electrospun Porous Ethyl Cellulose Fiber by THF/DMAc Binary Solvent System*. JOURNAL OF

- INDUSTRIAL & ENGINEERING CHEMISTRY, 2007. **13**(6): p. 1002-1008.
195. Alfonsi, K., J. Colberg, P.J. Dunn, T. Fevig, S. Jennings, T.A. Johnson, H.P. Kleine, C. Knight, M.A. Nagy, D.A. Perry, and M. Stefaniak, *Green chemistry tools to influence a medicinal chemistry and research chemistry based organisation*. Green Chem., 2008. **10**(1): p. 31-36.
196. ACS Green Chemistry Institute, P.R., *ACS GCI Pharmaceutical Roundtable Solvent Selection Guide*. 2011, ACS.
197. Gu, W., P.E. Heil, H. Choi, and K. Kim, *Comprehensive model for fine Coulomb fission of liquid droplets charged to Rayleigh limit*. Applied Physics Letters, 2007. **91**(6): p. 064104.
198. Almeria, B., W. Deng, T.M. Fahmy, and A. Gomez, *Controlling the morphology of electrospray-generated PLGA microparticles for drug delivery*. J Colloid Interface Sci, 2010. **343**(1): p. 125-33.
199. Li, Z. and C. Wang, *Effects of Working Parameters on Electrospinning*. 2013: p. 15-28.
200. Shenoy, S.L., W.D. Bates, H.L. Frisch, and G.E. Wnek, *Role of chain entanglements on fiber formation during electrospinning of polymer solutions: good solvent, non-specific polymer–polymer interaction limit*. Polymer, 2005. **46**(10): p. 3372-3384.
201. Luo, C. and M. Edirisinghe, *Core-Liquid-Induced Transition from Coaxial Electrospray to Electrospinning of Low-Viscosity Poly (lactide-*

- co-glycolide) Sheath Solution*. *Macromolecules*, 2014. **47**(22): p. 7930-7938.
202. Jaworek, A. and A. Krupa, *MAIN MODES OF ELECTROHYDRODYNAMIC SPRAYING OF LIQUIDS*, in *Third International Conference on Multiphase Flow*. 1998: Lyon, France. p. 8.
203. Rodoplu, D. and M. Mutlu, *Effects of Electrospinning Setup and Process Parameters on Nanofiber Morphology Intended for the Modification of Quartz Crystal Microbalance Surfaces*. *Journal of Engineered Fibers and Fabrics*, 2012. **7**(2): p. 118-123.
204. Andrade, P.F., A.F. de Faria, F.J. Quides, S.R. Oliveira, O.L. Alves, M.A.Z. Arruda, and M.d.C. Gonçalves, *Inhibition of bacterial adhesion on cellulose acetate membranes containing silver nanoparticles*. *Cellulose*, 2015. **22**(6): p. 3895-3906.
205. Chen, W.-J., B.-J. Xin, and X.-J. Wu, *Fabrication and characterization of PSA nanofibers via electrospinning*. *Journal of Industrial Textiles*, 2014. **44**(1): p. 159-179.
206. Hohman, M.M., M. Shin, G. Rutledge, and M.P. Brenner, *Electrospinning and electrically forced jets. I. Stability theory*. *Physics of Fluids*, 2001. **13**(8): p. 2201.
207. Hayati, I., A. Bailey, and T.F. Tadros, *Investigations into the Mechanism of Electrohydrodynamic Spraying of Liquids* *Journal of Colloid and Interface Science*, 1986. **117**(1).

208. Yang, Y., Z. Jia, J. Liu, Q. Li, L. Hou, L. Wang, and Z. Guan, *Effect of electric field distribution uniformity on electrospinning*. Journal of Applied Physics, 2008. **103**(10): p. 104307.
209. Han, T., D.H. Reneker, and A.L. Yarin, *Buckling of jets in electrospinning*. Polymer, 2007. **48**(20): p. 6064-6076.
210. Thompson, C.J., G.G. Chase, A.L. Yarin, and D.H. Reneker, *Effects of parameters on nanofiber diameter determined from electrospinning model*. Polymer, 2007. **48**(23): p. 6913-6922.
211. Ratner, B.D., A.S. Hoffman, F.J. Schoen, and J.E. Lemons, eds. *Biomaterials Science: An Introduction to Materials in Medicine*. 2004, Elsevier.
212. Lannutti, J., D. Reneker, T. Ma, D. Tomasko, and D. Farson, *Electrospinning for tissue engineering scaffolds*. Materials Science and Engineering: C, 2007. **27**(3): p. 504-509.
213. Sofokleous, P., E. Stride, W. Bonfield, and M. Edirisinghe, *Design, construction and performance of a portable handheld electrohydrodynamic multi-needle spray gun for biomedical applications*. Materials Science & Engineering C-Materials for Biological Applications, 2013. **33**(1): p. 213-223.
214. Luong-Van, E., L. Grondahl, K.N. Chua, K.W. Leong, V. Nurcombe, and S.M. Cool, *Controlled release of heparin from poly(epsilon-caprolactone) electrospun fibers*. Biomaterials, 2006. **27**(9): p. 2042-50.

215. Lovikka, V.A., L. Rautkari, and T.C. Maloney, *Changes in the hygroscopic behavior of cellulose due to variations in relative humidity*. Cellulose, 2017. **25**(1): p. 87-104.
216. Cai, Q., J. Bei, and S. Wang, *In vitro study on the drug release behavior from Polylactide-based blend matrices*. Polymers for Advanced Technologies, 2002. **13**(7): p. 534-540.
217. Pitt, C.G., F.I. Chasalow, Y.M. Hibionada, D.M. Klimas, and A. Schindler, *Aliphatic polyesters. I. The degradation of poly(ϵ -caprolactone) in vivo*. Journal of Applied Polymer Science, 1981. **26**(11): p. 3779-3787.
218. Peña, J., T. Corrales, I. Izquierdo-Barba, A. Doadrio, and M. Vallet-Regí, *Long Term Degradation of Poly(3-Caprolactone) Films in Biologically Related Fluids*. Vol. 91. 2006. 1424-1432.
219. Elzoghby, A.O., W.M. Samy, and N.A. Elgindy, *Albumin-based nanoparticles as potential controlled release drug delivery systems*. Journal of Controlled Release, 2012. **157**(2): p. 168-182.
220. Akbar, D.H., *Effect of metformin and sulfonylurea on C-reactive protein level in well-controlled type 2 diabetics with metabolic syndrome*. Endocrine, 2003. **20**(3): p. 215-218.
221. Dandona, P., A. Aljada, H. Ghanim, P. Mohanty, C. Tripathy, D. Hofmeyer, and A. Chaudhuri, *Increased Plasma Concentration of Macrophage Migration Inhibitory Factor (MIF) and MIF mRNA in Mononuclear Cells in the Obese and the Suppressive Action of*

- Metformin*. The Journal of Clinical Endocrinology & Metabolism, 2004. **89**(10): p. 5043-5047.
222. Shi, L., G.-S. Tan, and K. Zhang, *Relationship of the Serum CRP Level With the Efficacy of Metformin in the Treatment of Type 2 Diabetes Mellitus: A Meta-Analysis*. Journal of Clinical Laboratory Analysis, 2016. **30**(1): p. 13-22.
223. Ishibashi, Y., T. Matsui, M. Takeuchi, and S. Yamagishi, *Metformin inhibits advanced glycation end products (AGEs)-induced renal tubular cell injury by suppressing reactive oxygen species generation via reducing receptor for AGEs (RAGE) expression*. Hormone and Metabolic Research, 2012. **44**(12): p. 891-895.
224. Salminen, A., J.M.T. Hyttinen, and K. Kaarniranta, *AMP-activated protein kinase inhibits NF- κ B signaling and inflammation: impact on healthspan and lifespan*. Journal of Molecular Medicine, 2011. **89**(7): p. 667-676.
225. Carvalho-Filho, M.A., M. Ueno, S.M. Hirabara, A.B. Seabra, J.B.C. Carvalheira, M.G. de Oliveira, L.A. Velloso, R. Curi, and M.J.A. Saad, *S-Nitrosation of the Insulin Receptor, Insulin Receptor Substrate 1, and Protein Kinase B/Akt*. Diabetes, 2005. **54**(4): p. 959.
226. Otranto, M., A.P.d. Nascimento, and A. Monte-Alto-Costa, *Insulin resistance impairs cutaneous wound healing in mice*. Wound Repair and Regeneration, 2013. **21**(3): p. 464-472.

227. Altun, E., M.O. Aydogdu, M. Crabbe-Mann, J. Ahmed, F. Brako, B. Karademir, B. Aksu, M. Sennaroglu, M.S. Eroglu, G. Ren, O. Gunduz, and M. Edirisinghe, *Co-Culture of Keratinocyte-Staphylococcus aureus on Cu-Ag-Zn/CuO and Cu-Ag-W Nanoparticle Loaded Bacterial Cellulose:PMMA Bandages*. *Macromolecular Materials and Engineering*, 2019. **304**(1): p. 1800537.
228. Gerlier, D. and N. Thomasset, *Use of MTT colorimetric assay to measure cell activation*. *Journal of Immunological Methods*, 1986. **94**(1): p. 57-63.